

TIM LINDEN

THE RISE OF THE LEPTONS

PULSAR EMISSION DOMINATES THE TEV GAMMA-RAY SKY

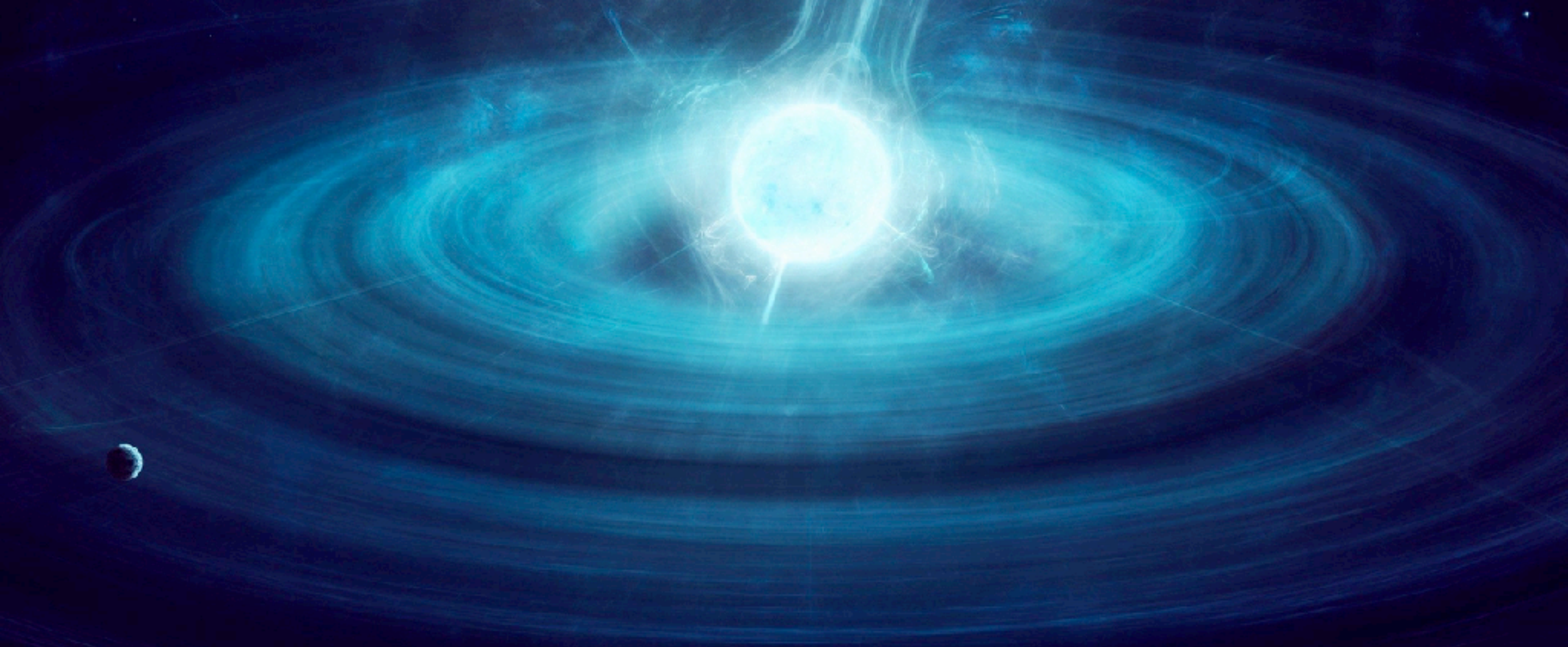
MSU High Energy Physics Seminar

November 14, 2017



THE OHIO STATE UNIVERSITY

CENTER FOR COSMOLOGY AND
ASTROPARTICLE PHYSICS



TIM LINDEN

THE RISE OF THE LEPTONS

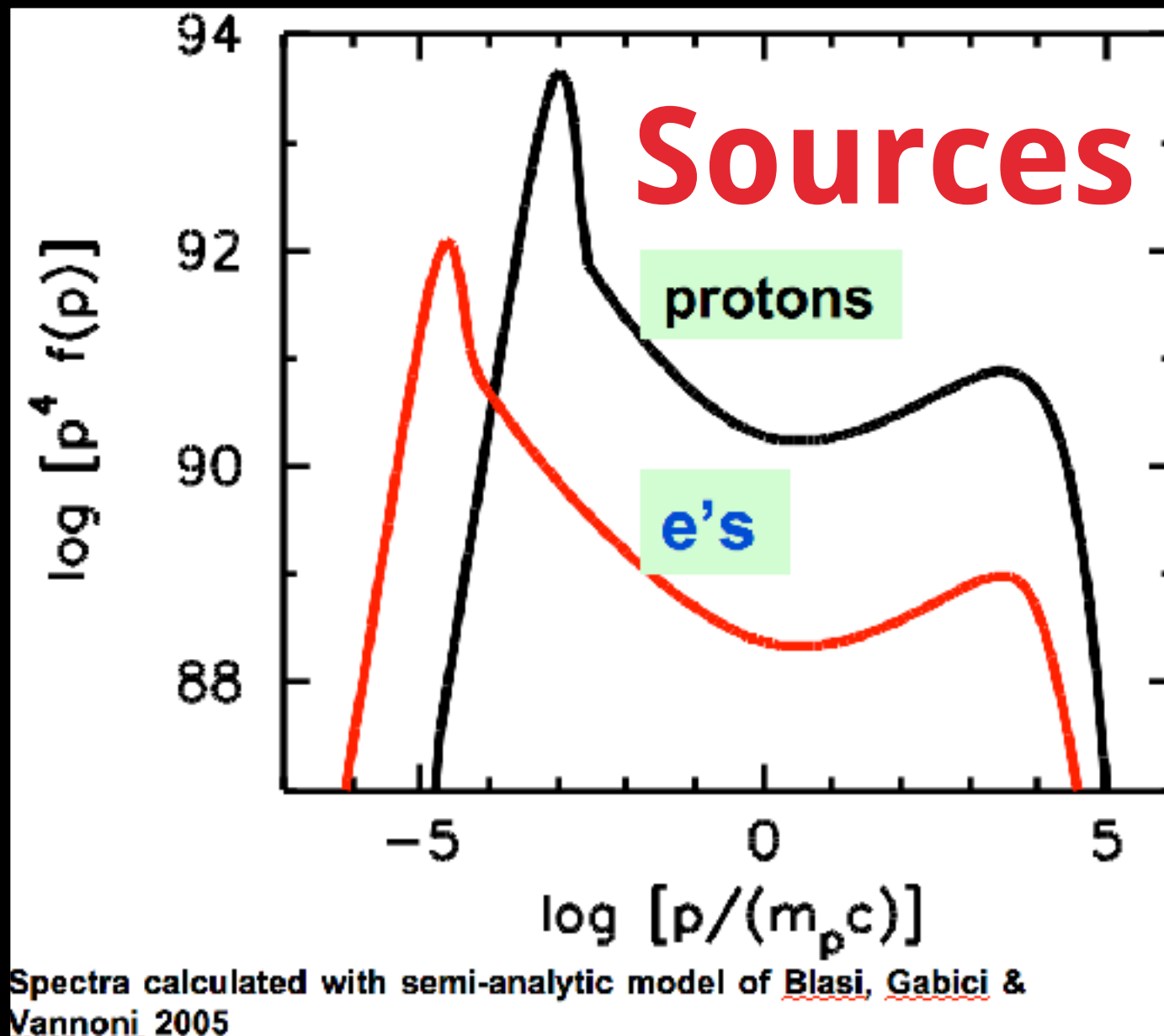
PULSAR EMISSION DOMINATES THE TEV GAMMA-RAY SKY

**WITH: KATIE AUCHETTL, BEN BUCKMAN, JOSEPH
BRAMANTE, ILIAS CHOLIS, CARMELO EVOLI, KE FANG, DAN
HOOPER, TANVI KARWAL, SHIRLEY LI, GIOVANNI MORLINO**

A UNIVERSE DOMINATED BY PROTONS

We normally think that the Milky Way cosmic-ray energy budget is dominated by protons.

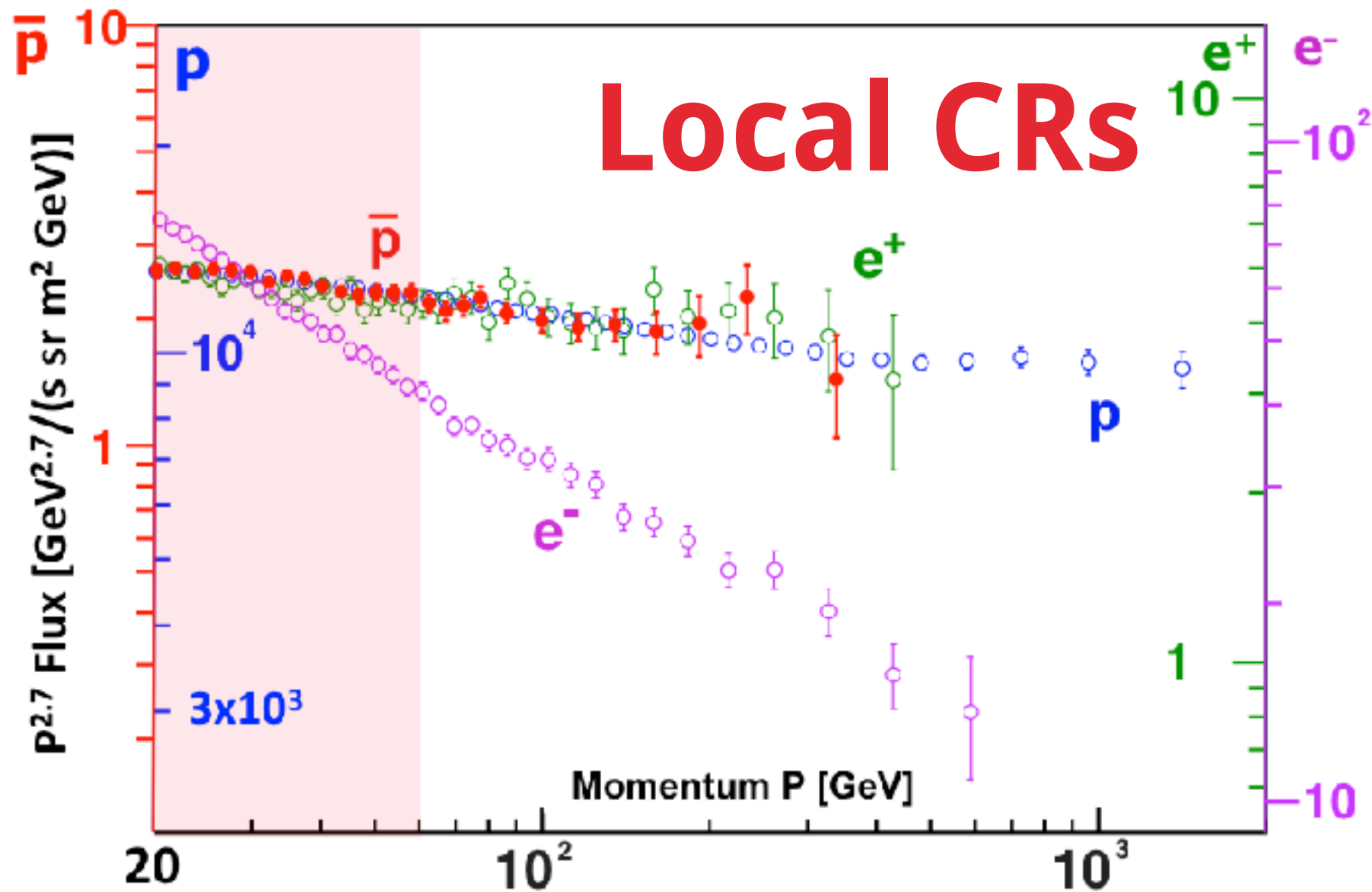
A UNIVERSE DOMINATED BY PROTONS



A UNIVERSE DOMINATED BY PROTONS

$\log [p^4 f(p)]$

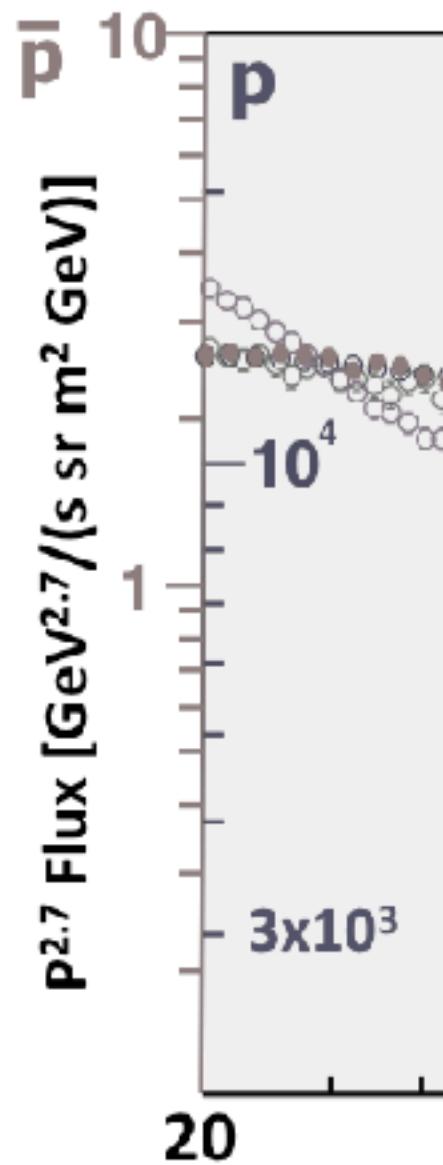
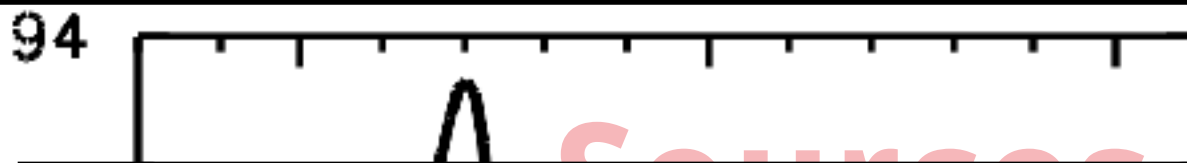
94



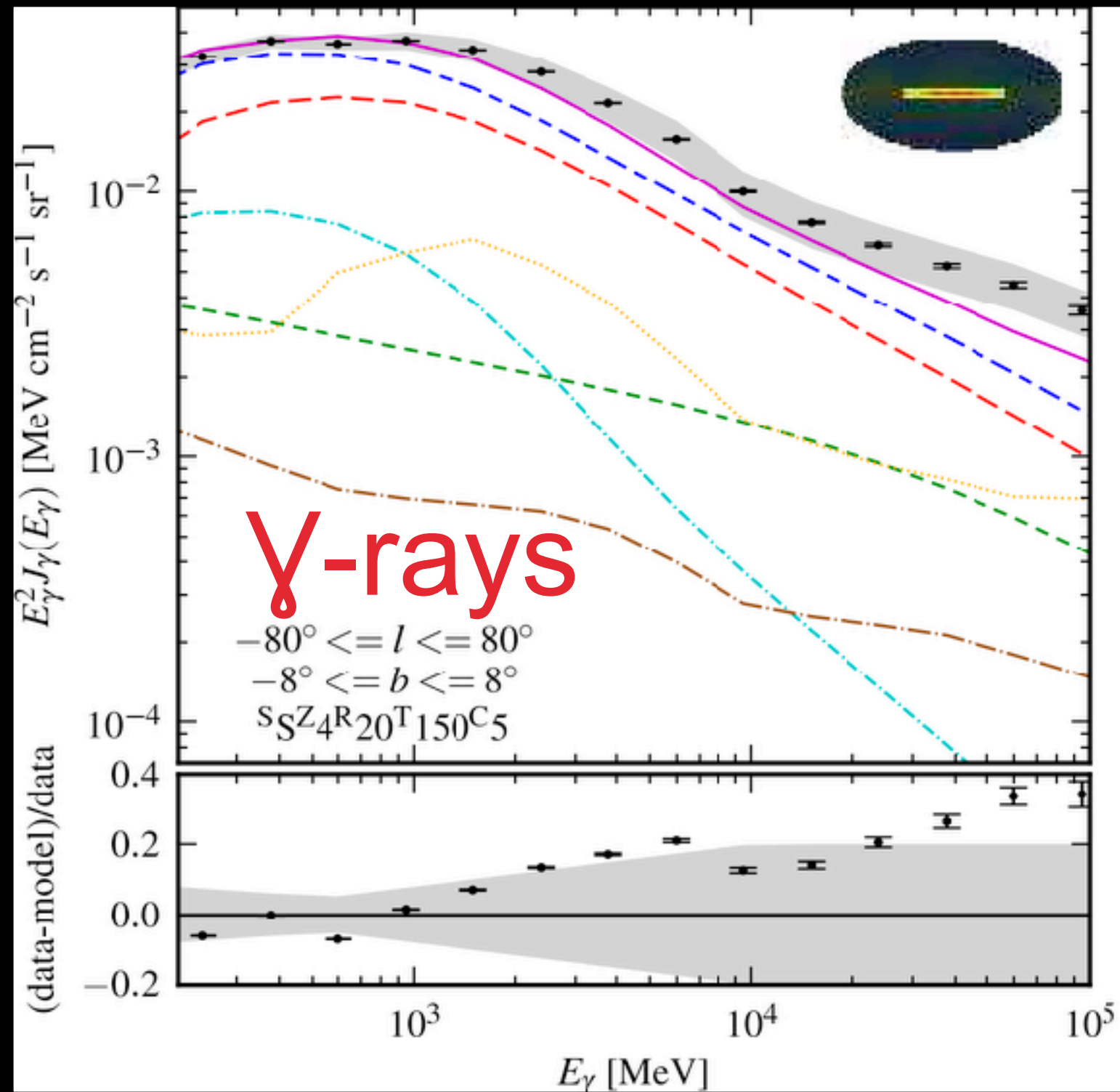
Spectra cal
Vannoni 20

A UNIVERSE DOMINATED BY PROTONS

$\log [p^4 f(p)]$



Spectra ca
Vannoni 20



COSMIC-RAY ACCELERATION AND PROPAGATION



Start with a source of relativistic cosmic-rays

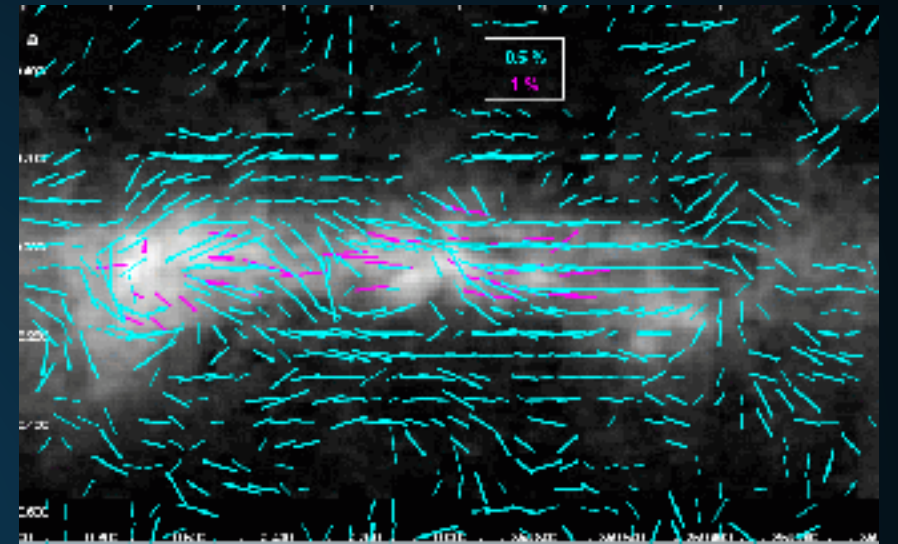
- ▶ **Supernova Explosions**
- ▶ **Supernova Remnants**
- ▶ **Pulsars**
- ▶ **Shocks/Mergers**

COSMIC-RAY ACCELERATION AND PROPAGATION



Start with a source of relativistic cosmic-rays

cosmic rays propagate



$$\frac{\partial \psi}{\partial t} = q(\vec{r}, p) + \vec{\nabla} \cdot (D_{xx} \vec{\nabla} \psi - \vec{V} \psi) + \frac{\partial}{\partial p} p^2 D_{pp} \frac{\partial}{\partial p} \frac{1}{p^2} \psi - \frac{\partial}{\partial p} \left[\dot{p} \psi - \frac{p}{3} (\vec{\nabla} \cdot \vec{V}) \psi \right] - \frac{1}{\tau_f} \psi - \frac{1}{\tau_r} \psi$$

Solved Numerically:
e.g. Galprop

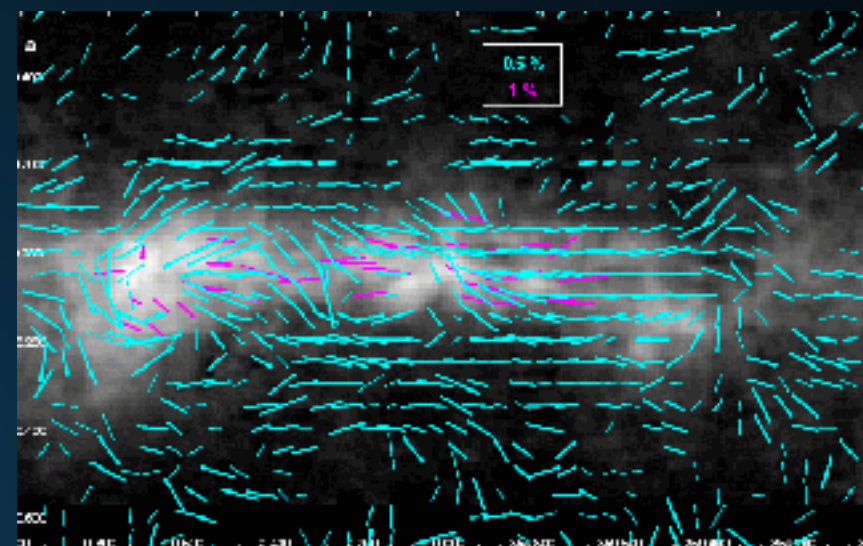
- ▶ If they propagate to Earth, can be detected:
 - ▶ AMS-02/PAMELA
 - ▶ CREAM/HEAT/CAPRICE

COSMIC-RAY ACCELERATION AND PROPAGATION



Start with a source of relativistic cosmic-rays

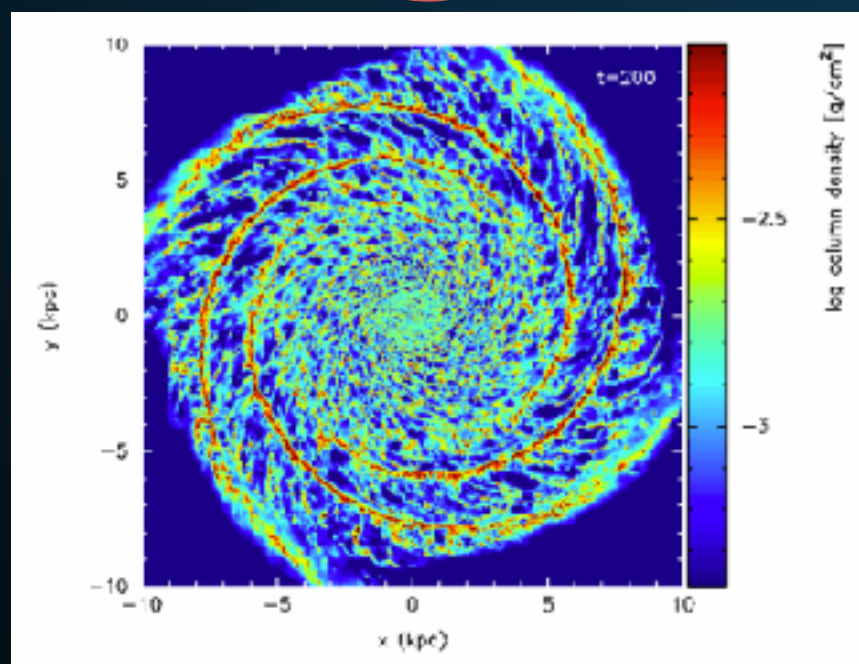
cosmic rays propagate



$$\frac{\partial \psi}{\partial t} = q(\vec{r}, p) + \vec{\nabla} \cdot (D_{xx} \vec{\nabla} \psi - \vec{V} \psi) + \frac{\partial}{\partial p} p^2 D_{pp} \frac{\partial}{\partial p} \frac{1}{p^2} \psi - \frac{\partial}{\partial p} \left[\dot{p} \psi - \frac{p}{3} (\vec{\nabla} \cdot \vec{V}) \psi \right] - \frac{1}{\tau_f} \psi - \frac{1}{\tau_r} \psi$$

Solved Numerically:
e.g. Galprop

Gas/ISRF



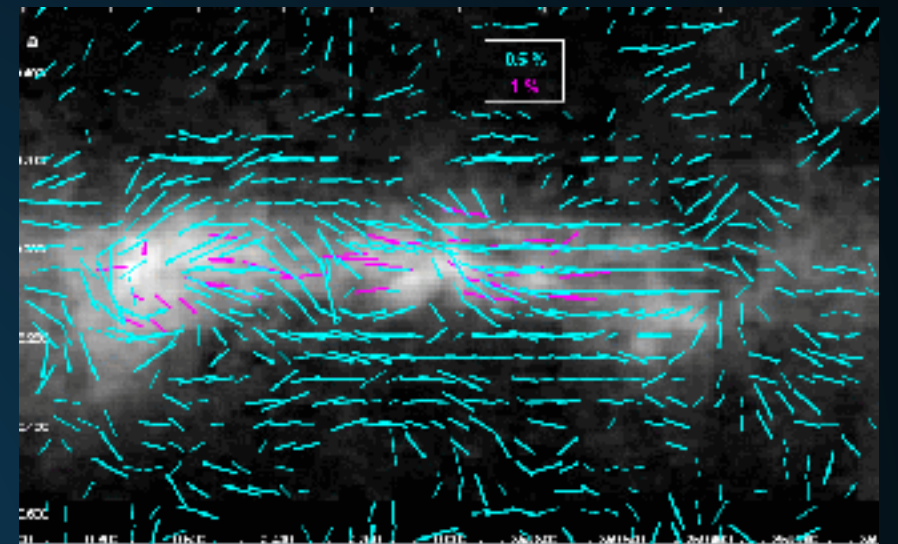
- ▶ Alternatively can collide with Galactic gas or the interstellar radiation field.

COSMIC-RAY ACCELERATION AND PROPAGATION



Start with a source of relativistic cosmic-rays

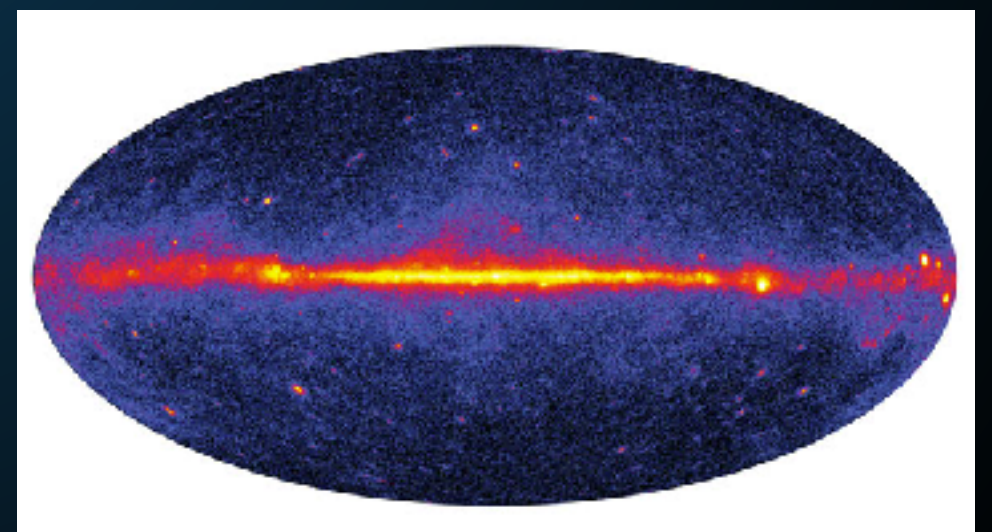
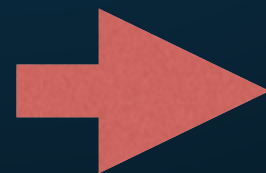
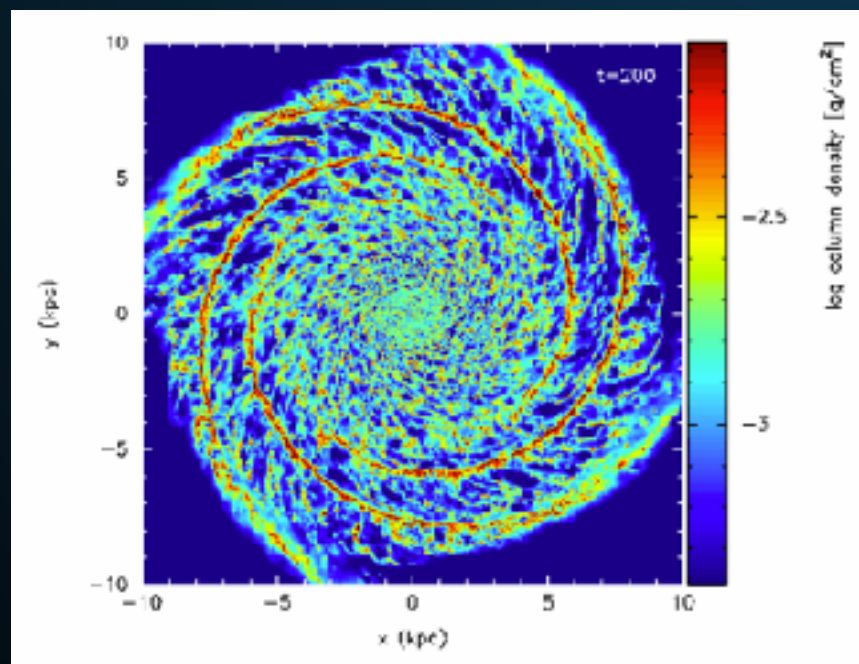
cosmic rays propagate



$$\frac{\partial \psi}{\partial t} = q(\vec{r}, p) + \vec{\nabla} \cdot (D_{xx} \vec{\nabla} \psi - \vec{V} \psi) + \frac{\partial}{\partial p} p^2 D_{pp} \frac{\partial}{\partial p} \frac{1}{p^2} \psi - \frac{\partial}{\partial p} \left[\dot{p} \psi - \frac{p}{3} (\vec{\nabla} \cdot \vec{V}) \psi \right] - \frac{1}{\tau_f} \psi - \frac{1}{\tau_r} \psi$$

Solved Numerically:
e.g. Galprop

Gas/ISRF



- ▶ **In this talk, I will argue that electrons and positrons dominate the Milky Way's energetics at TeV energies:**
 - ▶ **1.) Pulsars produce the majority of the TeV gamma-ray emission observed from the Milky Way**
 - ▶ **2.) Pulsars produce the majority of the bright TeV sources observed by CTA/HAWC/HESS etc.**
 - ▶ **3.) Pulsars are responsible for the rising positron fraction observed by PAMELA/AMS-02**

- ▶ **Always worry about the assumptions behind bold statements:**
 - ▶ **Observations necessitate these results.**
 - ▶ **Very few (and reasonable) modeling assumptions**

Let's start without a theoretical model.

What do TeV observations tell us about pulsars?

HAWC OBSERVATIONS OF GEMINGA AND MONOGEN

| Name | Tested radius [°] | Index | $F_7 \times 10^{16}$ [TeV ⁻¹ cm ⁻² s ⁻¹] | TeVCat |
|----------------|----------------------|------------------|---|---------|
| 2HWC J0534+220 | - | -2.58 ± 0.01 | 184.7 ± 2.4 | Crab |
| 2HWC J0631+169 | - | -2.57 ± 0.15 | 6.7 ± 1.5 | Geminga |
| " | 2.0 | -2.23 ± 0.08 | 48.7 ± 6.9 | Geminga |
| 2HWC J0635+180 | - | -2.56 ± 0.16 | 6.5 ± 1.5 | Geminga |
| 2HWC J0700+143 | 1.0 | -2.17 ± 0.16 | 13.8 ± 4.2 | - |
| " | 2.0 | -2.03 ± 0.14 | 23.0 ± 7.3 | - |

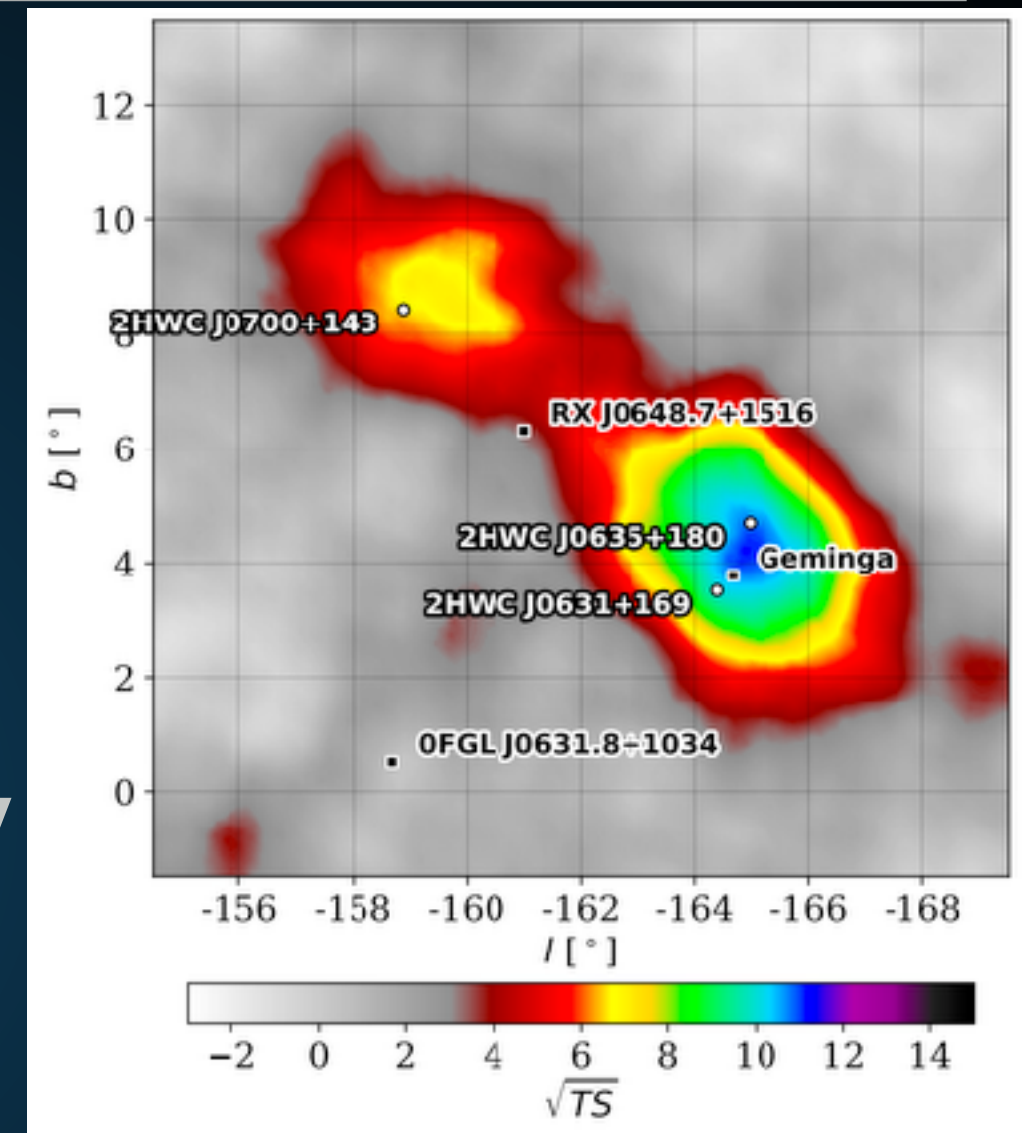
▶ HAWC observes Geminga

▶ $4.9 \times 10^{-14} \text{ TeV}^{-1} \text{ cm}^{-2} \text{ s}^{-1}$ at 7 TeV

▶ Luminosity $\sim 1.4 \times 10^{31} \text{ TeV s}^{-1}$

▶ Big Distance Uncertainties

▶ 300 kyr !



Beautiful !

HAWC OBSERVATIONS OF GEMINGA AND MONOGEM

| Name | Tested radius | Index | $F_7 \times 10^{15}$ | TeVCat |
|----------------|---------------|------------------|--|--------|
| | [$^\circ$] | | [$\text{TeV}^{-1} \text{cm}^{-2} \text{s}^{-1}$] | |
| 2HWC J0700+143 | 1.0 | -2.17 ± 0.16 | 13.8 ± 4.2 | - |
| " | 2.0 | -2.03 ± 0.14 | 23.0 ± 7.3 | - |

▶ HAWC observes B0656+14 (Monogem)

▶ $2.3 \times 10^{-14} \text{ TeV}^{-1} \text{ cm}^{-2} \text{ s}^{-1}$ at 7 TeV

▶ Luminosity $\sim 1.1 \times 10^{31} \text{ TeV s}^{-1}$

▶ Small distance uncertainties.

▶ 110 kyr !



Help ?

Table 1 HGPS sources considered as firmly identified pulsar wind nebulae in this paper.

| HGPS name | ATNF name | Canonical name | $\lg \dot{E}$ | τ_c (kyr) | d (kpc) | PSR offset (pc) | Γ | R_{PWN} (pc) | $L_{1-10 \text{ TeV}}$ ($10^{33} \text{ erg s}^{-1}$) |
|---------------------------|------------|------------------------------------|---------------|-------------------|--------------|--------------------|-----------------|--------------------------|--|
| J1813–178 ^[1] | J1813–1749 | | 37.75 | 5.60 | 4.70 | < 2 | 2.07 ± 0.05 | 4.0 ± 0.3 | 19.0 ± 1.5 |
| J1833–105 | J1833–1034 | G21.5–0.9 ^[2] | 37.53 | 4.85 | 4.10 | < 2 | 2.42 ± 0.19 | < 4 | 2.6 ± 0.5 |
| J1514–591 | B1509–58 | MSH 15–52 ^[3] | 37.23 | 1.56 | 4.40 | < 4 | 2.26 ± 0.03 | 11.1 ± 2.0 | 52.1 ± 1.8 |
| J1930+188 | J1930+1852 | G54.1+0.3 ^[4] | 37.08 | 2.89 | 7.00 | < 10 | 2.6 ± 0.3 | < 9 | 5.5 ± 1.8 |
| J1420–607 | J1420–6048 | Kookaburra (K2) ^[5] | 37.00 | 13.0 | 5.61 | 5.1 ± 1.2 | 2.20 ± 0.05 | 7.9 ± 0.6 | 44 ± 3 |
| J1849–000 | J1849–0001 | IGR J18490–0000 ^[6] | 36.99 | 42.9 | 7.00 | < 10 | 1.97 ± 0.09 | 11.0 ± 1.9 | 12 ± 2 |
| J1846–029 | J1846–0258 | Kes 75 ^[2] | 36.91 | 0.728 | 5.80 | < 2 | 2.41 ± 0.09 | < 3 | 6.0 ± 0.7 |
| J0835–455 | B0833–45 | Vela X ^[7] | 36.84 | 11.3 | 0.280 | 2.37 ± 0.18 | 1.89 ± 0.03 | 2.9 ± 0.3 | $0.83 \pm 0.11^*$ |
| J1837–069 ^[8] | J1838–0655 | | 36.74 | 22.7 | 6.60 | 17 ± 3 | 2.54 ± 0.04 | 41 ± 4 | 204 ± 8 |
| J1418–609 | J1418–6058 | Kookaburra (Rabbit) ^[5] | 36.69 | 10.3 | 5.00 | 7.3 ± 1.5 | 2.26 ± 0.05 | 9.4 ± 0.9 | 31 ± 3 |
| J1356–645 ^[9] | J1357–6429 | | 36.49 | 7.31 | 2.50 | 5.5 ± 1.4 | 2.20 ± 0.08 | 10.1 ± 0.9 | 14.7 ± 1.4 |
| J1825–137 ^[10] | B1823–13 | | 36.45 | 21.4 | 3.93 | 33 ± 6 | 2.38 ± 0.03 | 32 ± 2 | 116 ± 4 |
| J1119–614 | J1119–6127 | G292.2–0.5 ^[11] | 36.36 | 1.61 | 8.40 | < 11 | 2.64 ± 0.12 | 14 ± 2 | 23 ± 4 |
| J1303–631 ^[12] | J1301–6305 | | 36.23 | 11.0 | 6.65 | 20.5 ± 1.8 | 2.33 ± 0.02 | 20.6 ± 1.7 | 96 ± 5 |

- ▶ HESS finds a large population of “TeV PWN”
- ▶ HESS systems have a higher spin down power, but are more distant.

Table 4 Candidate pulsar wind nebulae from the pre-selection.

| HGPS name | ATNF name | $\lg \dot{E}$ | τ_c (kyr) | d (kpc) | PSR offset (pc) | Γ | R_{PWN} (pc) | $L_{1-10 \text{ TeV}}$ ($10^{33} \text{ erg s}^{-1}$) |
|---------------|----------------|---------------|-------------------|--------------|--------------------|-----------------|--------------------------|--|
| J1616–508 (1) | J1617–5055 | 37.20 | 8.13 | 6.82 | < 26 | 2.34 ± 0.06 | 28 ± 4 | 162 ± 9 |
| J1023–575 | J1023–5746 | 37.04 | 4.60 | 8.00 | < 9 | 2.36 ± 0.05 | 23.2 ± 1.2 | 67 ± 5 |
| J1809–193 (1) | J1811–1925 | 36.81 | 23.3 | 5.00 | 29 ± 7 | 2.38 ± 0.07 | 35 ± 4 | 53 ± 3 |
| J1857+026 | J1856+0245 | 36.66 | 20.6 | 9.01 | 21 ± 6 | 2.57 ± 0.06 | 41 ± 9 | 118 ± 13 |
| J1640–465 | J1640–4631 (1) | 36.64 | 3.35 | 12.8 | < 20 | 2.55 ± 0.04 | 25 ± 8 | 210 ± 12 |
| J1641–462 | J1640–4631 (2) | 36.64 | 3.35 | 12.8 | 50 ± 5 | 2.50 ± 0.11 | < 14 | 17 ± 4 |
| J1708–443 | B1706–44 | 36.53 | 17.5 | 2.60 | 17 ± 3 | 2.17 ± 0.08 | 12.7 ± 1.4 | 6.6 ± 0.9 |
| J1908+063 | J1907+0602 | 36.45 | 19.5 | 3.21 | 21 ± 3 | 2.26 ± 0.06 | 27.2 ± 1.5 | 28 ± 2 |
| J1018–589A | J1016–5857 (1) | 36.41 | 21.0 | 8.00 | 47.5 ± 1.6 | 2.24 ± 0.13 | < 4 | 8.1 ± 1.4 |
| J1018–589B | J1016–5857 (2) | 36.41 | 21.0 | 8.00 | 25 ± 7 | 2.20 ± 0.09 | 21 ± 4 | 23 ± 5 |
| J1804–216 | B1800–21 | 36.34 | 15.8 | 4.40 | 18 ± 5 | 2.69 ± 0.04 | 19 ± 3 | 42.5 ± 2.0 |
| J1809–193 (2) | J1809–1917 | 36.26 | 51.3 | 3.55 | < 17 | 2.38 ± 0.07 | 25 ± 3 | 26.9 ± 1.5 |
| J1616–508 (2) | B1610–50 | 36.20 | 7.42 | 7.94 | 60 ± 7 | 2.34 ± 0.06 | 32 ± 5 | 220 ± 12 |
| J1718–385 | J1718–3825 | 36.11 | 89.5 | 3.60 | 5.4 ± 1.6 | 1.77 ± 0.06 | 7.2 ± 0.9 | 4.6 ± 0.8 |
| J1026–582 | J1028–5819 | 35.92 | 90.0 | 2.33 | 9 ± 2 | 1.81 ± 0.10 | 5.3 ± 1.6 | 1.7 ± 0.5 |
| J1832–085 | B1830–08 (1) | 35.76 | 147 | 4.50 | 23.3 ± 1.5 | 2.38 ± 0.14 | < 4 | 1.7 ± 0.4 |
| J1834–087 | B1830–08 (2) | 35.76 | 147 | 4.50 | 32.3 ± 1.9 | 2.61 ± 0.07 | 17 ± 3 | 25.8 ± 2.0 |
| J1858+020 | J1857+0143 | 35.65 | 71.0 | 5.75 | 38 ± 3 | 2.39 ± 0.12 | 7.9 ± 1.6 | 7.1 ± 1.5 |
| J1745–303 | B1742–30 (1) | 33.93 | 546 | 0.200 | 1.42 ± 0.15 | 2.57 ± 0.06 | 0.62 ± 0.07 | 0.014 ± 0.003 |
| J1746–308 | B1742–30 (2) | 33.93 | 546 | 0.200 | < 1.1 | 3.3 ± 0.2 | 0.56 ± 0.12 | 0.009 ± 0.003 |

- ▶ HESS finds a large population of “TeV PWN”
- ▶ HESS systems have a higher spin down power, but are more distant.

THE SPECTRUM OF GEMINGA

► Geminga has a hard gamma-ray spectrum

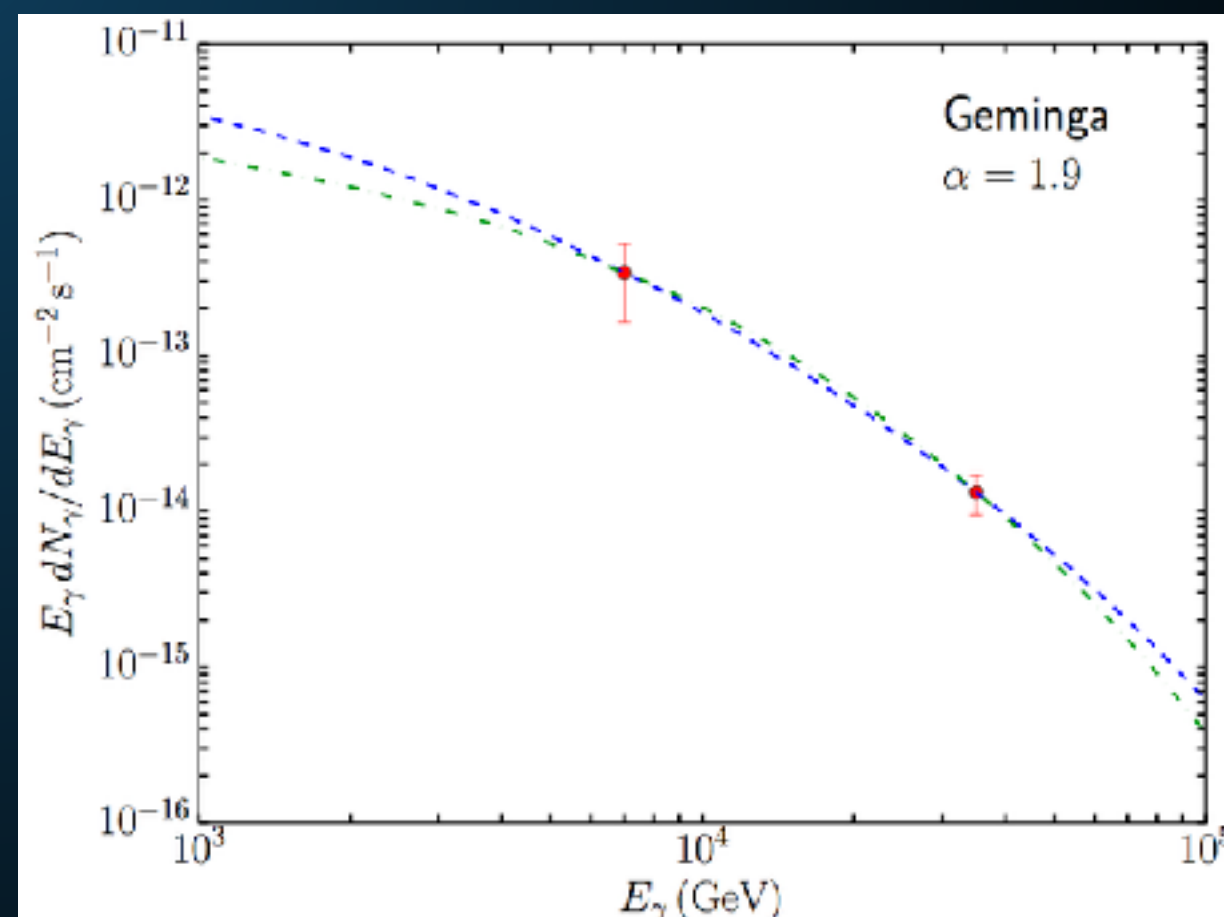
| Name | Tested radius [°] | Index | $F_7 \times 10^{15}$ [TeV ⁻¹ cm ⁻² s ⁻¹] | TeVCat |
|----------------|----------------------|------------------|---|---------|
| 2HWC J0631+169 | - | -2.57 ± 0.15 | 6.7 ± 1.5 | Geminga |
| " | 2.0 | -2.23 ± 0.08 | 48.7 ± 6.9 | Geminga |
| 2HWC J0635+180 | - | -2.56 ± 0.16 | 6.5 ± 1.5 | Geminga |

► We assuming an electron injection spectrum following a power-law with an exponential cutoff.

► Based on a joint fit to the HAWC and Milagro data, we calculate:

► $-1.9 < \alpha < -1.5$

► $E_{\text{cut}} \cong 50 \text{ TeV}$



Geminga Electron Power Corresponds to

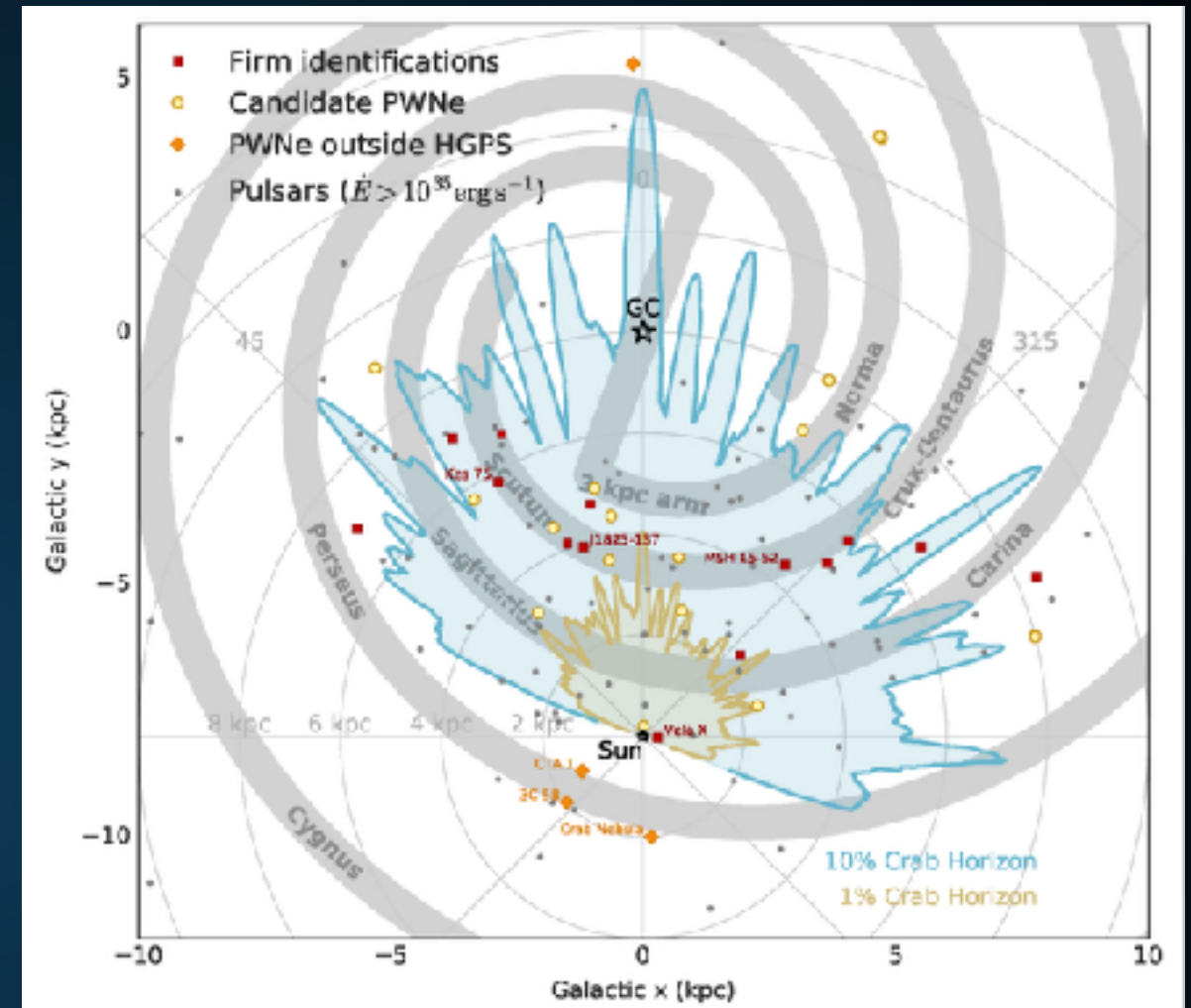
$\sim 3-9 \times 10^{33} \text{ erg s}^{-1} !$

9-27% of the total pulsar spin-down power!

A MODEL OF TEV HALOS

1702.08280

- ▶ **Assumption: Geminga (and Monogem) are typical pulsars.**
- ▶ This statement is well supported:
 - ▶ Observed because they are the two closest sources.
 - ▶ Many similar HESS Sources.
- ▶ We will call these sources, “TeV halos” - for reasons which will become clear later.



THE FIRST-ORDER MODEL OF TEV HALOS

$$\phi_{\text{TeV halo}} = \left(\frac{\dot{E}_{\text{psr}}}{\dot{E}_{\text{Geminga}}} \right) \left(\frac{d_{\text{Geminga}}^2}{d_{\text{psr}}^2} \right) \phi_{\text{Geminga}}$$

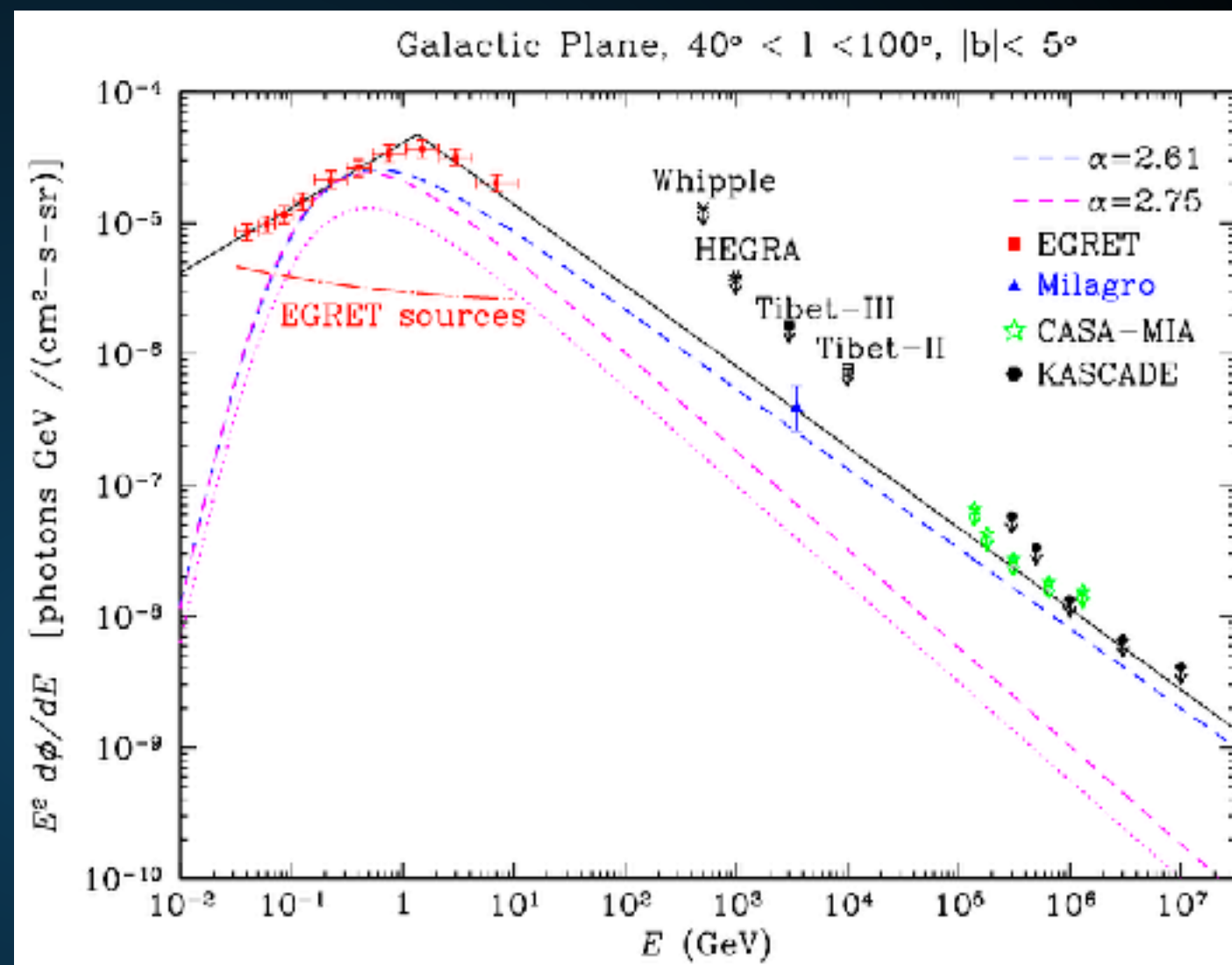
$$\theta_{\text{TeV halo}} = \left(\frac{d_{\text{Geminga}}}{d_{\text{psr}}} \right) \theta_{\text{Geminga}}$$

- ▶ **Assume that every pulsar converts an equivalent fraction of its spin-down power into the TeV halo flux.**
- ▶ **Can then calculate the TeV flux and extension of every TeV halo based on its spin-down power, and the observations of Geminga.**
- ▶ **Note: Using Monogem would increase fluxes by nearly a factor of 2. The power law of this correlation doesn't greatly affect the results.**

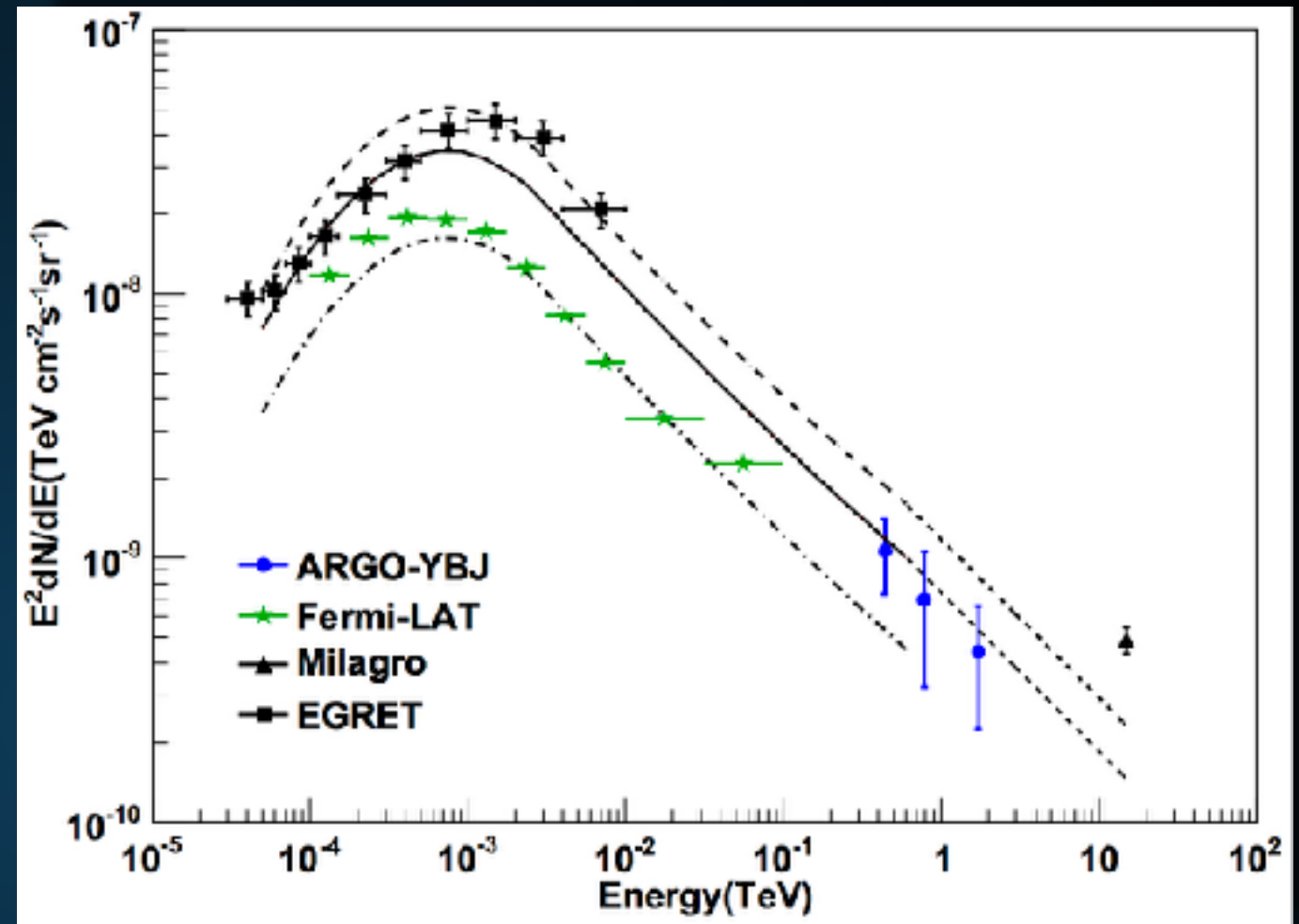
Implication I:

Most diffuse TeV emission is powered by pulsars

- ▶ Milagro detects bright diffuse TeV emission along the Galactic plane.
- ▶ Difficult to explain with pion decay, due to steeply falling local hadronic CR spectrum.
- ▶ Can harden gamma-ray emission to some extent using radially dependent diffusion constants (1504.00227).



- ▶ **Milagro detects bright diffuse TeV emission along the Galactic plane.**
- ▶ **Difficult to explain with pion decay, due to steeply falling local hadronic CR spectrum.**
- ▶ **Can harden gamma-ray emission to some extent using radially dependent diffusion constants (1504.00227).**



- ▶ Use a generic model for pulsar luminosities
- ▶ $B_0 = 10^{12.5} \text{ G } (+/- 10^{0.3} \text{ G})$
- ▶ $P_0 = 0.3 \text{ s } (+/- 0.15 \text{ s})$
- ▶ Spindown Timescale of $\sim 10^4 \text{ yr}$ (depends on B_0)
- ▶ Galprop model for supernova distances

PsrPopPy: An open-source package for pulsar population simulations

D. Bates^{1,2}, D. R. Lorimer^{1,3}, A. Rane¹ and J. Swiggum¹

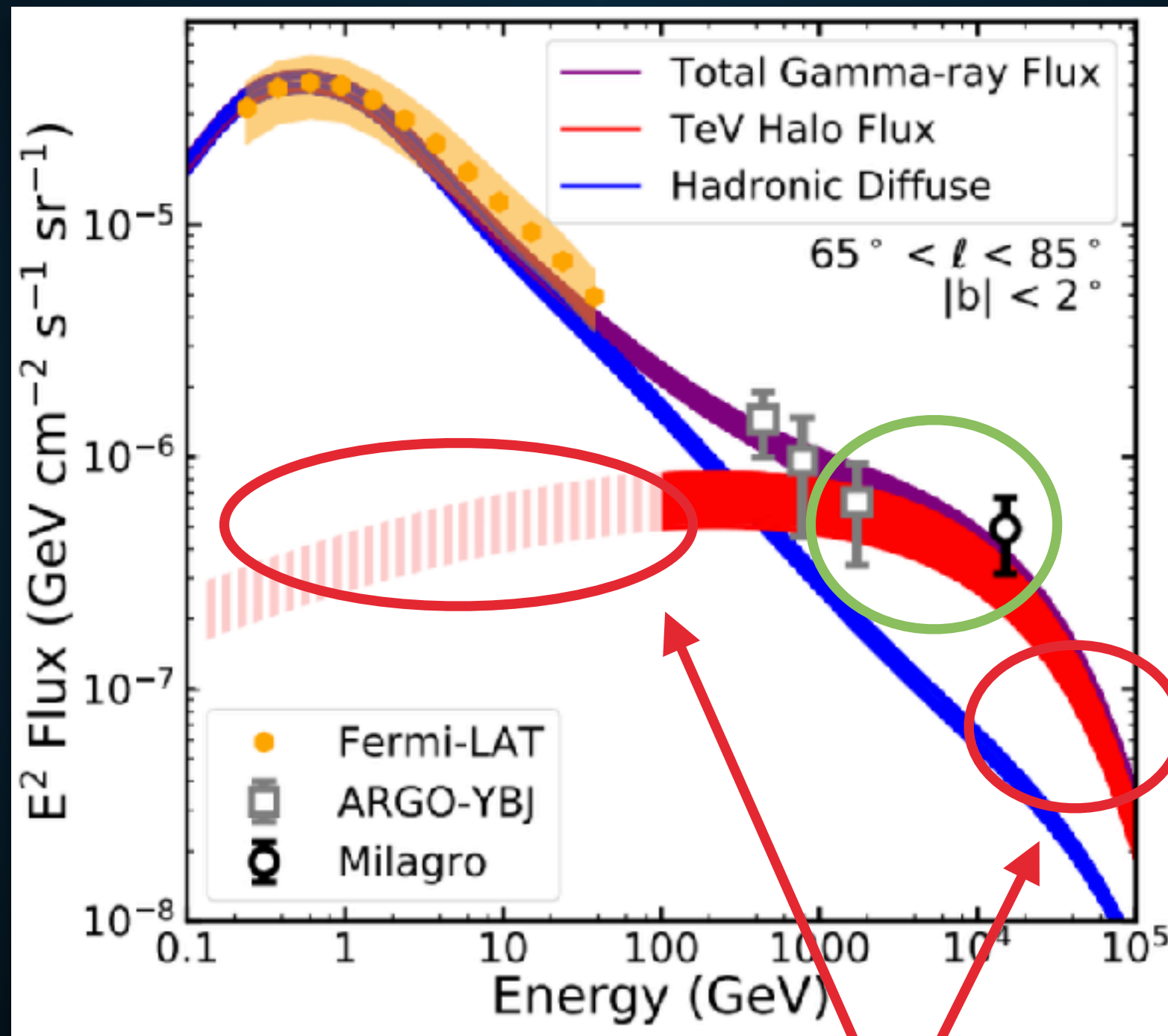
¹Department of Physics and Astronomy, West Virginia University, Morgantown, WV, 26506 USA

²Centre for Astrophysics, School of Physics and Astronomy, The University of Manchester, Manchester M13 9PL, UK

³Astronomy Observatory, PO Box 2, Green Bank, WV 24944, USA

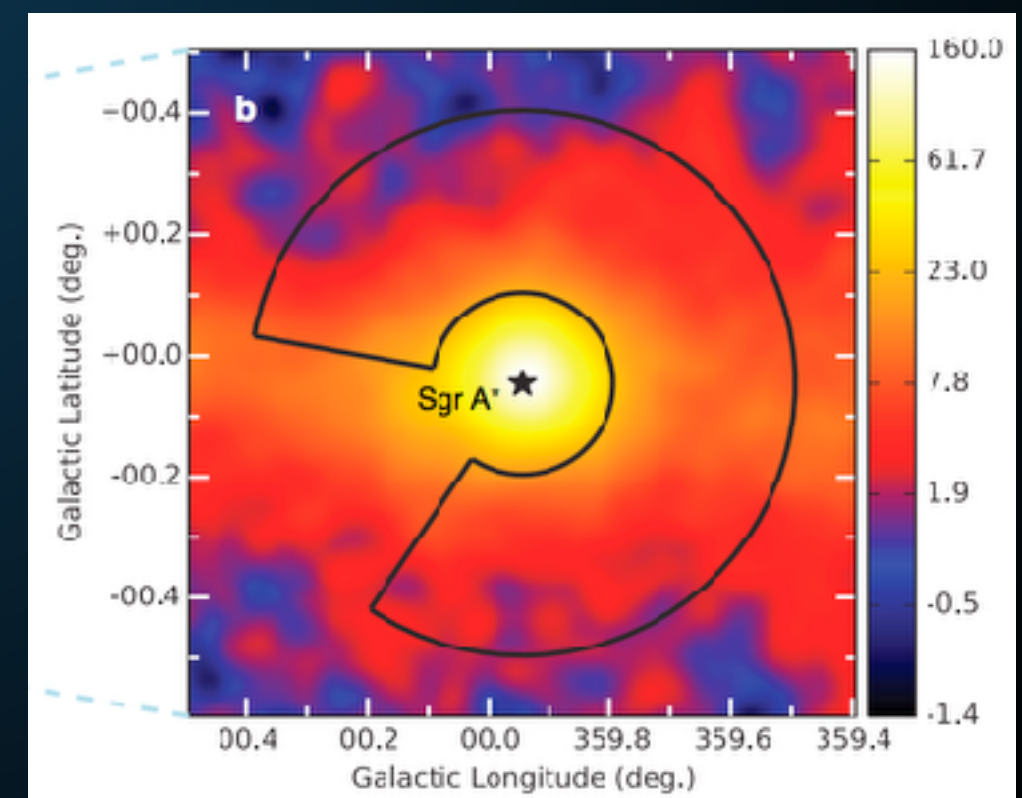
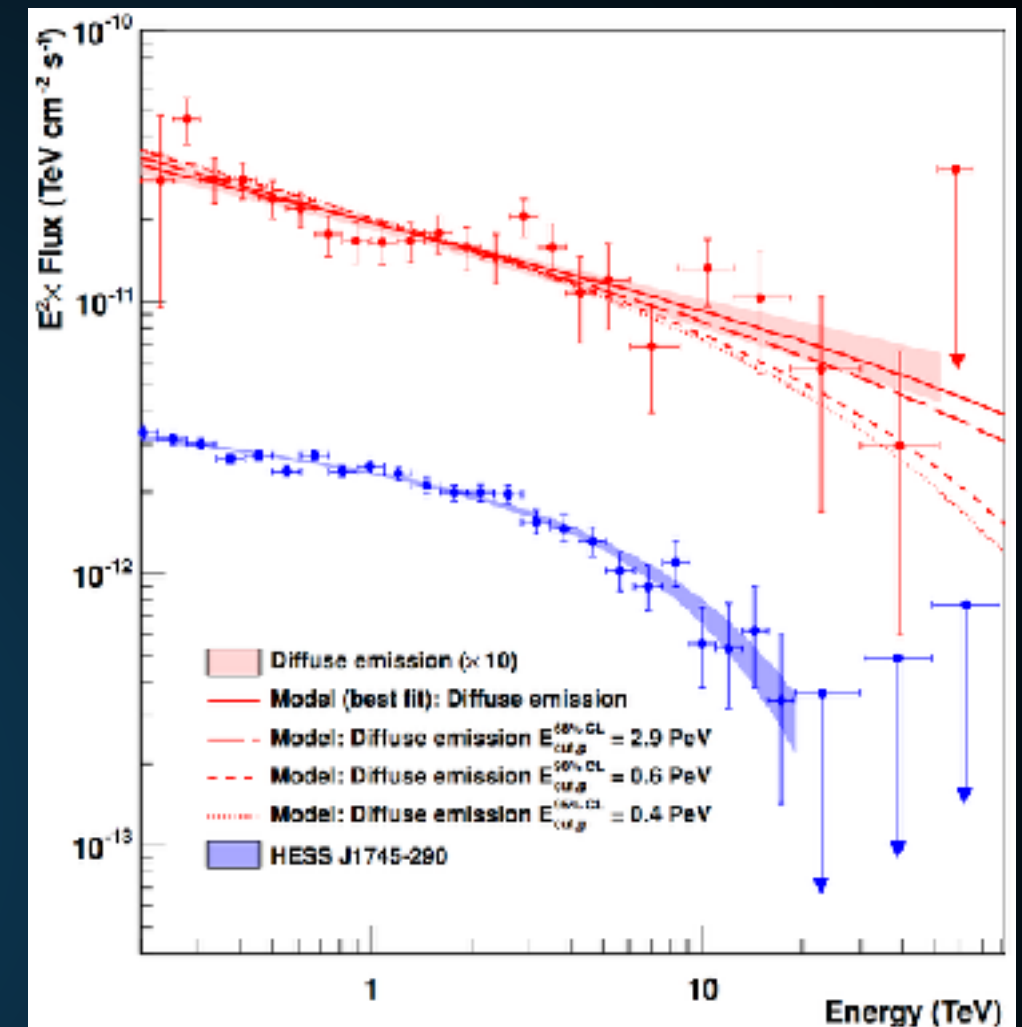
software package for the simulation of pulsar populations. The codebase is written in Python, which remain in their original language, and improving the simulation support.

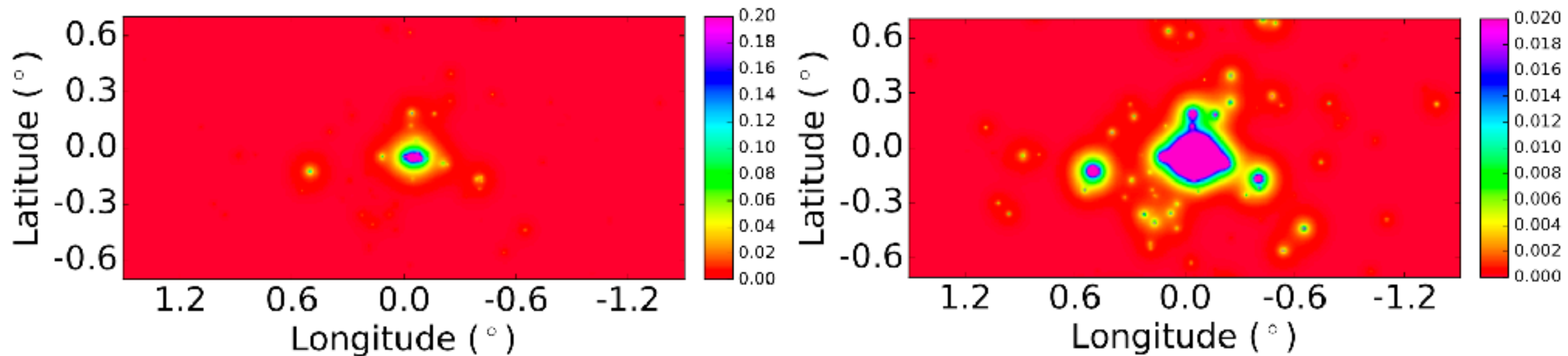
► TeV halos naturally explain the TeV excess!



spectral assumption!

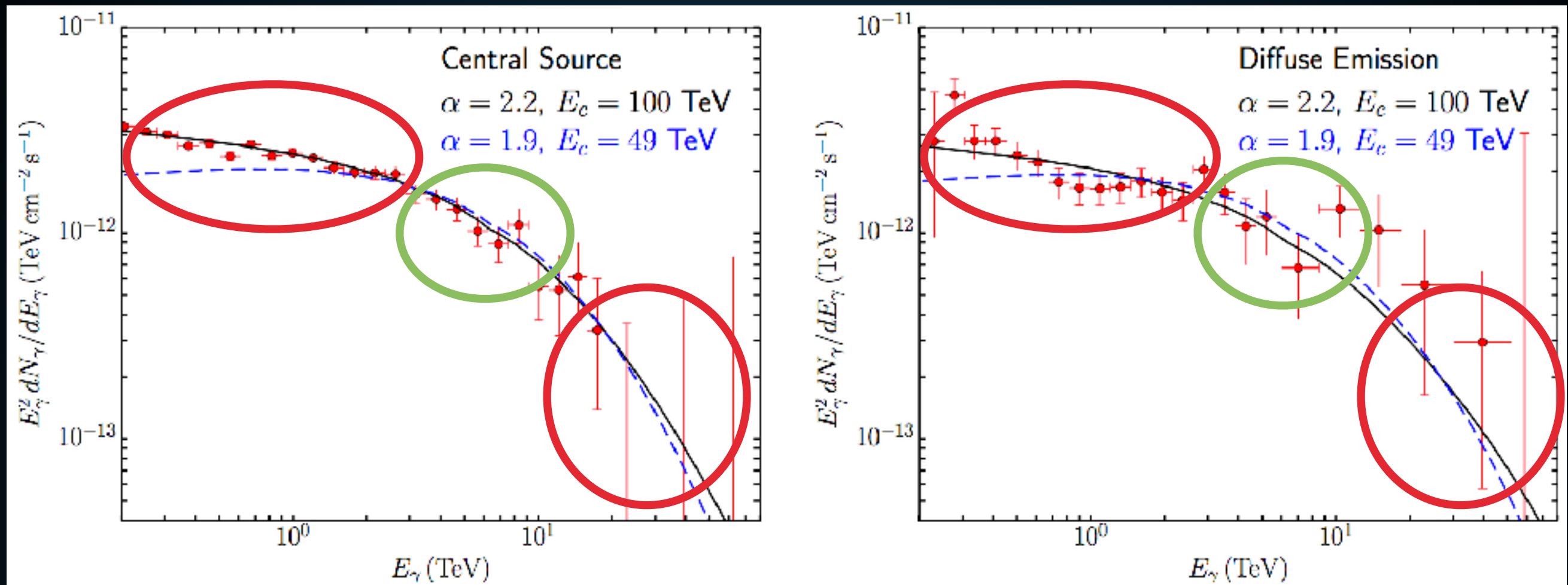
- ▶ HESS observations indicate diffuse ~ 50 TeV emission from the Galactic center
- ▶ If this emission is hadronic, it indicates PeV particle acceleration in the GC
- ▶ Spherical symmetry hints at Galactic Center source.





- ▶ **Significant star (pulsar) formation in the Galactic center**
- ▶ **Pulsars formed in the central parsec will be kicked into surrounding medium.**
- ▶ **Source of diffuse gamma-rays in the Galactic center.**

INTENSITY OF TEV HALO EMISSION IN GALACTIC CENTER



- ▶ **Assumptions: Standard values for the pulsar birthrate and kick velocity**
 - ▶ Birth rate between 100-750 pulsars/Myr
 - ▶ Pulsar kicks $\sim 400 \text{ km/s}$
- ▶ We reproduce the intensity and morphology of the HESS emission.

Implication II:

Most TeV gamma-ray sources are TeV halos.

TEV HALOS ARE A GENERIC FEATURE OF PULSARS

- ▶ **5 / 39 sources in the 2HWC catalog are correlated with bright, middle-aged (100 – 400 kyr) pulsars.**

| 2HWC Name | ATNF Name | Distance (kpc) | Angular Separation | Projected Separation | Expected Flux ($\times 10^{-15}$) | Actual Flux ($\times 10^{-15}$) | Flux Ratio | Expected Extension | Actual Extension | Age (kyr) | Chance Overlap |
|-----------|------------|----------------|--------------------|----------------------|-------------------------------------|-----------------------------------|------------|--------------------|------------------|-----------|----------------|
| J0700+143 | B0656+14 | 0.29 | 0.18° | 0.91 pc | 43.0 | 23.0 | 1.87 | 2.0° | 1.73° | 111 | 0.0 |
| J0531+169 | J0633+1746 | 0.25 | 0.89° | 3.88 pc | 48.7 | 48.7 | 1.0 | 2.0° | 2.0° | 342 | 0.0 |
| J1912+099 | J1913+1011 | 4.61 | 0.34° | 27.36 pc | 13.0 | 36.6 | 0.36 | 0.11° | 0.7° | 169 | 0.30 |
| J2031+415 | J2032+4127 | 1.70 | 0.11° | 3.26 pc | 5.59 | 61.6 | 0.091 | 0.29° | 0.7° | 181 | 0.002 |
| J1831-098 | J1831-0952 | 3.68 | 0.04° | 2.57 pc | 7.70 | 95.8 | 0.080 | 0.14° | 0.9° | 128 | 0.006 |

- ▶ **12 others with young pulsars**

- ▶ **2.3 chance overlaps**
- ▶ **TeV emission may be contaminated by SNR**

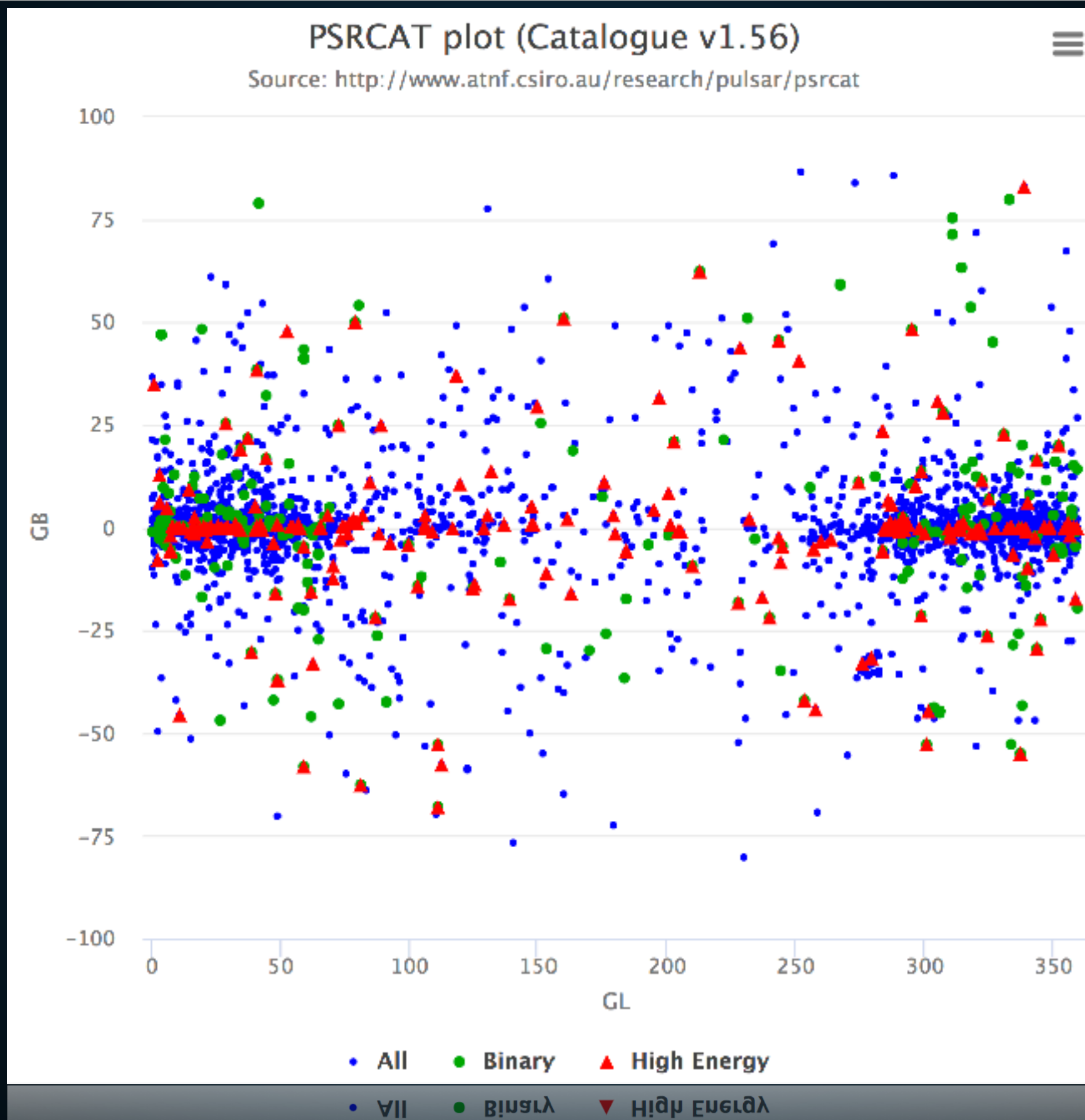
| 2HWC Name | ATNF Name | Distance (kpc) | Angular Separation | Projected Separation | Expected Flux ($\times 10^{-15}$) | Actual Flux ($\times 10^{-15}$) | Flux Ratio | Expected Extension | Actual Extension | Age (kyr) | Chance Overlap |
|-----------|------------|----------------|--------------------|----------------------|-------------------------------------|-----------------------------------|------------|--------------------|------------------|-----------|----------------|
| J1930+188 | J1930+1852 | 7.0 | 0.03° | 3.67 pc | 23.2 | 9.8 | 2.37 | 0.07° | 0.0° | 2.89 | 0.002 |
| J1814-173 | J1813-1749 | 4.7 | 0.54° | 44.30 pc | 243 | 152 | 1.60 | 0.11° | 1.0° | 5.6 | 0.61 |
| J2019+367 | J2021+3651 | 1.8 | 0.27° | 8.48 pc | 99.8 | 58.2 | 1.71 | 0.28° | 0.7° | 17.2 | 0.04 |
| J1928+177 | J1928+1746 | 4.34 | 0.03° | 2.27 pc | 8.08 | 10.0 | 0.81 | 0.11° | 0.0° | 82.6 | 0.002 |
| J1908+063 | J1907+0602 | 2.58 | 0.36° | 16.21 pc | 40.0 | 85.0 | 0.47 | 0.2° | 0.8° | 19.5 | 0.26 |
| J2020+403 | J2021+4026 | 2.15 | 0.18° | 6.75 pc | 2.48 | 18.5 | 0.134 | 0.23° | 0.0° | 77 | 0.01 |
| J1857+027 | J1856+0245 | 6.32 | 0.12° | 13.24 pc | 11.0 | 97.0 | 0.11 | 0.08° | 0.9° | 20.6 | 0.06 |
| J1825-134 | J1826-1334 | 3.61 | 0.20° | 12.66 pc | 20.5 | 249 | 0.082 | 0.14° | 0.9° | 21.4 | 0.14 |
| J1837-065 | J1838-0655 | 6.60 | 0.38° | 43.77 pc | 12.0 | 341 | 0.035 | 0.08° | 2.0° | 22.7 | 0.48 |
| J1837-065 | J1837-0604 | 4.78 | 0.50° | 41.71 pc | 8.3 | 341 | 0.024 | 0.10° | 2.0° | 33.8 | 0.68 |
| J2006+341 | J2004+3429 | 10.8 | 0.42° | 80.07 pc | 0.48 | 24.5 | 0.019 | 0.04° | 0.9° | 18.5 | 0.08 |

STEP I: TEV HALOS ARE A GENERIC FEATURE OF PULSARS

| ATNF Name | Dec. (°) | Distance (kpc) | Age (kyr) | Spindown Lum. (erg s^{-1}) | Spindown Flux ($\text{erg s}^{-1} \text{kpc}^{-2}$) | 2HWC |
|------------|----------|----------------|-----------|---------------------------------------|---|----------------|
| J0633+1746 | 17.77 | 0.25 | 342 | $3.2\text{e}34$ | $4.1\text{e}34$ | 2HWC J0631+169 |
| B0656+14 | 14.23 | 0.29 | 111 | $3.8\text{e}34$ | $3.6\text{e}34$ | 2HWC J0700+143 |
| B1951+32 | 32.87 | 3.00 | 107 | $3.7\text{e}36$ | $3.3\text{e}34$ | — |
| J1740+1000 | 10.00 | 1.23 | 114 | $2.3\text{e}35$ | $1.2\text{e}34$ | — |
| J1913+1011 | 10.18 | 4.61 | 169 | $2.9\text{e}36$ | $1.1\text{e}34$ | 2HWC J1912+099 |
| J1831-0952 | -9.86 | 3.68 | 128 | $1.1\text{e}36$ | $6.4\text{e}33$ | 2HWC J1831-098 |
| J2032+4127 | 41.45 | 1.70 | 181 | $1.7\text{e}35$ | $4.7\text{e}33$ | 2HWC J2031+415 |
| B1822-09 | -9.58 | 0.30 | 232 | $4.6\text{e}33$ | $4.1\text{e}33$ | — |
| B1830-08 | -8.45 | 4.50 | 147 | $5.8\text{e}35$ | $2.3\text{e}33$ | — |
| J1913+0904 | 9.07 | 3.00 | 147 | $1.6\text{e}35$ | $1.4\text{e}33$ | — |
| B0540+23 | 23.48 | 1.56 | 253 | $4.1\text{e}34$ | $1.4\text{e}33$ | — |

- ▶ Can produce a ranked list of the 57 ATNF pulsars in the HAWC field of view – these are the brightest 11.
- ▶ 10 year HAWC observations should detect:
 - ▶ TeV halos from a dozen middle-aged ATNF pulsars.
 - ▶ TeV halos from ~40 additional young pulsars.

WHY DO WE CARE?



- ▶ **Tauris and Manchester (1998) calculated the beaming angle from a population of young and middle-aged pulsars.**

$$f = \left[1.1 \left(\log_{10} \left(\frac{\tau}{100 \text{ Myr}} \right) \right)^2 + 15 \right] \%$$

- ▶ **This varies between 15-30%.**
- ▶ **1/f pulsars are unseen in radio surveys.**

MISSING TEV HALOS

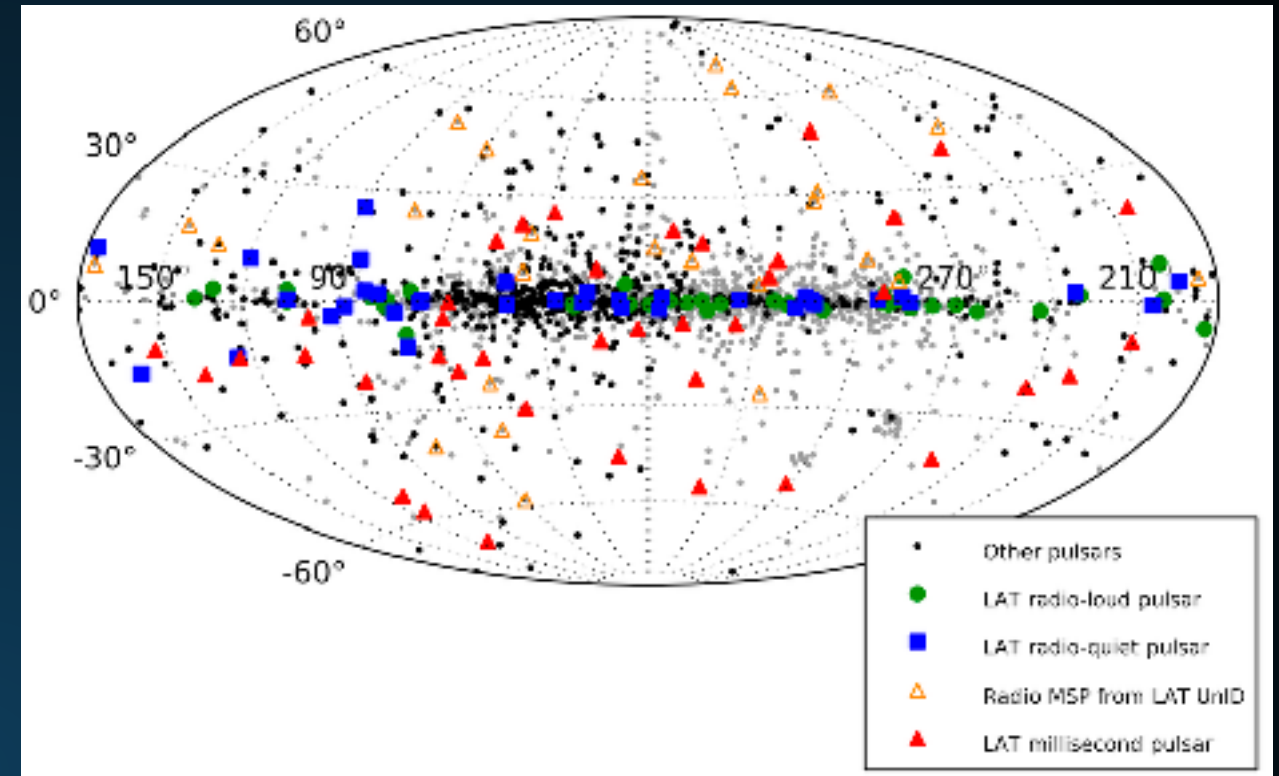
| 2HWC Name | ATNF Name | Distance (kpc) | Angular Separation | Projected Separation | Expected Flux ($\times 10^{-15}$) | Actual Flux ($\times 10^{-15}$) | Flux Ratio | Expected Extension | Actual Extension | Age (kyr) | Chance Overlap |
|-----------|------------|----------------|--------------------|----------------------|-------------------------------------|-----------------------------------|------------|--------------------|------------------|-----------|----------------|
| J0700+143 | B0656+14 | 0.29 | 0.18° | 0.91 pc | 43.0 | 23.0 | 1.87 | 2.0° | 1.73° | 111 | 0.0 |
| J0631+169 | J0633+1746 | 0.25 | 0.89° | 3.88 pc | 48.7 | 48.7 | 1.0 | 2.0° | 2.0° | 342 | 0.0 |
| J1912+099 | J1913+1011 | 4.61 | 0.34° | 27.36 pc | 13.0 | 36.6 | 0.36 | 0.11° | 0.7° | 169 | 0.30 |
| J2031+415 | J2032+4127 | 1.70 | 0.11° | 3.26 pc | 5.59 | 61.6 | 0.091 | 0.29° | 0.7° | 181 | 0.002 |
| J1831-098 | J1831-0952 | 3.68 | 0.04° | 2.57 pc | 7.70 | 95.8 | 0.080 | 0.14° | 0.9° | 128 | 0.006 |

| 2HWC Name | ATNF Name | Distance (kpc) | Angular Separation | Projected Separation | Expected Flux ($\times 10^{-15}$) | Actual Flux ($\times 10^{-15}$) | Flux Ratio | Expected Extension | Actual Extension | Age (kyr) | Chance Overlap |
|-----------|------------|----------------|--------------------|----------------------|-------------------------------------|-----------------------------------|------------|--------------------|------------------|-----------|----------------|
| J1930+188 | J1930+1852 | 7.0 | 0.03° | 3.67 pc | 23.2 | 9.8 | 2.37 | 0.07° | 0.0° | 2.89 | 0.002 |
| J1814-173 | J1813-1749 | 4.7 | 0.54° | 44.30 pc | 243 | 152 | 1.60 | 0.11° | 1.0° | 5.6 | 0.61 |
| J2019+367 | J2021+3651 | 1.8 | 0.27° | 8.48 pc | 99.8 | 58.2 | 1.71 | 0.28° | 0.7° | 17.2 | 0.04 |
| J1928+177 | J1928+1746 | 4.34 | 0.03° | 2.27 pc | 8.08 | 10.0 | 0.81 | 0.11° | 0.0° | 82.6 | 0.002 |
| J1908+063 | J1907+0602 | 2.58 | 0.36° | 16.21 pc | 40.0 | 85.0 | 0.47 | 0.2° | 0.8° | 19.5 | 0.26 |
| J2020+403 | J2021+4026 | 2.15 | 0.18° | 6.75 pc | 2.48 | 18.5 | 0.134 | 0.23° | 0.0° | 77 | 0.01 |
| J1857+027 | J1856+0245 | 6.32 | 0.12° | 13.24 pc | 11.0 | 97.0 | 0.11 | 0.08° | 0.9° | 20.6 | 0.06 |
| J1825-134 | J1826-1334 | 3.61 | 0.20° | 12.66 pc | 20.5 | 249 | 0.082 | 0.14° | 0.9° | 21.4 | 0.14 |
| J1837-065 | J1838-0655 | 6.60 | 0.38° | 43.77 pc | 12.0 | 341 | 0.035 | 0.08° | 2.0° | 22.7 | 0.48 |
| J1837-065 | J1837-0604 | 4.78 | 0.50° | 41.71 pc | 8.3 | 341 | 0.024 | 0.10° | 2.0° | 33.8 | 0.68 |
| J2006+341 | J2004+3429 | 10.8 | 0.42° | 80.07 pc | 0.48 | 24.5 | 0.019 | 0.04° | 0.9° | 18.5 | 0.08 |

- ▶ Correcting for the beaming fraction implies that 56_{-11}^{+15} TeV halos are currently observed by HAWC.
- ▶ However, only 39 total HAWC sources.
- ▶ Chance overlaps, SNR contamination must be taken into account.

FERMI-LAT DETECTIONS

- ▶ **Fermi-LAT has detected 54 new pulsars**
- ▶ **35 younger than 100 kyr**
- ▶ **Only 5/35 in HAWC field of view**



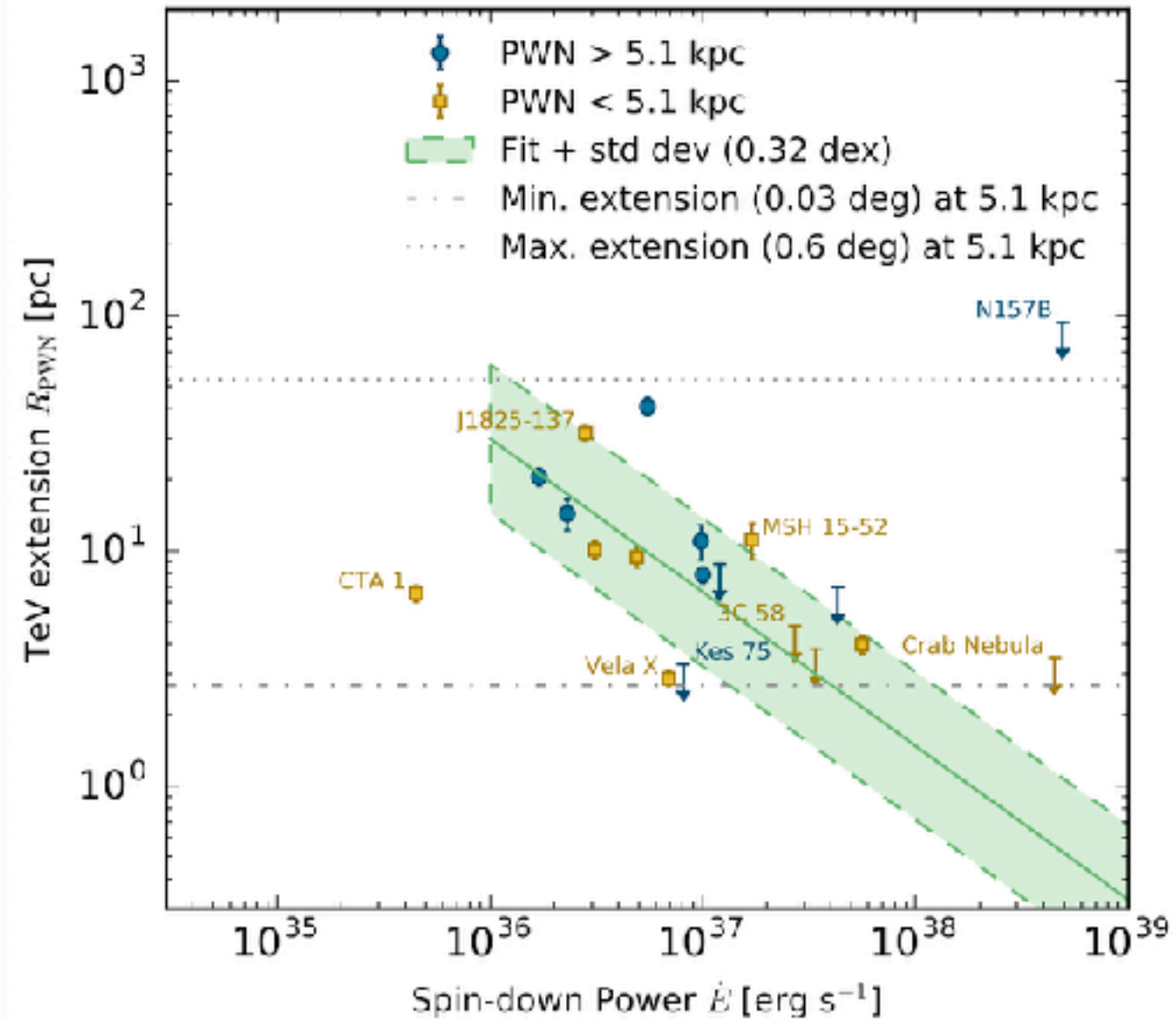
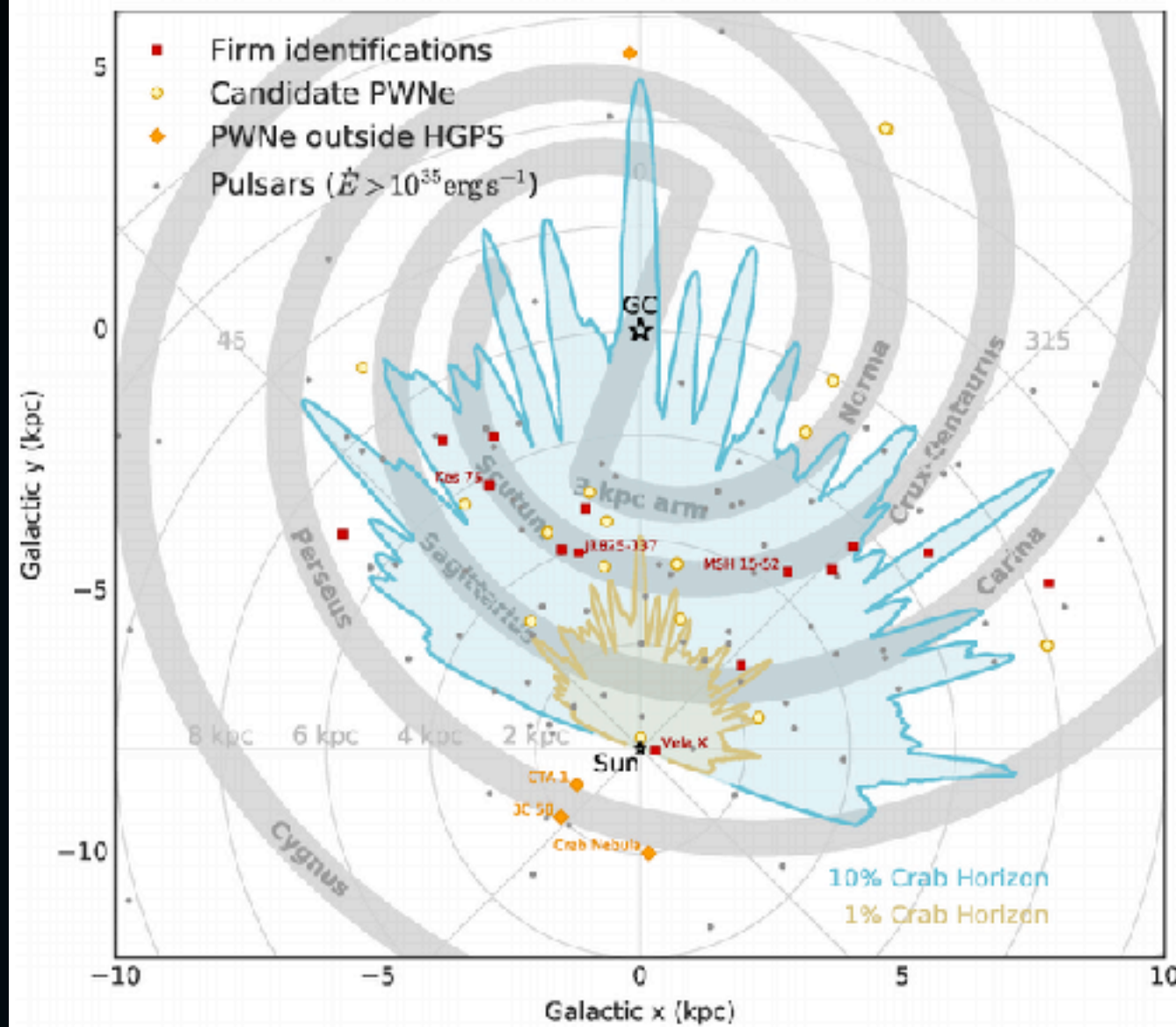
- ▶ **Fermi-LAT has detected only ~5 of these 37 systems.**

X-RAY PWN DETECTIONS

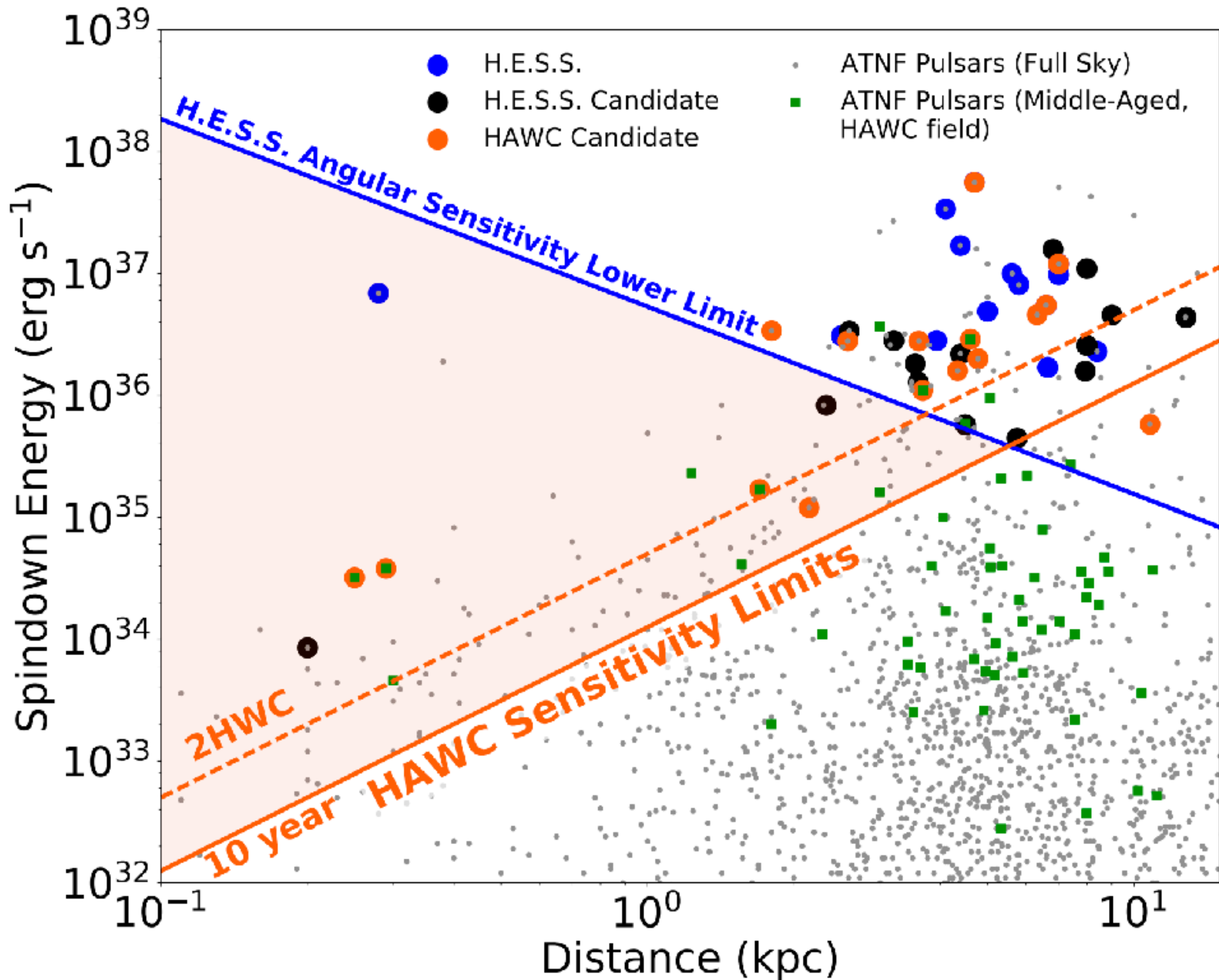
| PWNe With No Detected Pulsar | | | | | | |
|------------------------------|------------------------|---|---|---|---|-------|
| Gname | other name(s) | R | X | O | G | |
| G0.13-0.11 | | | | | ? | notes |
| G0.9+0.1 | | | | | N | notes |
| G7.4-2.0 | GeV J1809-2327, Tazzie | | | | Y | notes |
| G16.7+0.1 | | | | | N | notes |
| G18.5-0.4 | GeV J1825-1310, Fcl | | | | Y | notes |
| G20.0-0.2 | | | | | N | notes |
| G24.7+0.6 | | | | | N | notes |
| G27.8+0.6 | | | | | N | notes |
| G39.2-0.3 | 3C 396 | | | | Y | notes |
| G63.7+1.1 | | | | | N | notes |
| G74.9+1.2 | CTB 87 | | | | Y | notes |
| G119.5+10.2 | CTA 1 | | | | Y | notes |
| G189.1+3.0 | IC 443 | | | | ? | notes |
| G279.8-35.8 | B0453-685 | | | | N | notes |
| G291.0-0.1 | MSH 11-62 | | | | Y | notes |
| G293.8+0.6 | | | | | N | notes |
| G313.3+0.1 | Rabbit | | | | Y | notes |
| G318.9+0.4 | | | | | N | notes |
| G322.5-0.1 | | | | | N | notes |
| G326.3-1.8 | MSH 15-56 | | | | N | notes |
| G327.1-1.1 | | | | | N | notes |
| G328.4+0.2 | MSH 15-57 | | | | N | notes |
| G358.6-17.2 | RX J1856.5-3754 | N | N | | N | notes |
| G359.89-0.08 | | | | | Y | notes |

- ▶ X-Ray PWN have detected only ~6 of these 37 systems.

HESS/VERITAS DETECTION OF TEV HALOS



- ▶ Targeted ACTs are sensitive to the flux from TeV halos.
- ▶ ACTs are not sensitive to sources extended $>0.5^\circ$.
- ▶ Large parameter space available only to HAWC.

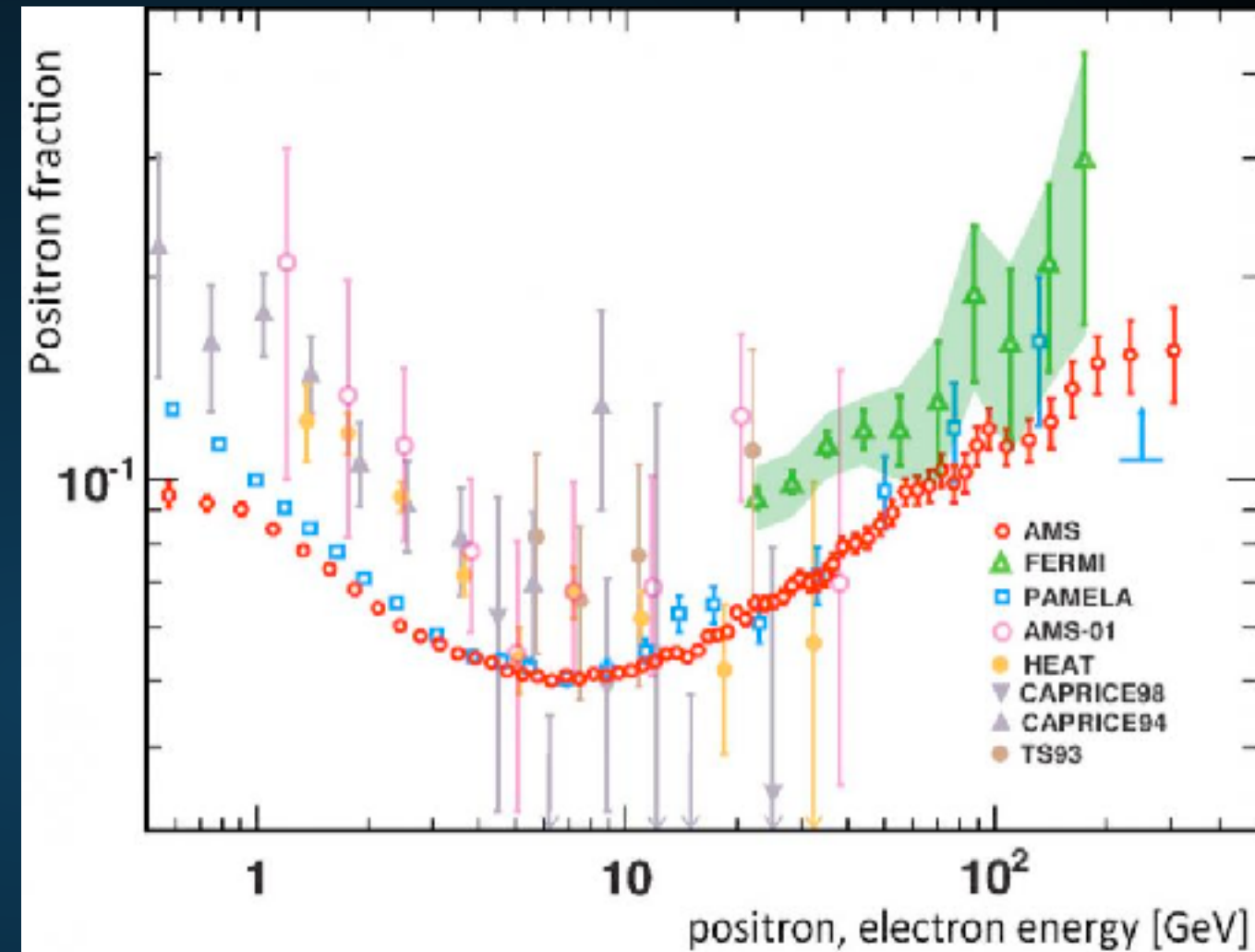


**Implication III: The positron excess is
due to pulsar activity**

THE POSITRON EXCESS

- ▶ Rising fraction of cosmic-ray positrons at energies above 10 GeV

- ▶ Standard Cosmic-Ray Secondary Production predicts the positron fraction falls as $\sim E^{-0.4}$.



- ▶ Indicates a new primary source of high energy e^+e^- pairs.

ENERGY LOSSES ARE DOMINATED BY THE ISM

- ▶ It is not energetically possible for Geminga to produce the magnetic field or ISRF that these electrons interact with.

$$\begin{aligned} U &= \frac{1}{8\pi} B^2 = \frac{(10 \mu\text{G})^2}{8\pi} \\ &= 4 \times 10^{-12} \frac{\text{erg}}{\text{cm}^3} \\ \int_0^{10 \text{ pc}} U dV &= 5 \times 10^{47} \text{ erg} \\ \hookrightarrow \text{Magnetic Flux} &\approx 5 \times 10^{38} \frac{\text{erg}}{\text{s}} \end{aligned}$$

$$\begin{aligned} \text{ISRF} &= 1 \frac{\text{eV}}{\text{cm}^3} \\ \int \text{ISRF} dV &= 8 \times 10^{47} \text{ erg} \\ \hookrightarrow \text{Flux} &= 8 \times 10^{38} \frac{\text{erg}}{\text{s}} \end{aligned}$$

- ▶ We can use typical ISM values ($5 \mu\text{G}$; 1 eV cm^{-3}) to characterize interactions.
- ▶ Nearly equal energy to synchrotron and ICS.

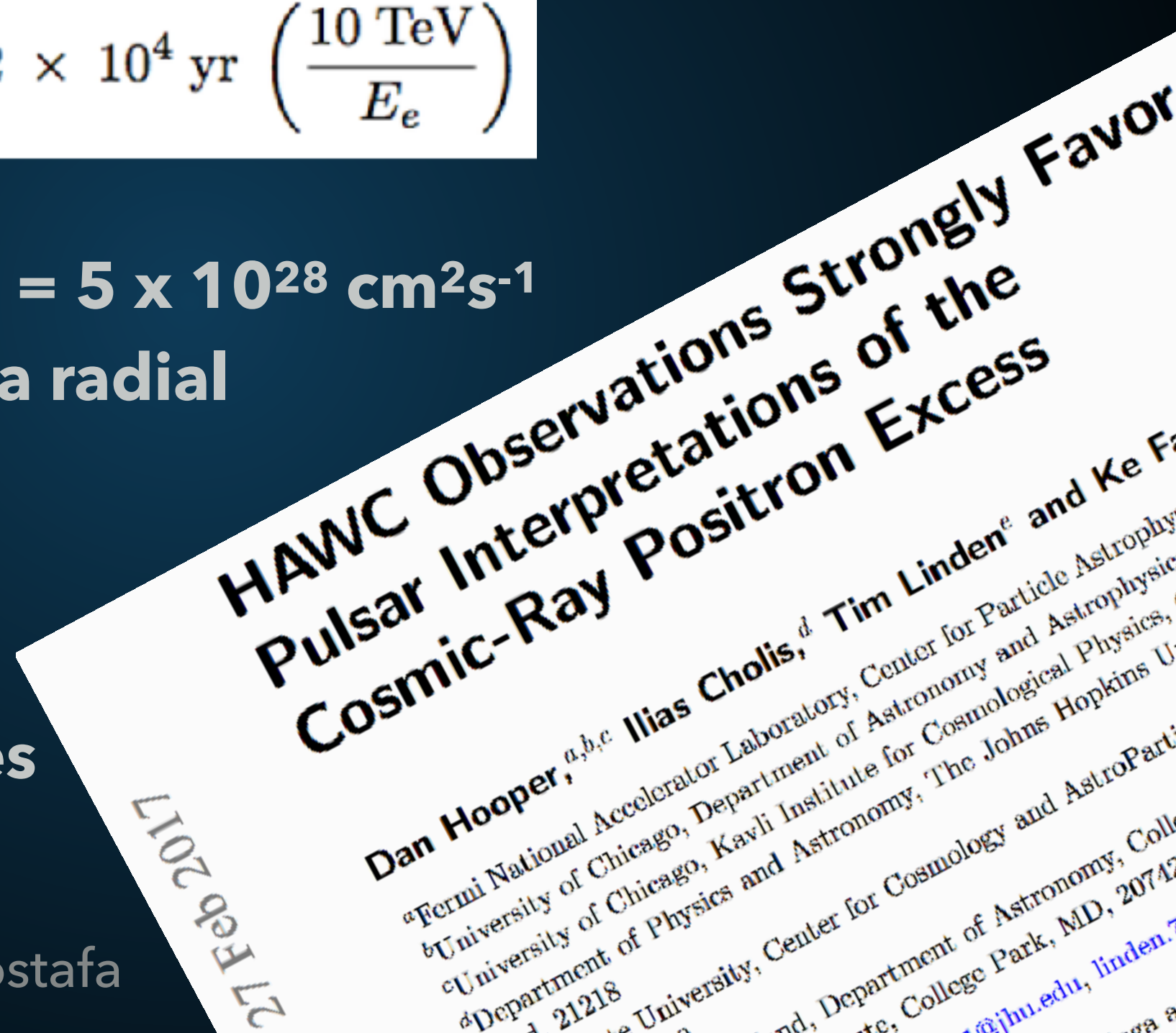
- ▶ The energy loss timescale in the ISM ($5 \mu\text{G}$; 1 eV cm^{-3}) is approximately:

$$\tau_{\text{loss}} \approx 2 \times 10^4 \text{ yr} \left(\frac{10 \text{ TeV}}{E_e} \right)$$

- ▶ For ISM Diffusion ($D_0 = 5 \times 10^{28} \text{ cm}^2 \text{ s}^{-1}$ $\delta=0.33$), this implies a radial extent of $\sim 250 \text{ pc}$.

- ▶ 10 pc extent indicates $D_0 \sim 7 \times 10^{25} \text{ cm}^2 \text{ s}^{-1}$

see also the talk by Miguel Mostafa



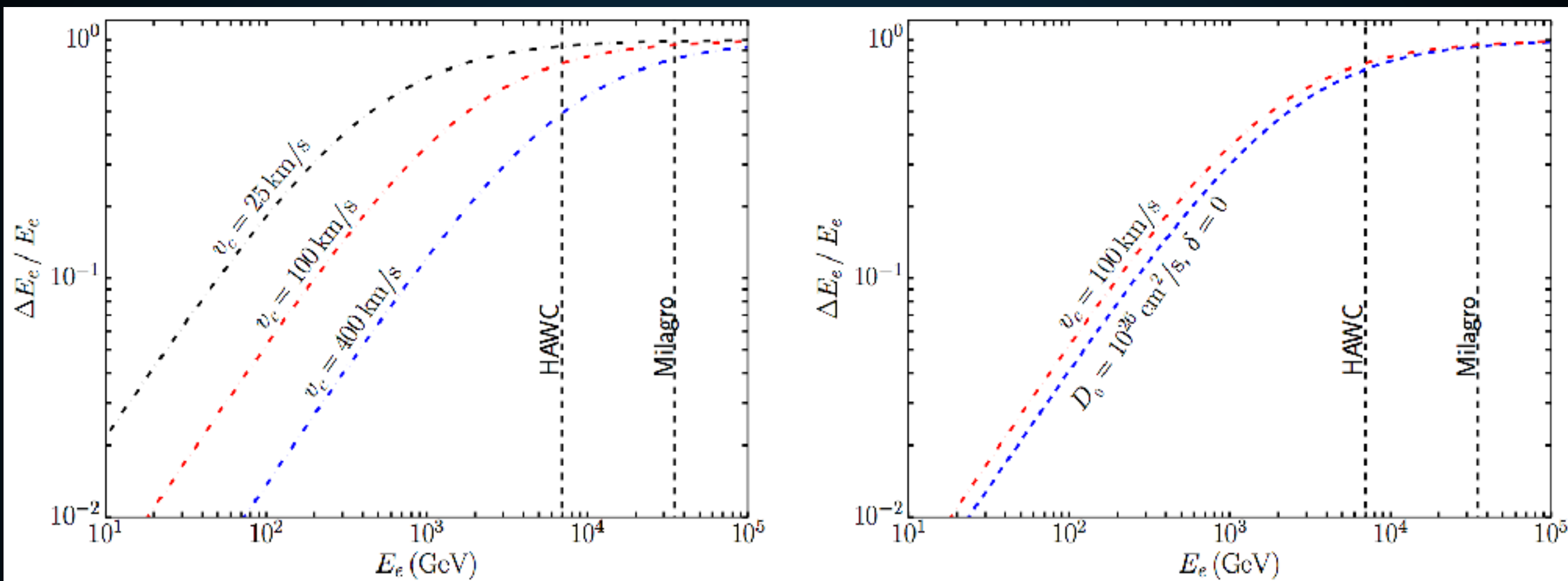
COSMIC-RAY DIFFUSION IS STANDARD

$$\tau_{\text{Diff}} \propto \frac{L^2}{D_0 E^\delta} \quad \tau_{\text{loss}} \propto E^{-1}$$
$$\left(\frac{\Delta E}{E} \right) \sim \frac{\tau_{\text{Diff}}}{\tau_{\text{loss}}} \propto E^{1-\delta}$$

- ▶ In general, low-energy electrons travel farther before losing their energy.
- ▶ How much bigger can the region of inhibited diffusion be?
- ▶ Low-energy electrons should escape!

WHAT ABOUT THE LOW-ENERGY ELECTRONS?

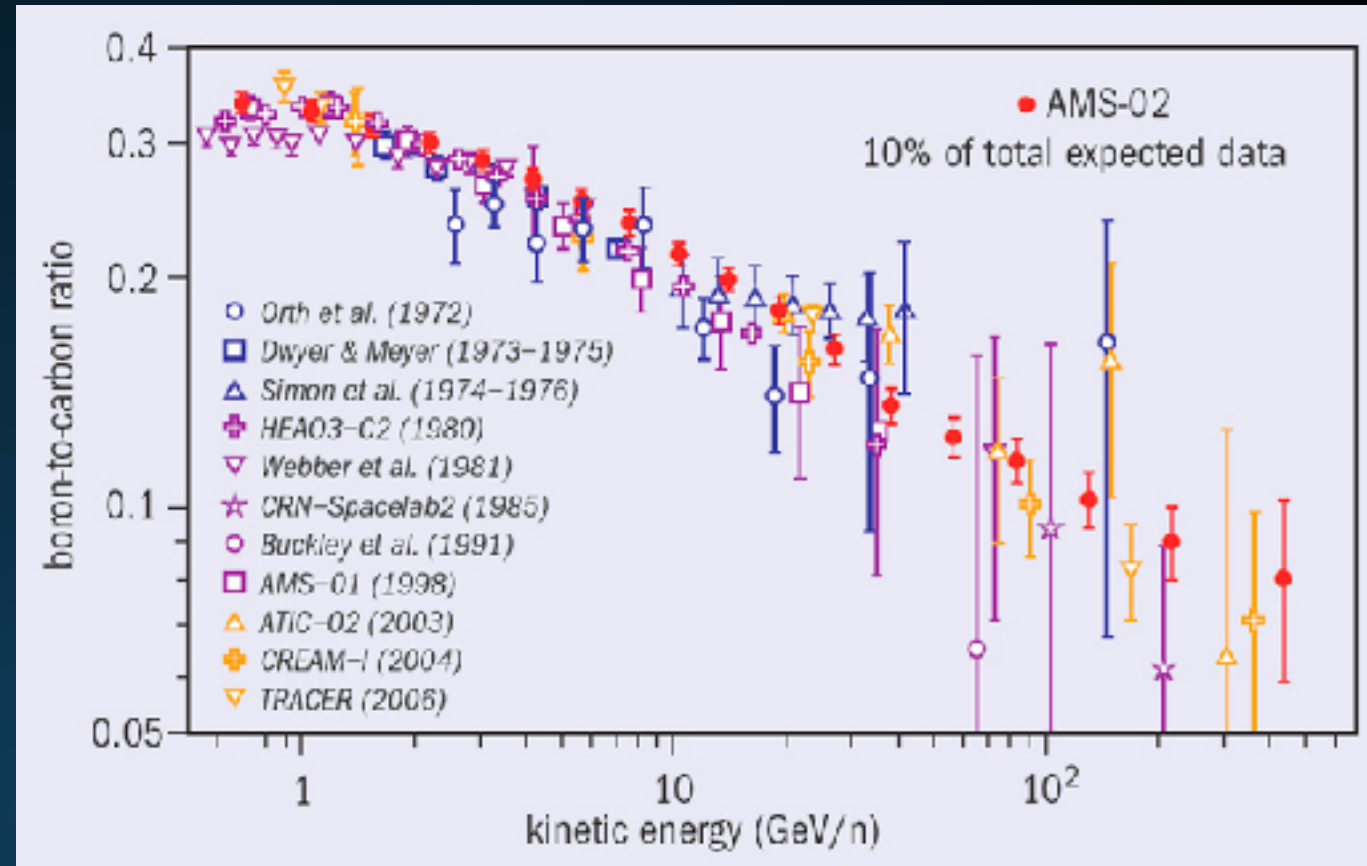
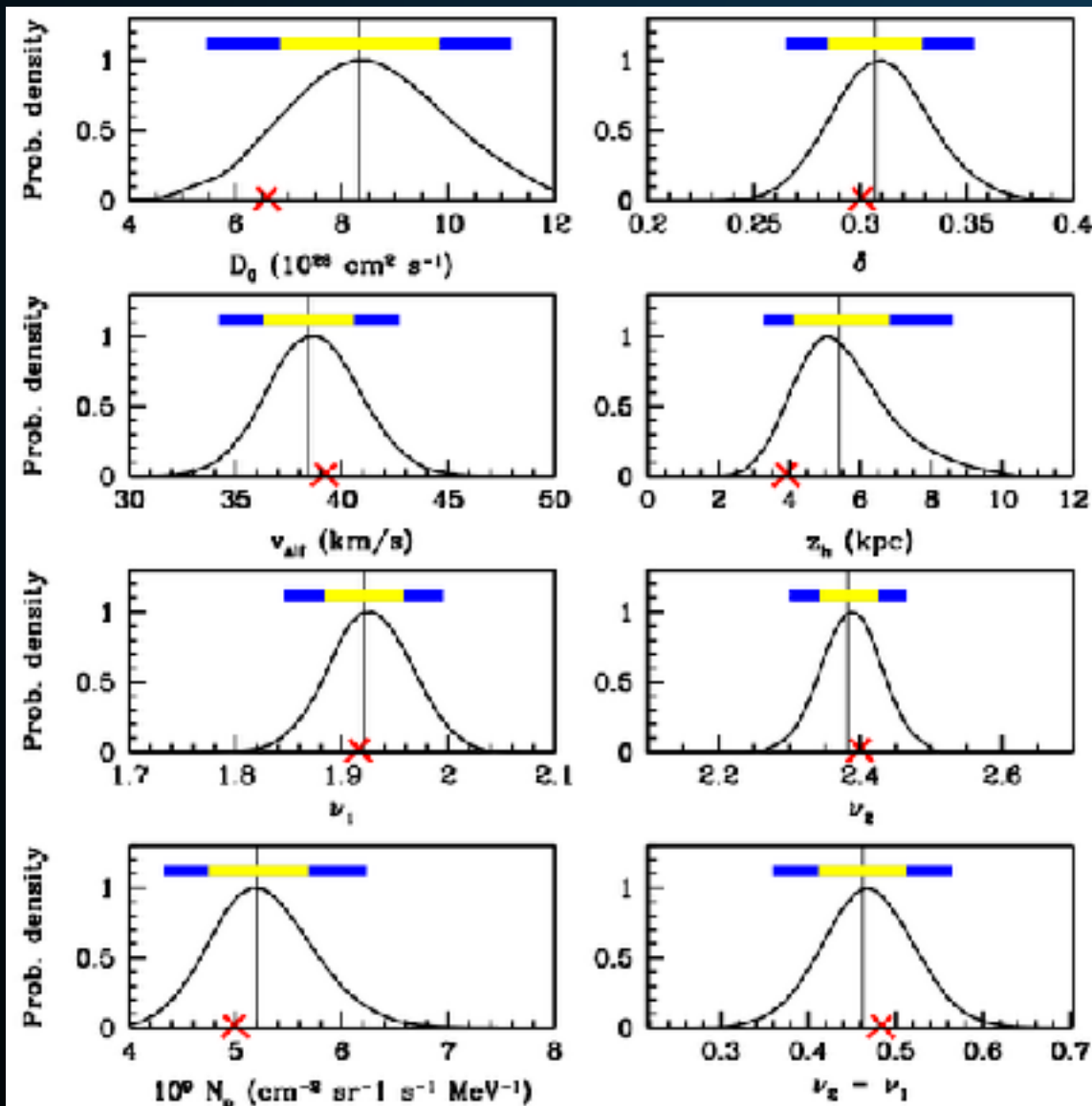
Fraction of energy lost before Electrons Travel a constant distance



- ▶ Low-energy electrons lose energy slower, must travel farther.
- ▶ This is true in both convective case (shown here) as well as most diffusive (e.g. Kolmogorov, Kraichnian) scenarios.
- ▶ Where do these electrons go?

EFFECT OF TEV HALOS ON ISM PROPAGATION

- Multiple cosmic-ray observations indicate that the average diffusion constant is $\sim 5 \times 10^{28} \text{ cm}^2 \text{ s}^{-1}$



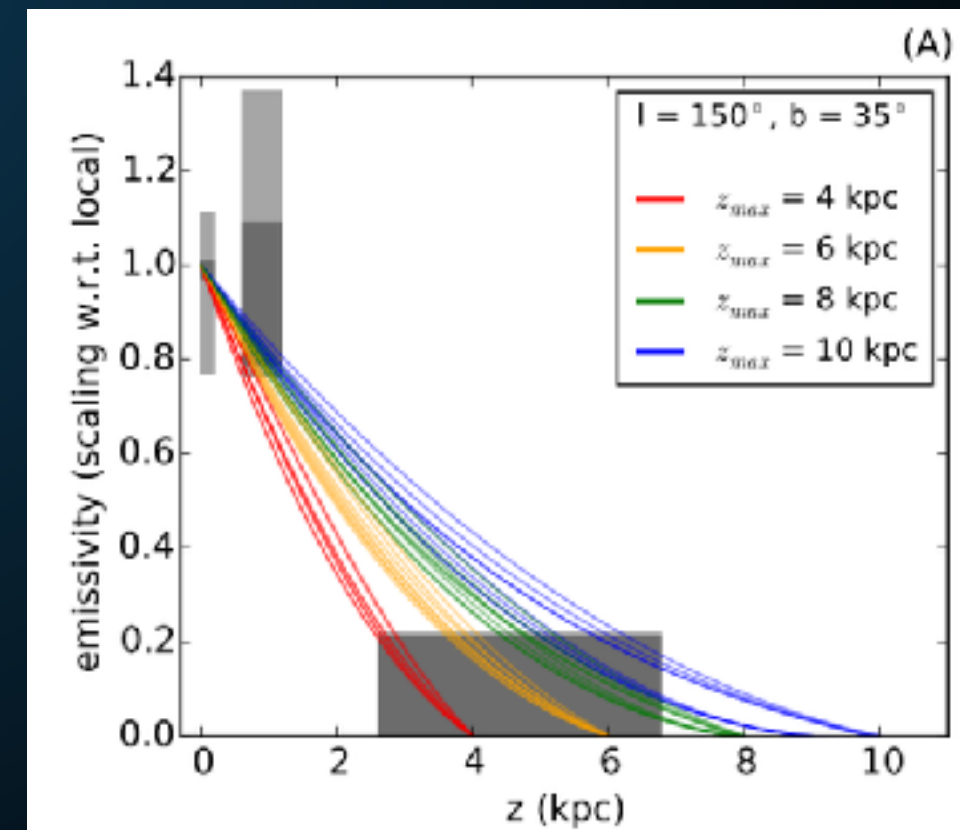
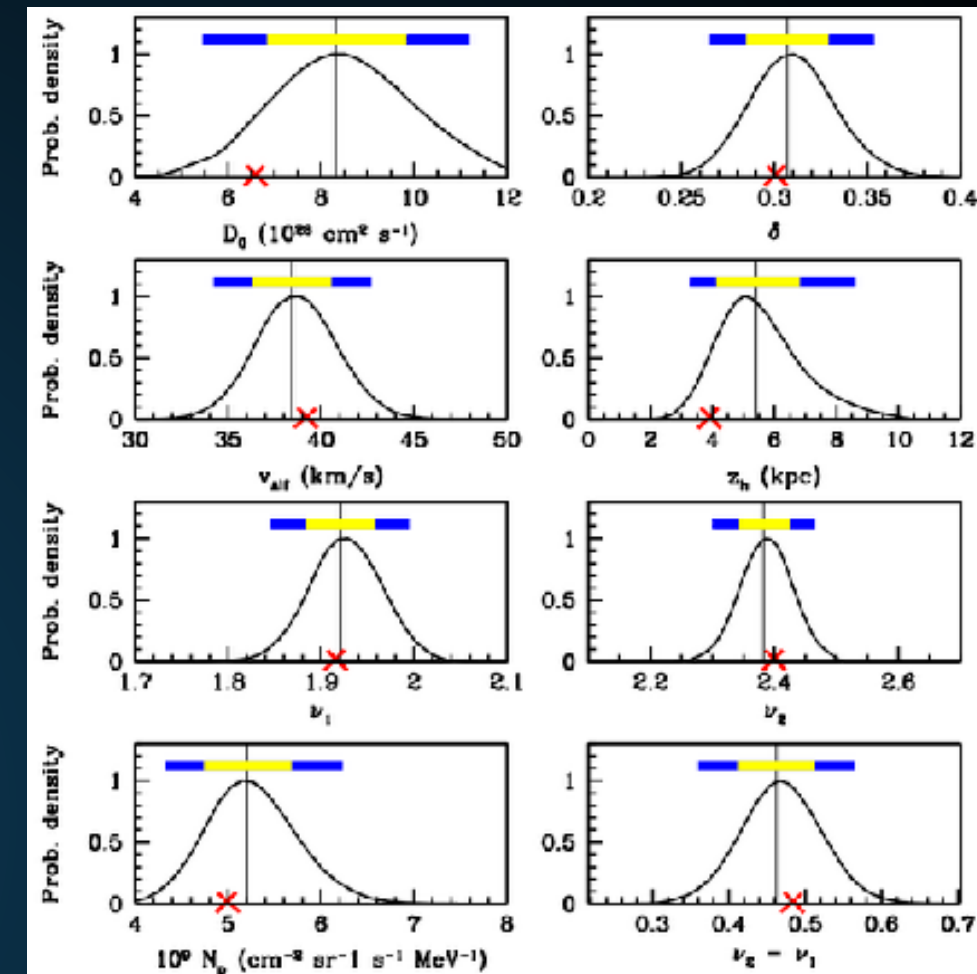
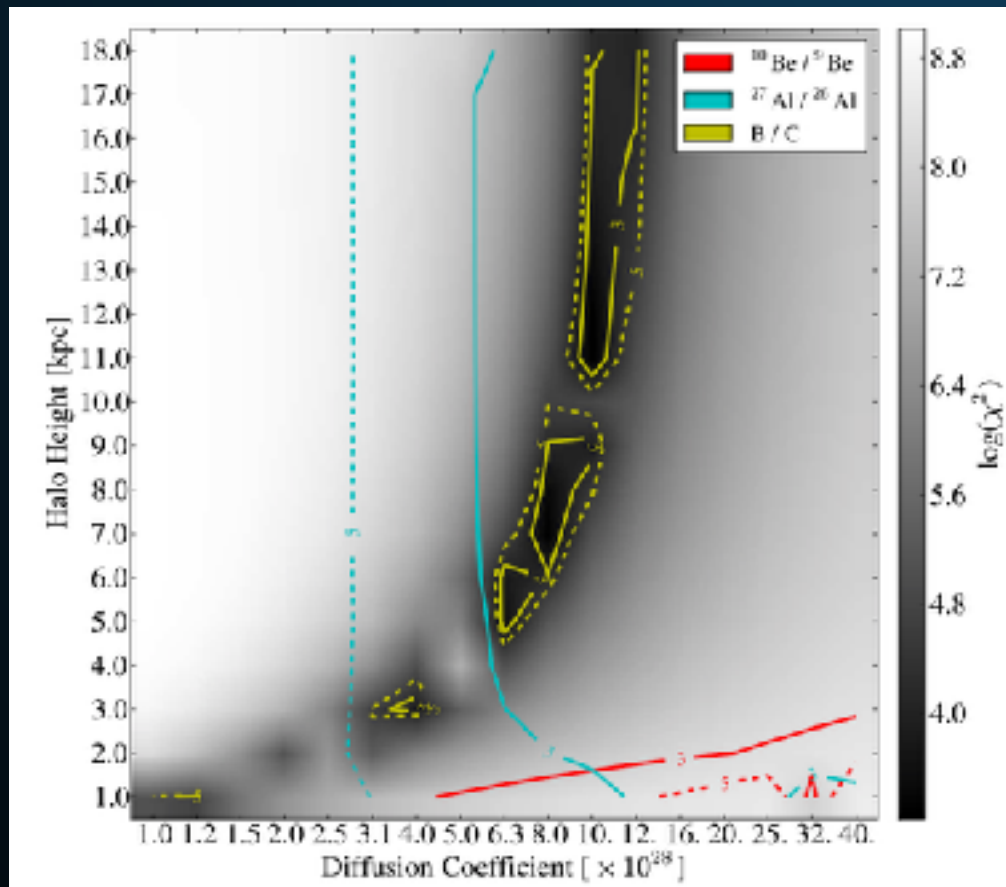
- Assume that diffusion reverts back to the standard case outside the TeV halo.
- Primary difference between our results and those from HAWC.

CAN THE DIFFUSION CONSTANT BETWEEN GEMINGA AND US BE LOW?

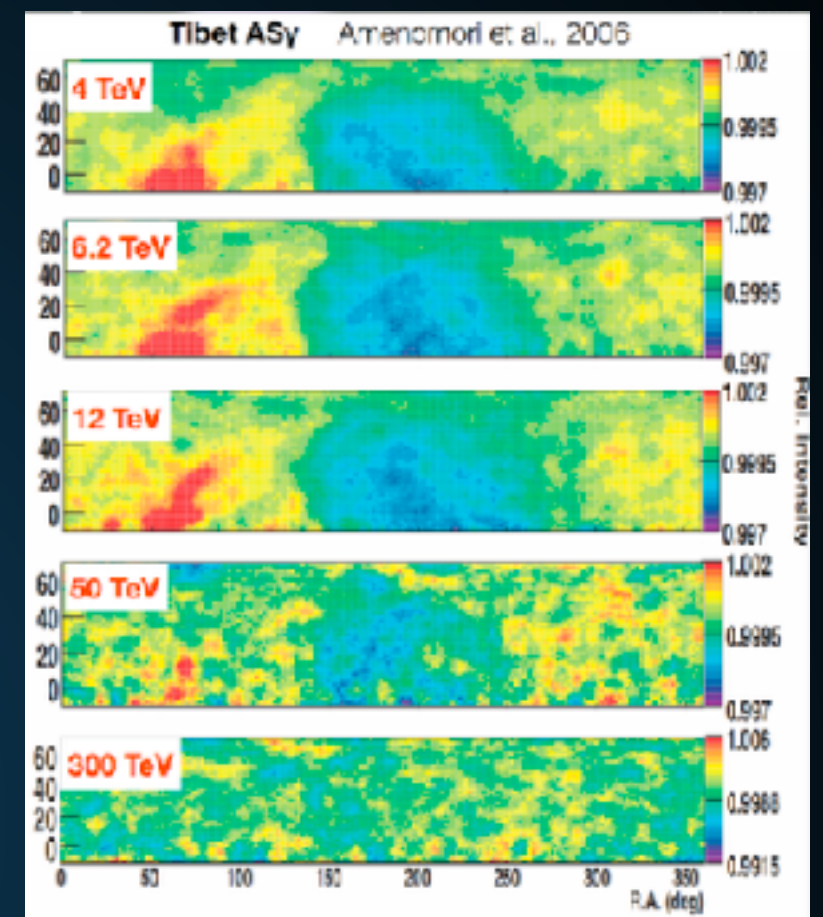
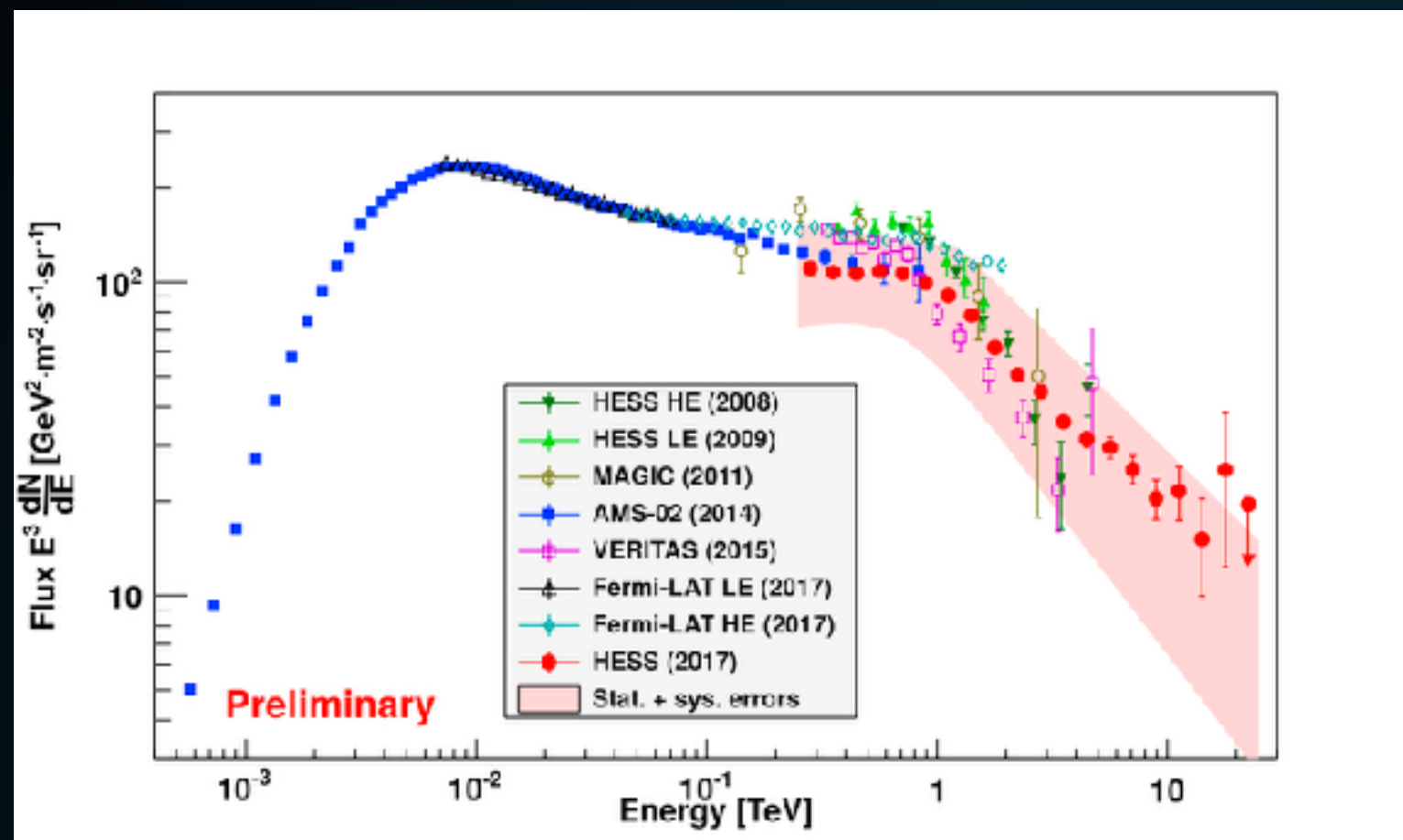


SCENARIO 1: THE MILKY WAY DIFFUSION CONSTANT IS LOW

- ▶ Cosmic-Ray primary to secondary ratios tell us about:
 - ▶ The average grammage encountered by cosmic-rays before they escape the galaxy (e.g. B/C)
 - ▶ The average time cosmic-rays are confined in the galaxy ($^{10}\text{Be}/^9\text{Be}$).



CAN THE LOCAL DIFFUSION CONSTANT BE LOW?



► If the local diffusion constant is low, we still run into problems.

► 1.) Where do 10 TeV electrons come from?

► 2.) Why are cosmic-rays isotropic?

$$\tau_{\text{loss}} \approx 2 \times 10^4 \text{ yr} \left(\frac{10 \text{ TeV}}{E_e} \right)$$

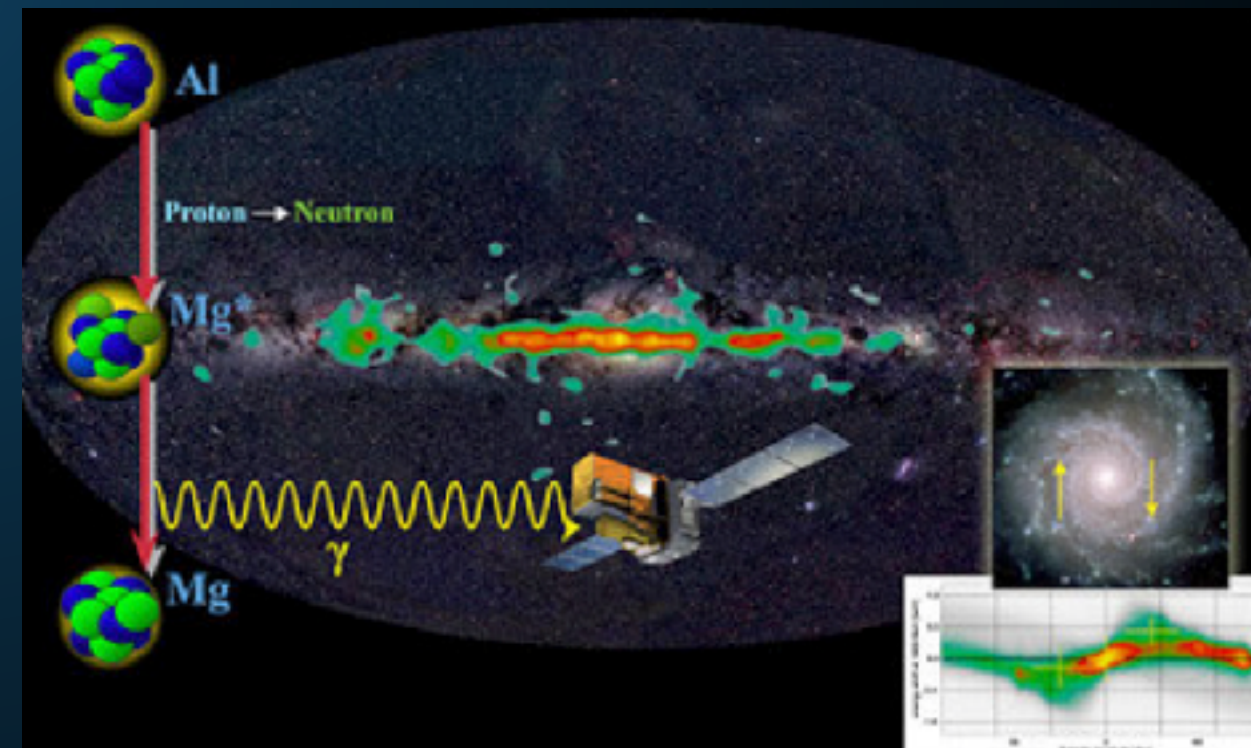
► $D_0 \sim 7 \times 10^{25} \text{ cm}^2 \text{ s}^{-1}$

$$L = \sqrt{6tD_0E^{0.33}} \approx 30 \text{ pc}$$

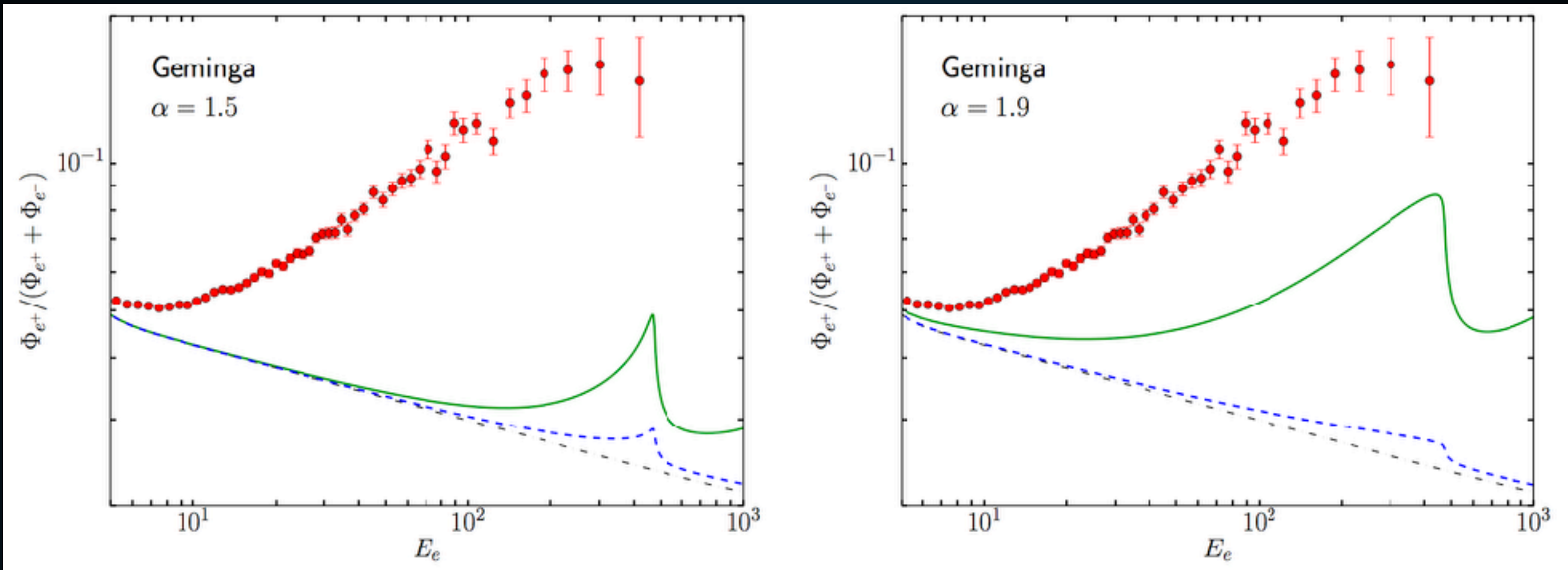
GEMINGA ISN'T SPECIAL

$$f \sim \frac{N_{\text{region}} \times \frac{4\pi}{3} r_{\text{region}}^3}{\pi R_{\text{MW}}^2 \times 2z_{\text{MW}}}$$
$$\sim 0.25 \times \left(\frac{r_{\text{region}}}{100 \text{ pc}} \right)^3 \left(\frac{\dot{N}_{\text{SN}}}{0.03 \text{ yr}^{-1}} \right) \left(\frac{\tau_{\text{region}}}{10^6 \text{ yr}} \right) \left(\frac{20 \text{ kpc}}{R_{\text{MW}}} \right)^2 \left(\frac{200 \text{ pc}}{z_{\text{MW}}} \right)$$

- ▶ Galactic Supernova rate is $\sim 0.02 \text{ yr}^{-1}$.
- ▶ If each supernova (and natal pulsar) produces a large diffusion region, the diffusion constant should be low everywhere.
- ▶ Only alternative is that a very unique event produced the local bubble.

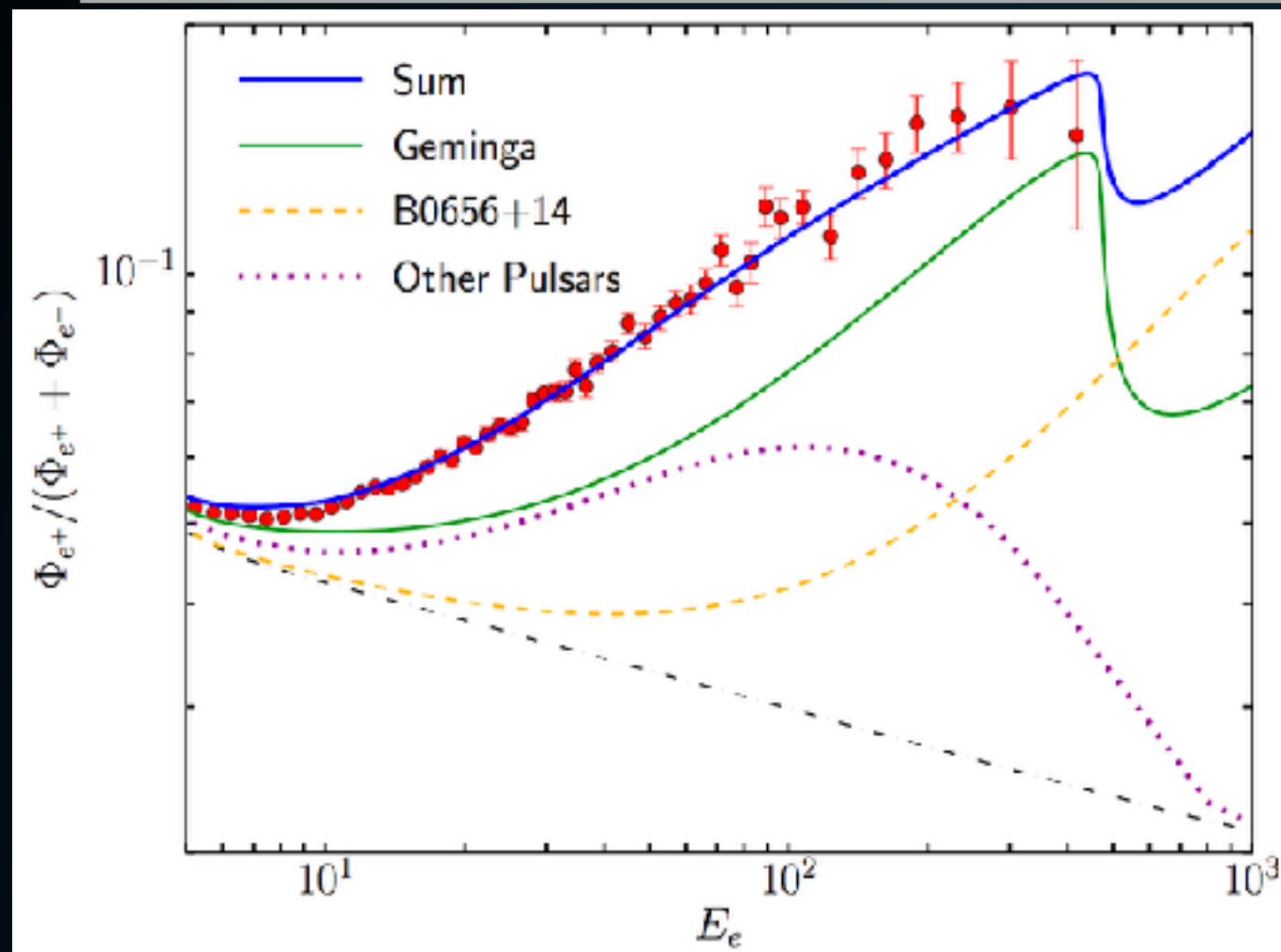


THE POSITRON FRACTION FROM TEV HALOS



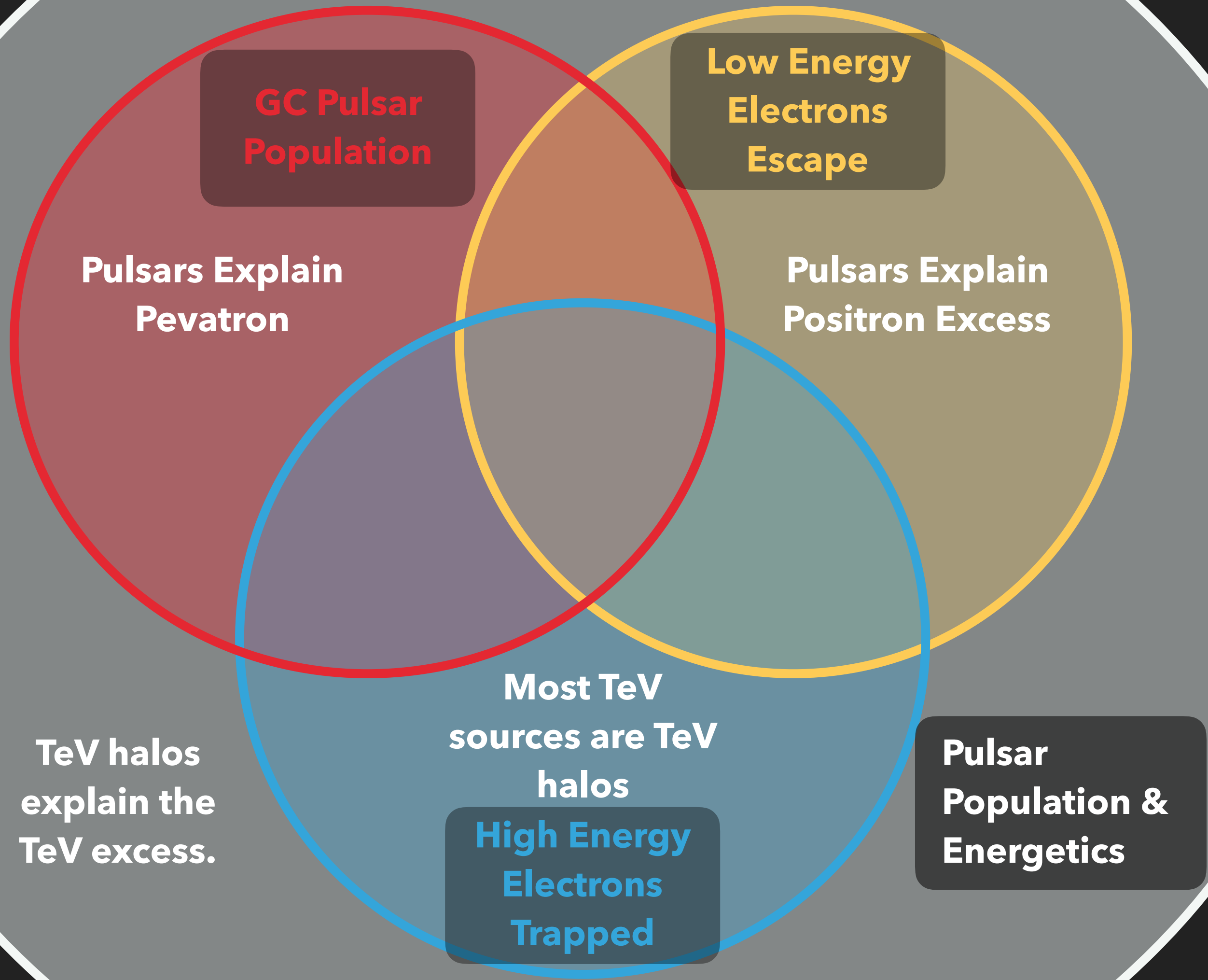
- ▶ **Geminga can individually produce nearly half of the positron excess.**
- ▶ **Models not fit to the data - this contribution must exist.**

THE POSITRON FRACTION FROM TEV HALOS



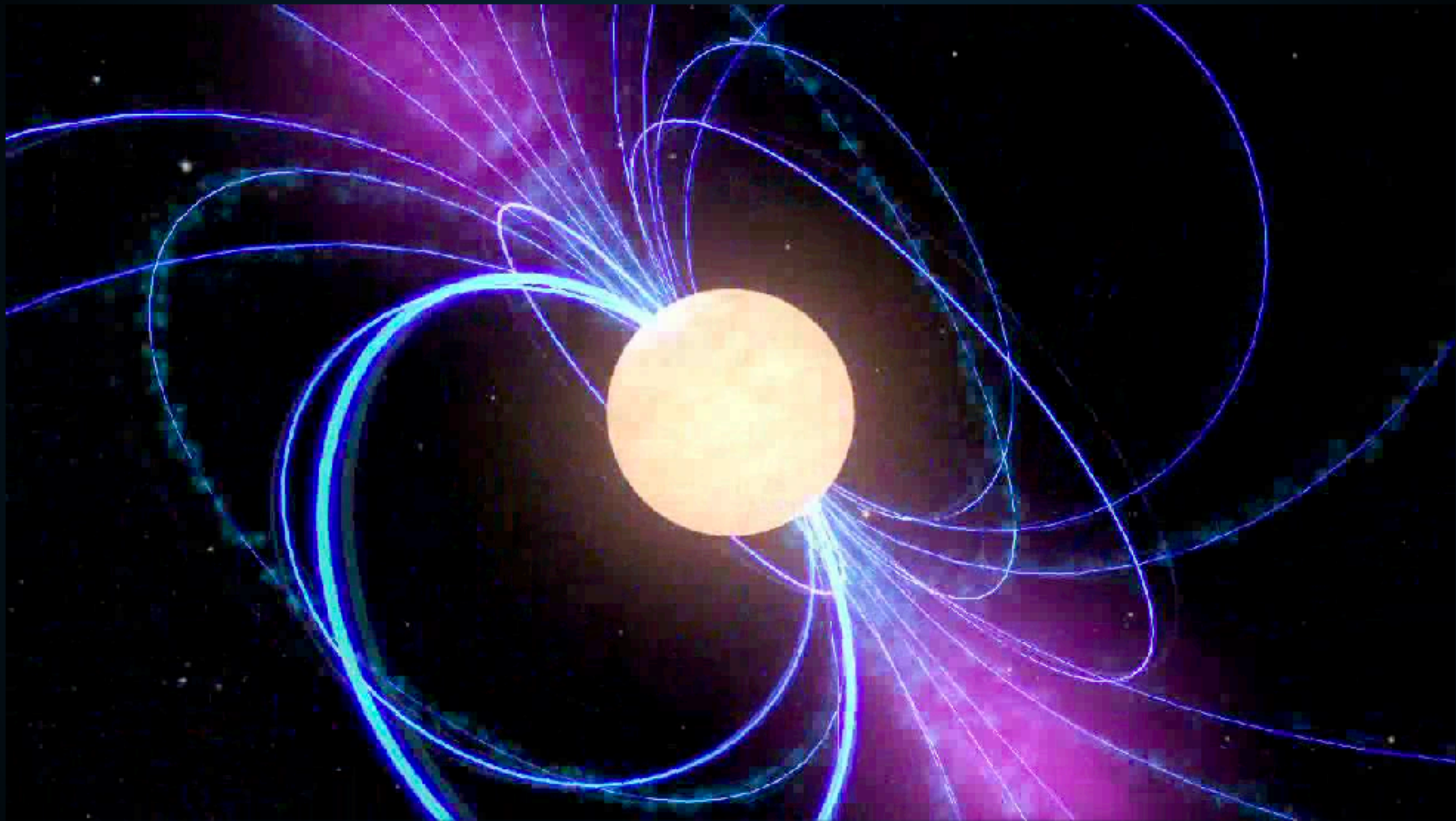
***Braking index slightly changed to fit model to data.**

- ▶ **Total Contribution from:**
 - ▶ **Geminga**
 - ▶ **Monogem**
 - ▶ **Average of other young pulsars**
- ▶ **Reasonable models can be exactly fit to the excess.**



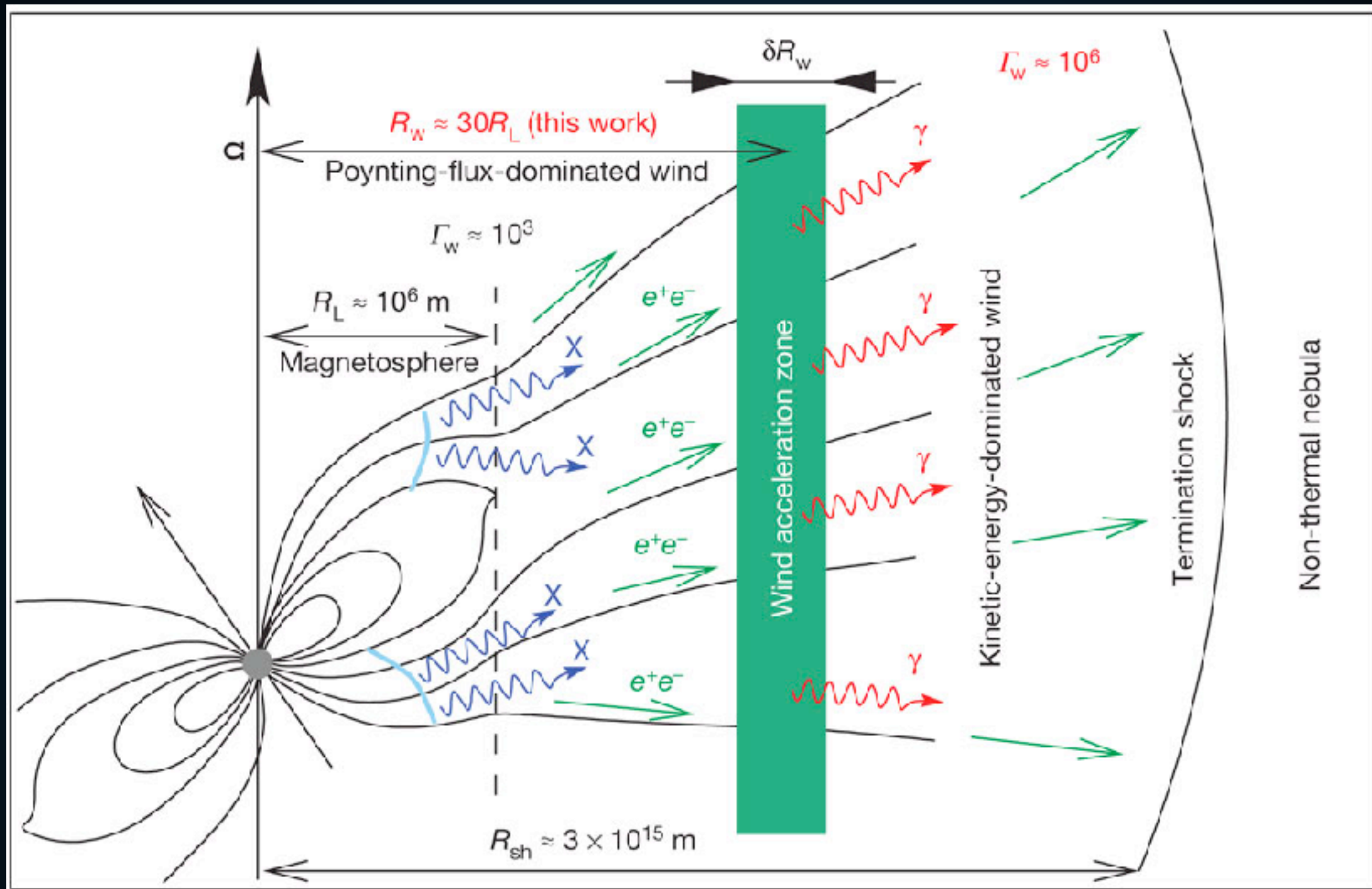
A Simple Model for TeV Halos

PULSARS AS ASTROPHYSICAL ACCELERATORS



- ▶ **Rotational Kinetic Energy of the neutron star is the ultimate power source of all emission in this problem.**

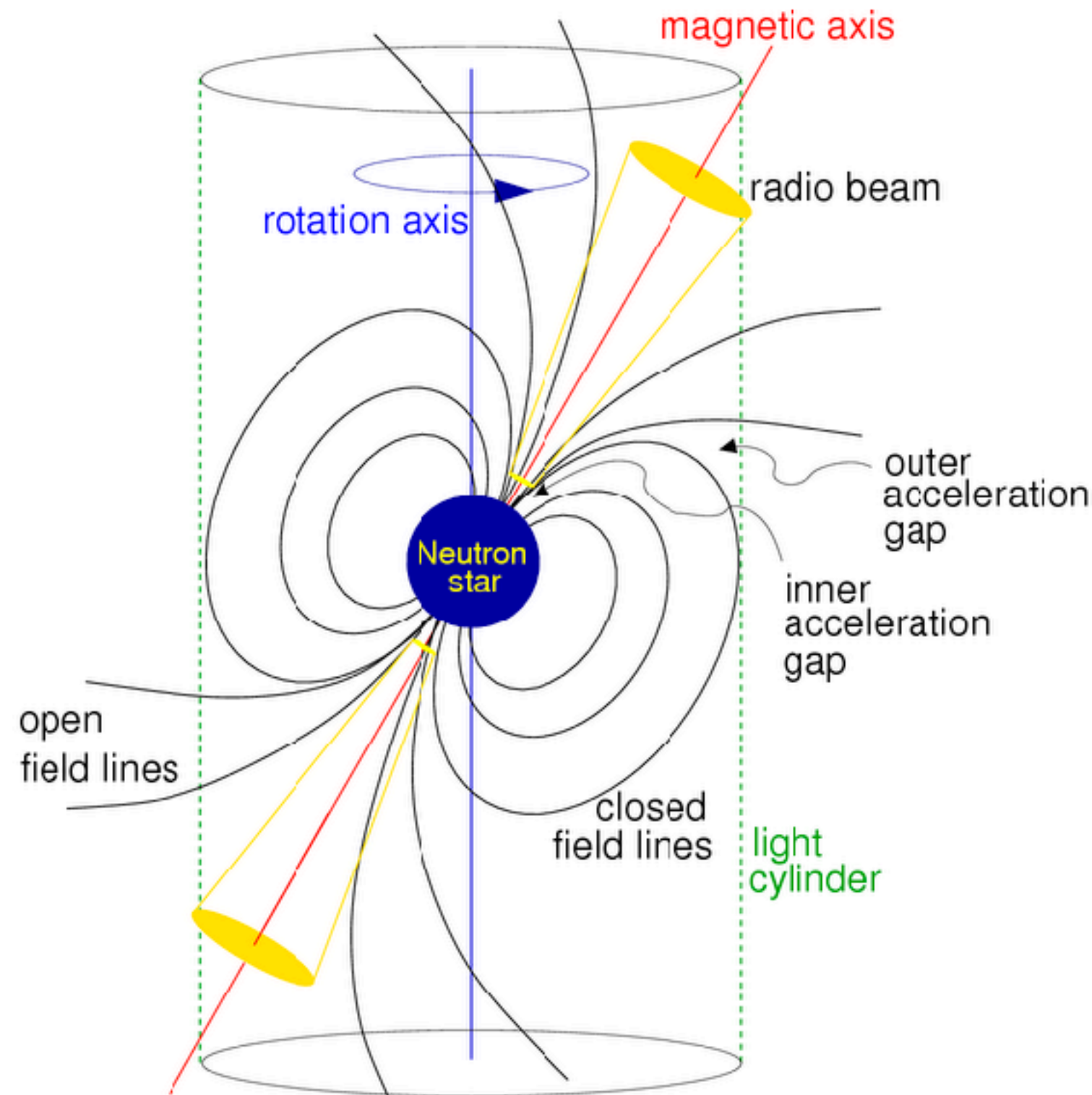
PRODUCTION OF ELECTRON AND POSITRON PAIRS



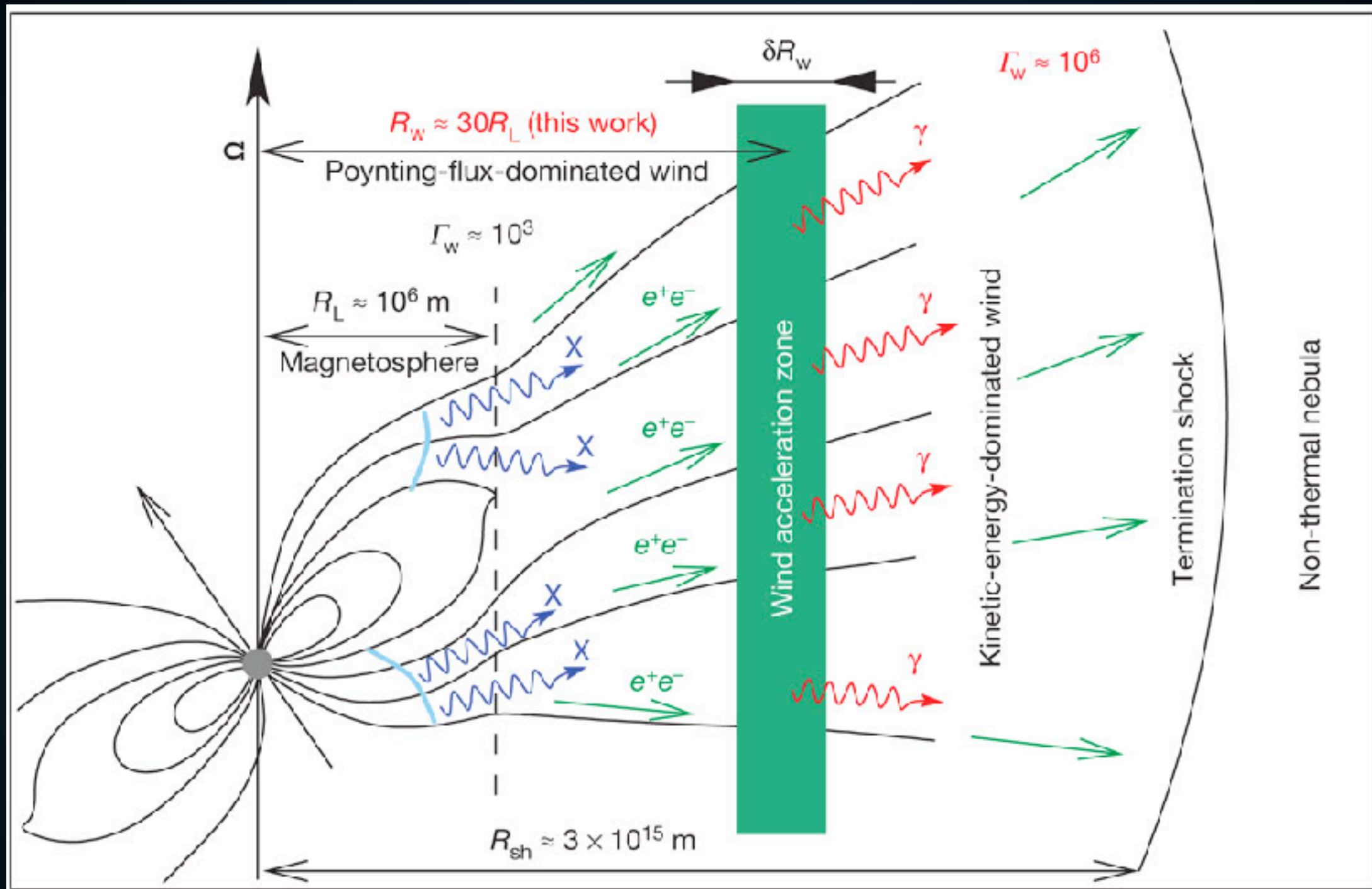
- ▶ Electrons boiled off the pulsar surface produce e^+e^- pairs
- ▶ Pair multiplicity is high, but model dependent.

PULSARS AS ASTROPHYSICAL ACCELERATORS

- ▶ radio beam
- ▶ gamma-ray beam
- ▶ e^+e^- acceleration in pulsar magnetosphere
- ▶ e^+e^- acceleration at termination shock



PRODUCTION OF ELECTRON AND POSITRON PAIRS



- ▶ Final e^+e^- spectrum is model dependent.
- ▶ Understanding this is important for MSPs.

REACCELERATION IN THE PULSAR WIND NEBULA



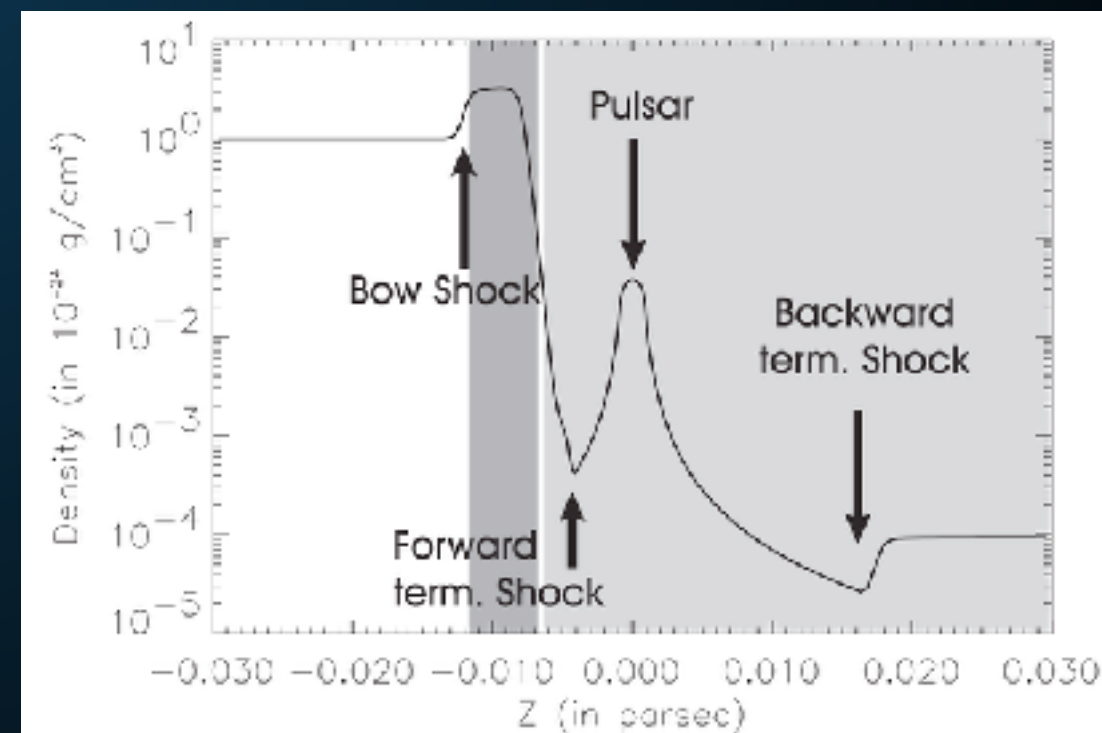
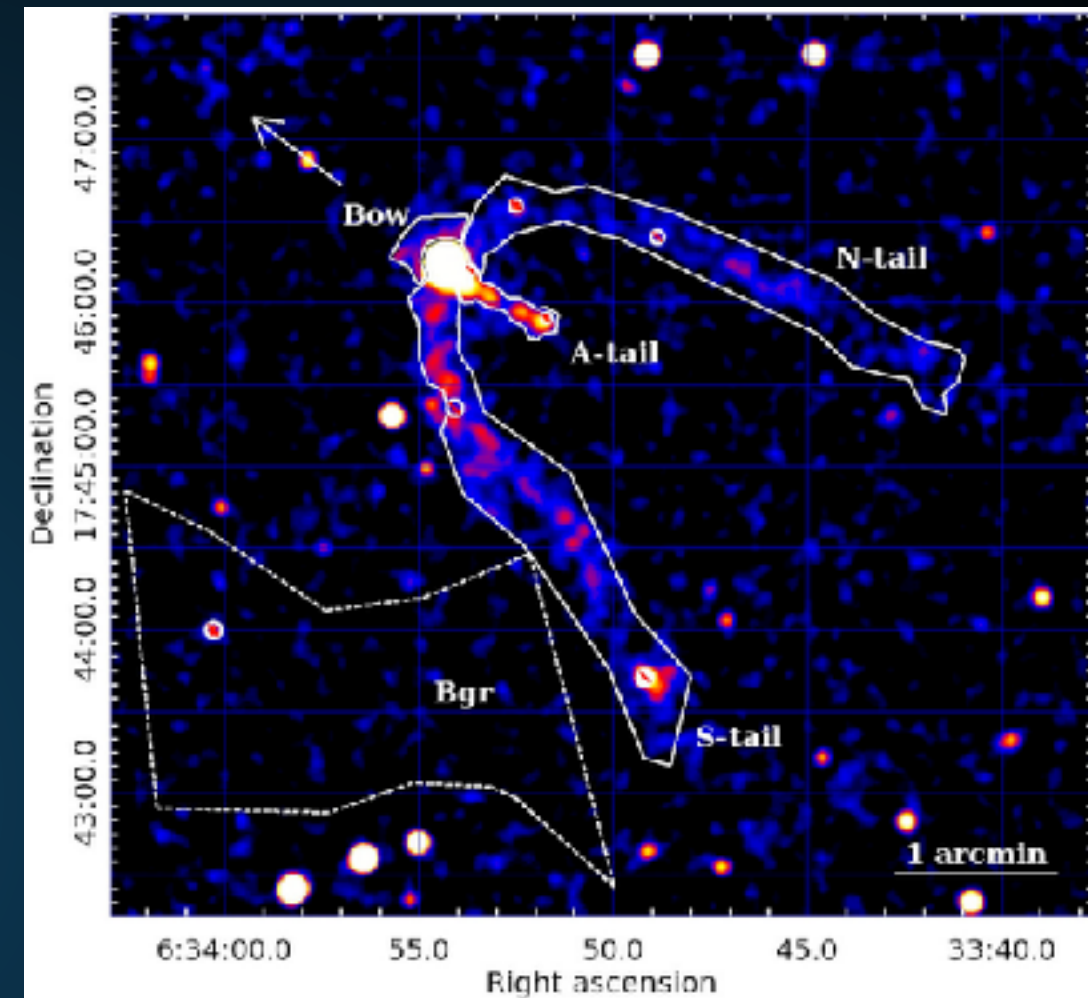
Blandford & Ostriker (1978)
Hoshino et al. (1992)
Coroniti (1990)
Sironi & Spitkovsky (2011)

- ▶ **PWN termination shock:**
 - ▶ **Voltage Drop > 30 PV**
 - ▶ **e^+e^- energy > 1 PeV**
(known from synchrotron)
- ▶ **Resets e^+e^- spectrum.**
- ▶ **Many Possible Models:**
 - ▶ **1st Order Fermi-Acceleration**
 - ▶ **Magnetic Reconnection**
 - ▶ **Shock-Driven Reconnection**

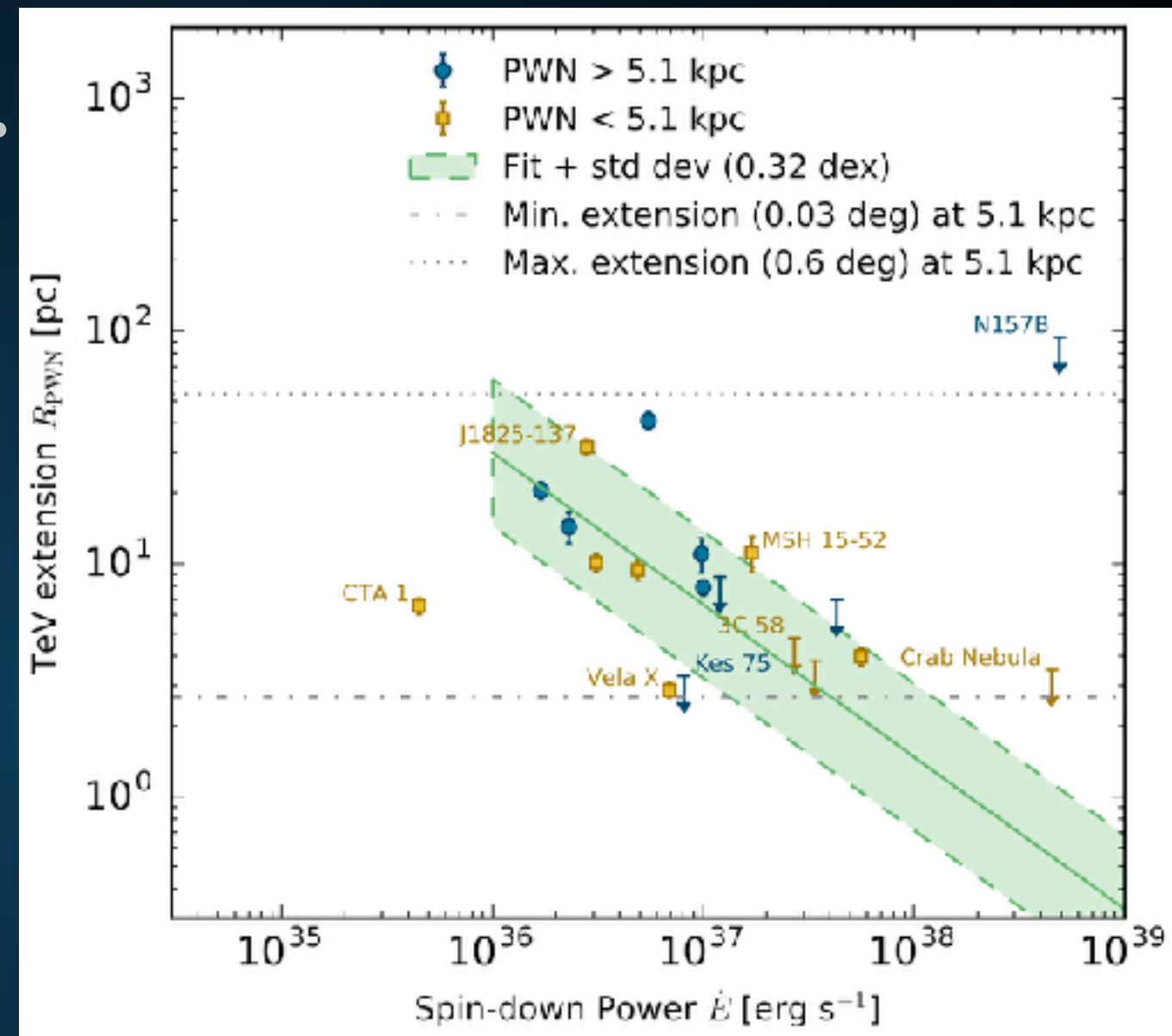
- ▶ **Extent of radio and X-Ray PWN is approximately 1 pc.**
- ▶ **Termination shock produced when ISM energy density overwhelms and stops the relativistic pulsar wind.**

$$R_{\text{PWN}} \simeq 1.5 \left(\frac{\dot{E}}{10^{35} \text{ erg/s}} \right)^{1/2} \times \left(\frac{n_{\text{gas}}}{1 \text{ cm}^{-3}} \right)^{-1/2} \left(\frac{v}{100 \text{ km/s}} \right)^{-3/2} \text{ pc}$$

- ▶ **NOTE: The radial extent of PWN is explained by a known physical mechanism.**



- ▶ TeV Halos are much larger.
- ▶ Particularly true in low-energy systems.

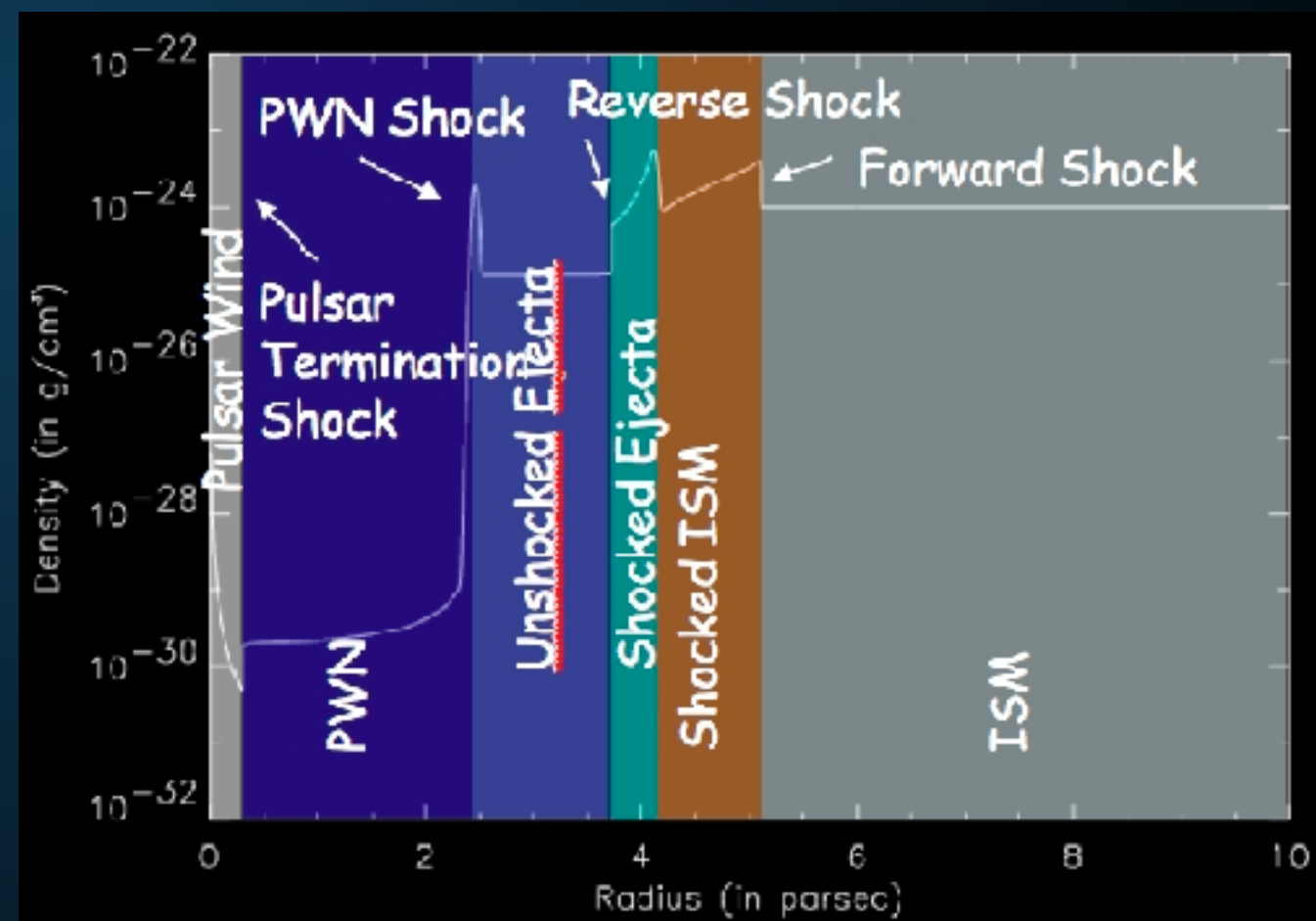


NOTE: This has the opposite energy dependence as the X-Ray PWN.

$$R_{\text{PWN}} \simeq 1.5 \left(\frac{\dot{E}}{10^{35} \text{ erg/s}} \right)^{1/2} \times \left(\frac{n_{\text{gas}}}{1 \text{ cm}^{-3}} \right)^{-1/2} \left(\frac{v}{100 \text{ km/s}} \right)^{-3/2} \text{ pc}$$

TeV HALOS

- ▶ **TeV halos are a new feature**
 - ▶ **3 orders of magnitude larger than PWN in volume**
 - ▶ **Opposite energy dependence**
- ▶ **PWN are morphologically connected to the physics of the termination shock**
- ▶ **TeV halos need a similar morphological description.**



- ▶ **Low-diffusion constants can be induced in regions with significant cosmic-ray injection**

$$D_{\text{loc}}(p) = \frac{\beta(p) c r_L(p)}{3} \left[\frac{2\pi}{3c_k} \frac{c f_0 p_0^4}{dU_0} \beta(p) r_L(p) \left(\frac{p}{p_0} \right)^{4-\alpha} \exp \left(-\frac{p}{p_c} \right) \right]^{-2/3}$$

$$B_0 = 1 \mu\text{G}$$

$$c_k = 5.2 \times 10^{-2}$$

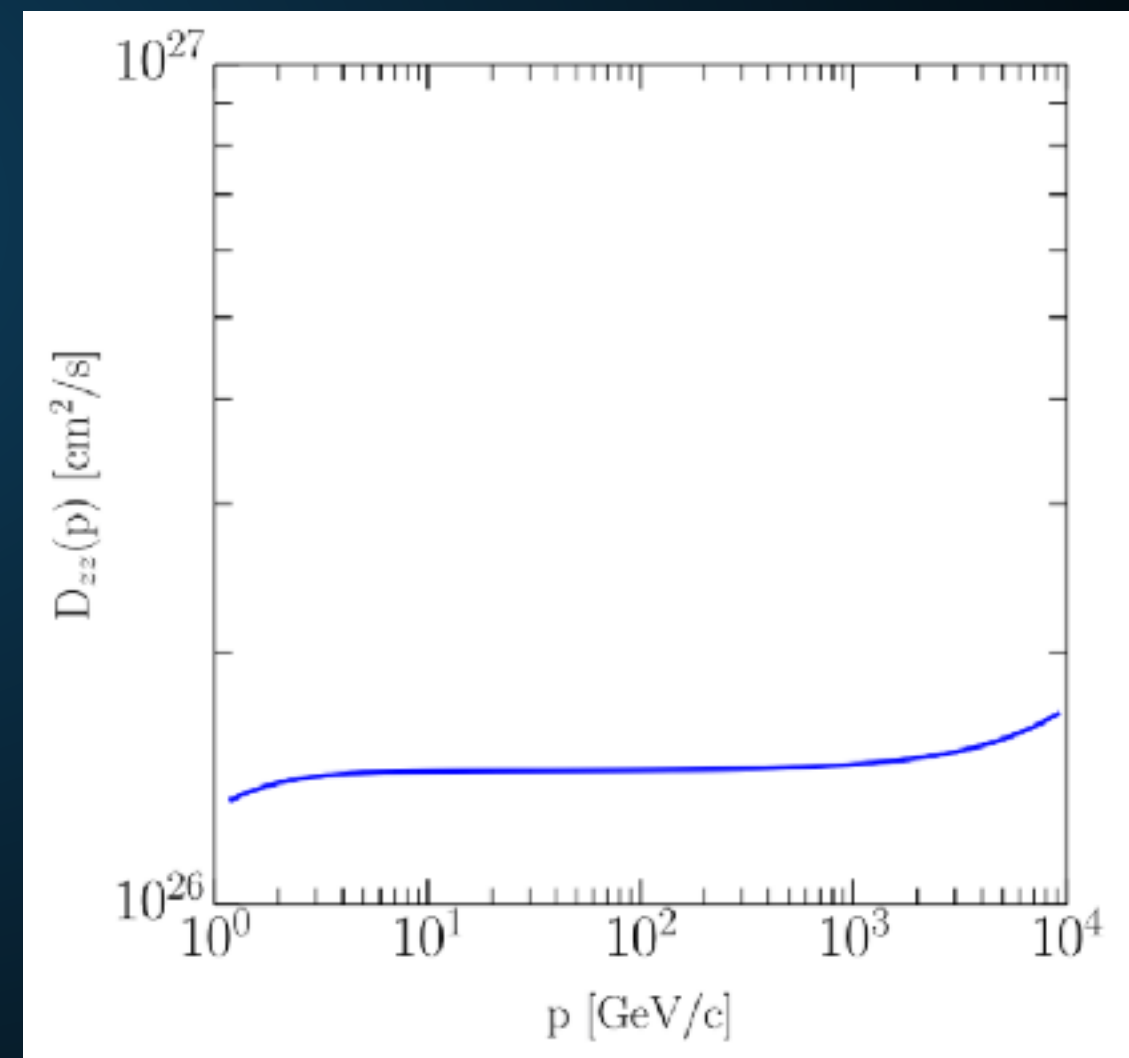
$$d = 50 \text{ pc}$$

$$p_0 = 1 \text{ GeV}/c$$

$$p_c = 39 \text{ TeV}/c$$

$$\alpha = 3.5$$

$$f_0 = 10^{-10} (\text{GeV}/c)^{-3} \text{ cm}^{-3}$$



$b [\text{GeV}/c]$

10^{-10} 10^{-9} 10^{-8} 10^{-7} 10^{-6} 10^{-5} 10^{-4} 10^{-3} 10^{-2} 10^{-1} 10^0 10^1 10^2 10^3 10^4

CONFIRMING TEV HALOS

- ▶ **Several Methods to confirm TeV halo detections:**
 - ▶ **X-Ray halos**
 - ▶ **X-Ray PWN**

X-RAY HALOS

- ▶ An X-Ray halo with an identical morphology as the TeV halo must exist.

$$\begin{aligned} U &= \frac{1}{8\pi} B^2 = \frac{(10 \mu G)^2}{8\pi} \\ &= 4 \times 10^{-12} \frac{\text{erg}}{\text{cm}^3} \\ \int_0^{10 \text{ pc}} U dV &= 5 \times 10^{47} \text{ erg} \\ \hookrightarrow \text{Magnetic Flux} &\approx 5 \times 10^{38} \frac{\text{erg}}{\text{s}} \end{aligned}$$

$$\begin{aligned} \text{ISRF} &= 1 \frac{\text{eV}}{\text{cm}^3} \\ \int \text{ISRF} dV &= 8 \times 10^{47} \text{ erg} \\ \hookrightarrow \text{Flux} &= 8 \times 10^{38} \frac{\text{erg}}{\text{s}} \end{aligned}$$

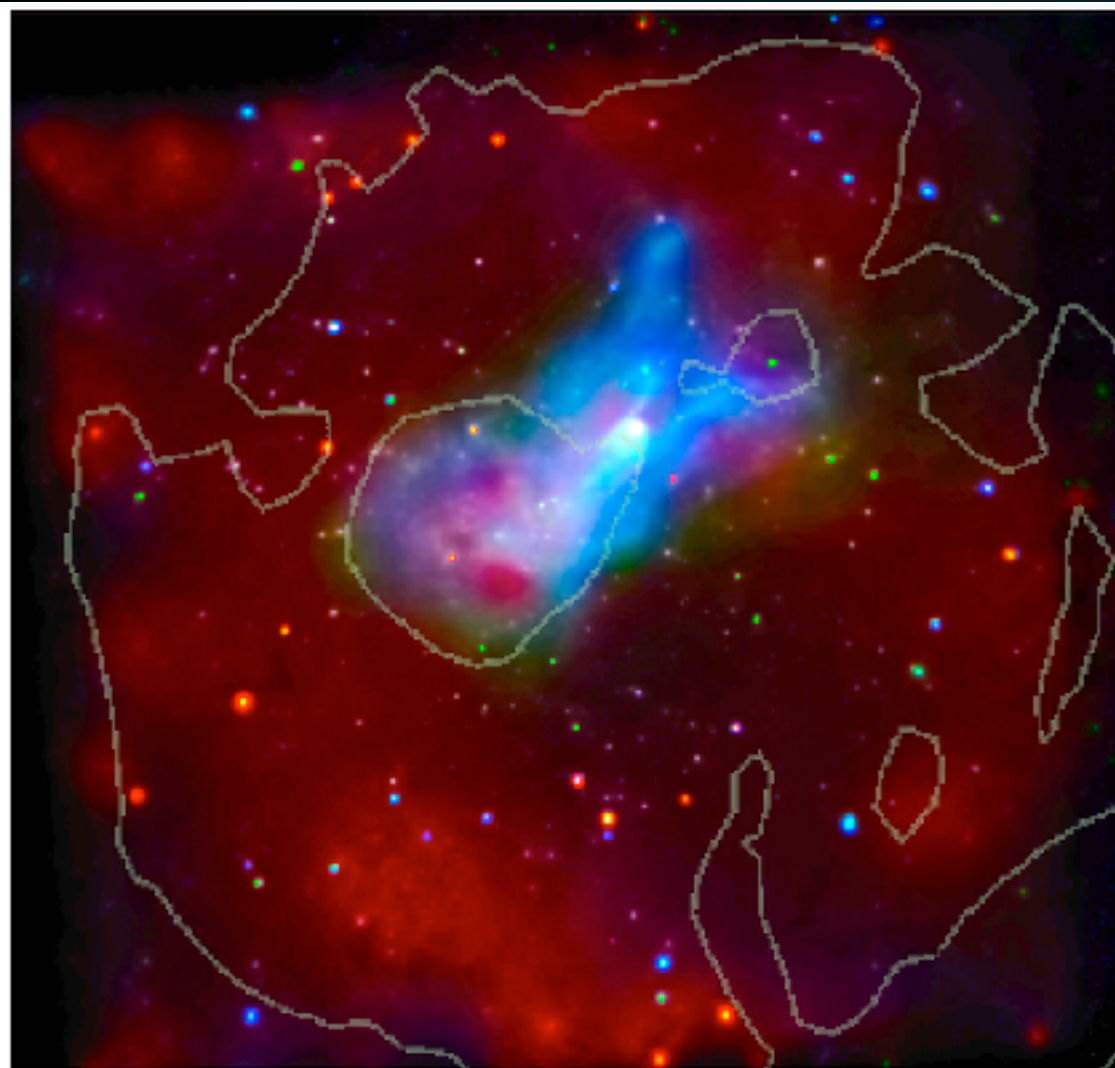
$$E_{\text{sync,critical}} = 22 \text{ eV} \left(\frac{B}{5 \mu G} \right) \left(\frac{E_e}{10 \text{ TeV}} \right)^2$$

- ▶ However, the signal has a low surface brightness and peaks at a low energy.

X-RAY PULSAR WIND NEBULAE



- ▶ **Larger magnetic fields make compact PWN easier to observe**
 - ▶ **Synchrotron dominated**
 - ▶ **Higher energy peak**
- ▶ **More distant sources easier to see.**
- ▶ **Significant observation times require careful HAWC analysis.**



- ▶ Possible Detection! (G327-1.1)
- ▶ Young Pulsar (17.4 kyr)
- ▶ Two PWN
 - ▶ Diffuse PWN has significantly softer spectrum

| | Region | Area (arcsec ²) | Cts (1000) | N _H (10 ²² cm ⁻²) | Photon Index | Amplitude (10 ⁻⁴) | kT (keV) | τ (10 ¹² s cm ⁻³) | Norm. (10 ⁻³) | F ₁ (10 ⁻¹²) | F ₂ | Red. χ^2 |
|----|----------------|--------------------------------|---------------|--|--|--|--|--|------------------------------------|--|----------------|------------------|
| 1 | Compact Source | 84.657 | 6.34 | 1.93 ^{+0.08} _{-0.08} | 1.61 ^{+0.08} _{-0.07} | 1.05 ^{+0.11} _{-0.10} | ... | ... | ... | 0.45 | ... | 0.80 |
| 2 | Cometary PWN | 971.22 | 7.75 | 1.93 | 1.62 ^{+0.08} _{-0.07} | 1.47 ^{+0.16} _{-0.14} | ... | ... | ... | 1.09 | ... | ... |
| 3 | Trail East | 537.42 | 2.13 | 1.93 | 1.84 ^{+0.12} _{-0.12} | 0.44 ^{+0.07} _{-0.06} | ... | ... | ... | 0.27 | ... | ... |
| 4 | Trail West | 766.56 | 3.12 | 1.93 | 1.80 ^{+0.11} _{-0.11} | 0.61 ^{+0.09} _{-0.08} | ... | ... | ... | 0.39 | ... | ... |
| 5 | Trail 1 | 424.45 | 1.98 | 1.93 | 1.76 ^{+0.12} _{-0.12} | 0.39 ^{+0.05} _{-0.05} | ... | ... | ... | 0.26 | ... | ... |
| 6 | Trail 2 | 588.19 | 2.13 | 1.93 | 1.95 ^{+0.11} _{-0.11} | 0.49 ^{+0.07} _{-0.06} | ... | ... | ... | 0.28 | ... | ... |
| 7 | Trail 3 | 994.92 | 2.99 | 1.93 | 2.09 ^{+0.10} _{-0.10} | 0.78 ^{+0.09} _{-0.08} | ... | ... | ... | 0.42 | ... | ... |
| 8 | Trail 4 | 839.48 | 2.38 | 1.93 | 2.28 ^{+0.12} _{-0.12} | 0.74 ^{+0.09} _{-0.09} | ... | ... | ... | 0.37 | ... | ... |
| 9 | Prong East | 828.58 | 1.66 | 1.93 | 1.72 ^{+0.14} _{-0.14} | 0.30 ^{+0.06} _{-0.05} | ... | ... | ... | 0.27 | ... | ... |
| 10 | Prong West | 971.22 | 2.06 | 1.93 | 1.85 ^{+0.14} _{-0.14} | 0.44 ^{+0.08} _{-0.07} | ... | ... | ... | 1.09 | ... | ... |
| 11 | Diffuse PWN* | 20007 | 27.7 | 1.93 | 2.11 ^{+0.04} _{-0.05} | 6.91 ^{+0.37} _{-0.74} | 0.23 ^{+0.14} _{-0.05} | 0.21 ^{+0.88} _{-0.16} | 6.0 ⁺¹⁶ _{-4.0} | 3.68 | 17.7 | 0.82 |
| 12 | Relic PWN* | 26787 | 17.2 | 1.93 | 2.58 ^{+0.07} _{-0.10} | 6.51 ^{+0.53} _{-0.71} | 0.23 | 0.21 | 6.9 ⁺¹⁸ _{-5.5} | 3.14 | 20.3 | ... |

X-RAY PWN DETECTIONS

| PWNe With No Detected Pulsar | | | | | | |
|------------------------------|------------------------|---|---|---|---|-------|
| Gname | other name(s) | R | X | O | G | |
| G0.13-0.11 | | | | | ? | notes |
| G0.9+0.1 | | | | | N | notes |
| G7.4-2.0 | GeV J1809-2327, Tazzie | | | | Y | notes |
| G16.7+0.1 | | | | | N | notes |
| G18.5-0.4 | GeV J1825-1310, Fcl | | | | Y | notes |
| G20.0-0.2 | | | | | N | notes |
| G24.7+0.6 | | | | | N | notes |
| G27.8+0.6 | | | | | N | notes |
| G39.2-0.3 | 3C 396 | | | | Y | notes |
| G63.7+1.1 | | | | | N | notes |
| G74.9+1.2 | CTB 87 | | | | Y | notes |
| G119.5+10.2 | CTA 1 | | | | Y | notes |
| G189.1+3.0 | IC 443 | | | | ? | notes |
| G279.8-35.8 | B0453-685 | | | | N | notes |
| G291.0-0.1 | MSH 11-62 | | | | Y | notes |
| G293.8+0.6 | | | | | N | notes |
| G313.3+0.1 | Rabbit | | | | Y | notes |
| G318.9+0.4 | | | | | N | notes |
| G322.5-0.1 | | | | | N | notes |
| G326.3-1.8 | MSH 15-56 | | | | N | notes |
| G327.1-1.1 | | | | | N | notes |
| G328.4+0.2 | MSH 15-57 | | | | N | notes |
| G358.6-17.2 | RX J1856.5-3754 | N | N | | N | notes |
| G359.89-0.08 | | | | | Y | notes |

- ▶ X-Ray PWN have detected only ~6 of these 37 systems.

- ▶ **TeV observations open up a new window into understanding Milky Way pulsars.**
- ▶ **Early indications:**
 - ▶ **TeV halos produce most of the TeV sources observed by ACTs and HAWC**
 - ▶ **TeV halos dominate the diffuse TeV emission in our galaxy.**
 - ▶ **Positron Excess is due to pulsar activity**

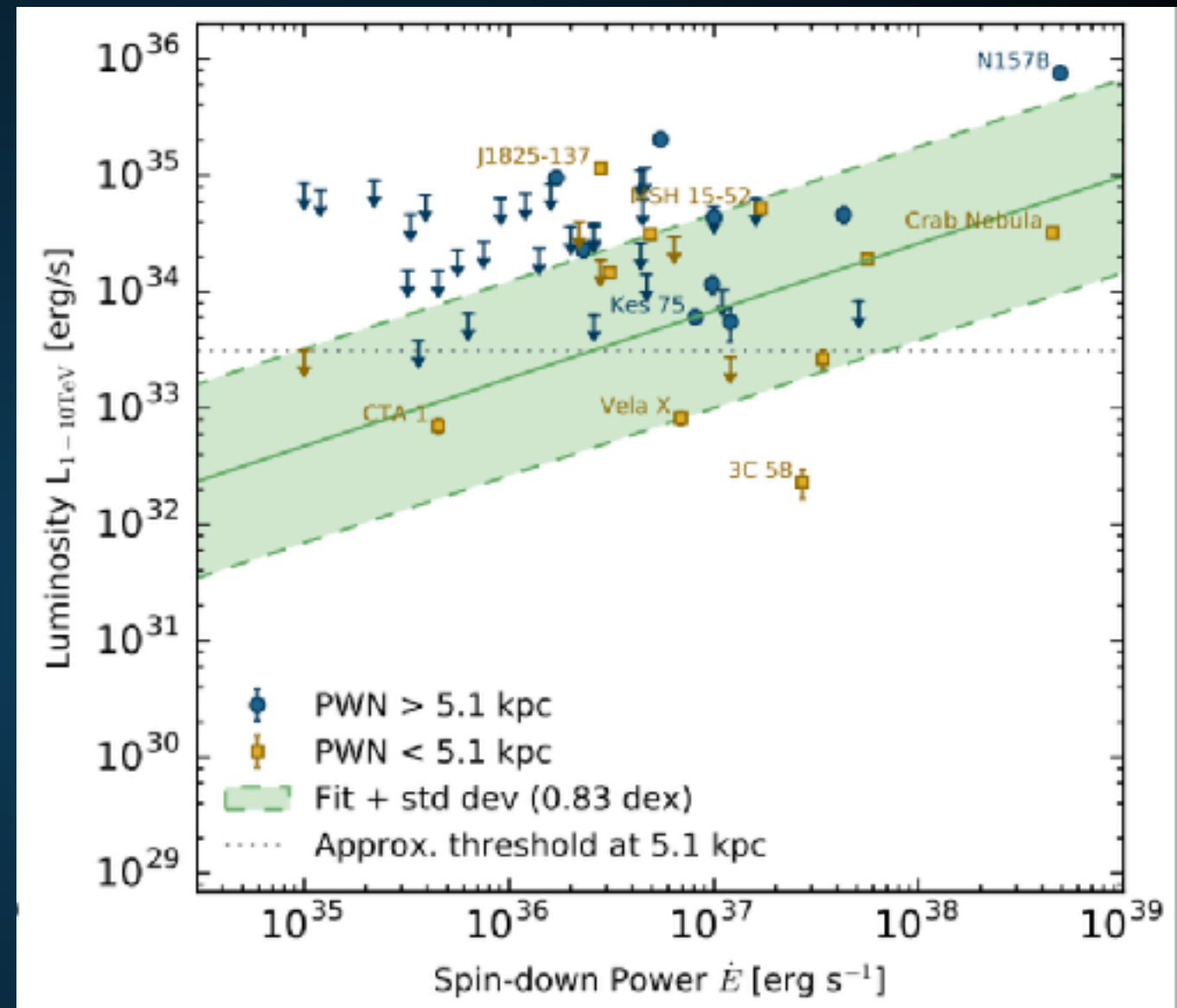
- ▶ **Additional implications:**
 - ▶ **Young pulsar braking index**
 - ▶ **MSPs?**
 - ▶ **Galactic cosmic-ray diffusion**
 - ▶ **Source of IceCube neutrinos**
 - ▶ **TeV Dark Matter Constraints**

Extra Slides

**What if the “Geminga”-like
model is wrong?**

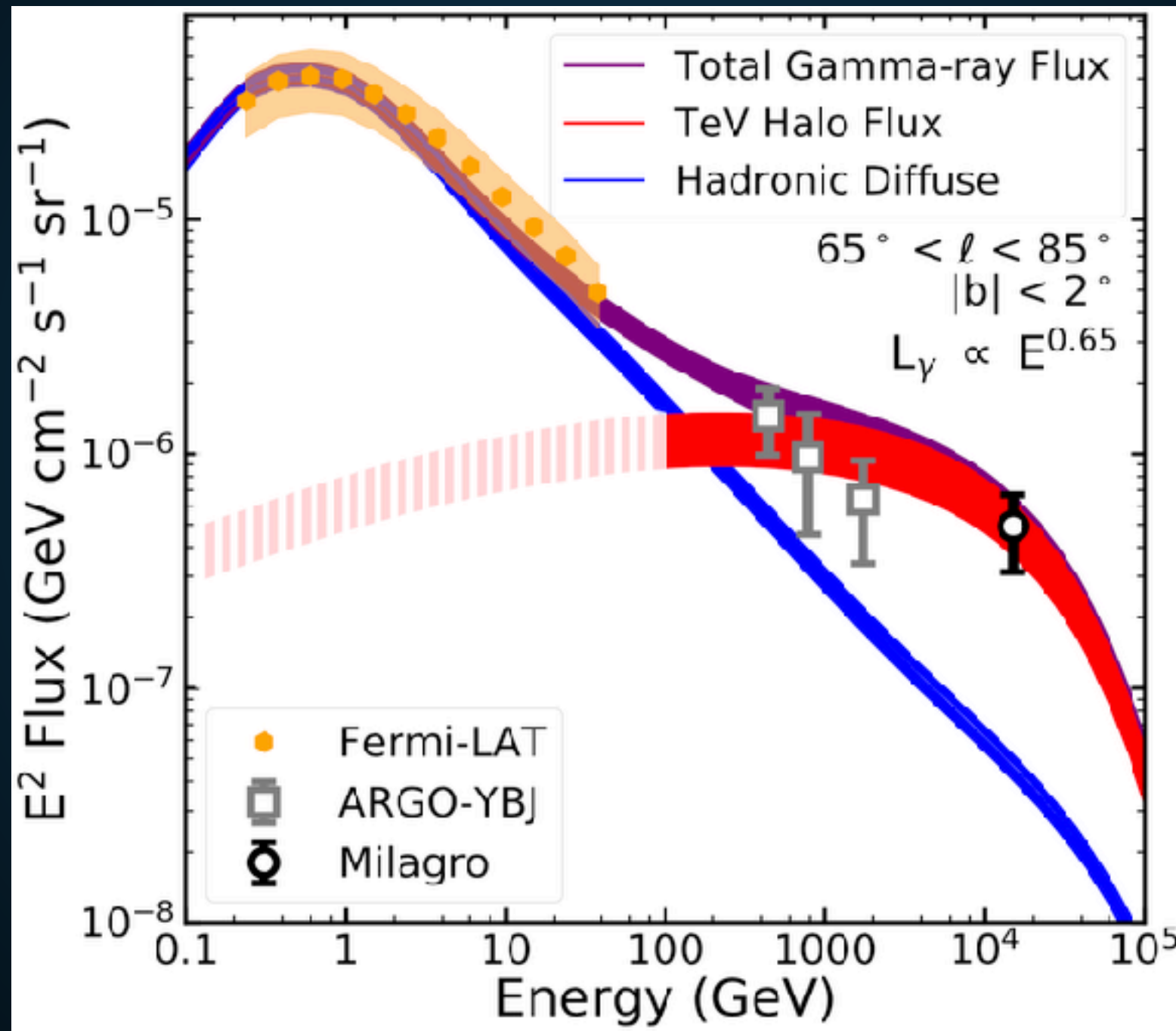
- Alternatively can utilize HESS results which find:

$$L = \dot{E}_{\text{dot}}^{0.59}$$



$$\phi_{\text{TeV halo}} = \left(\frac{\dot{E}_{\text{psr}}}{\dot{E}_{\text{Geminga}}} \right) \left(\frac{d_{\text{Geminga}}^2}{d_{\text{psr}}^2} \right) \phi_{\text{Geminga}}$$

► TeV halos naturally explain the TeV excess!

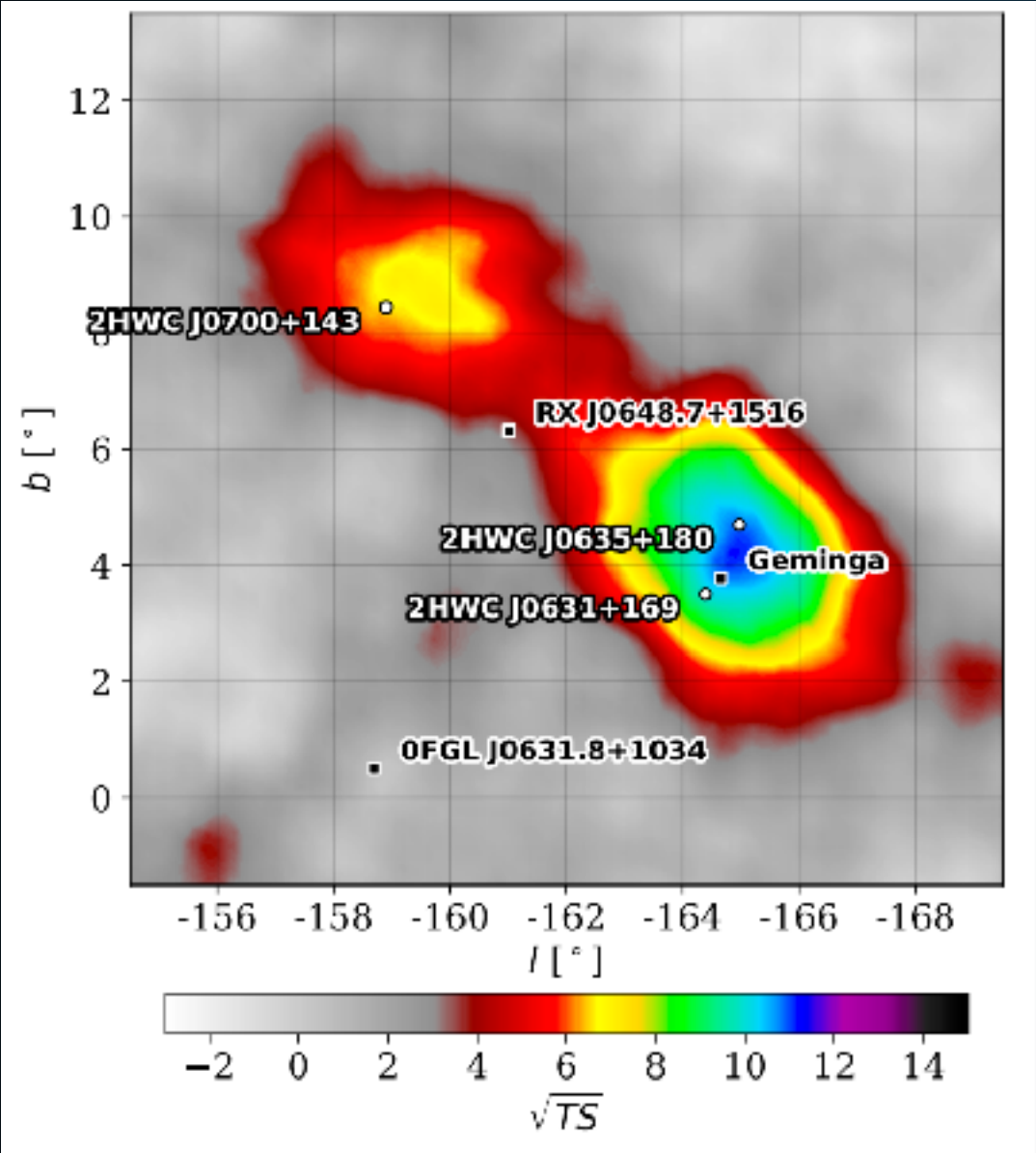


**How can we prove that
we've found a TeV halo?**

**What produces the
electron population?**

TWO CONTRASTING OBSERVABLES

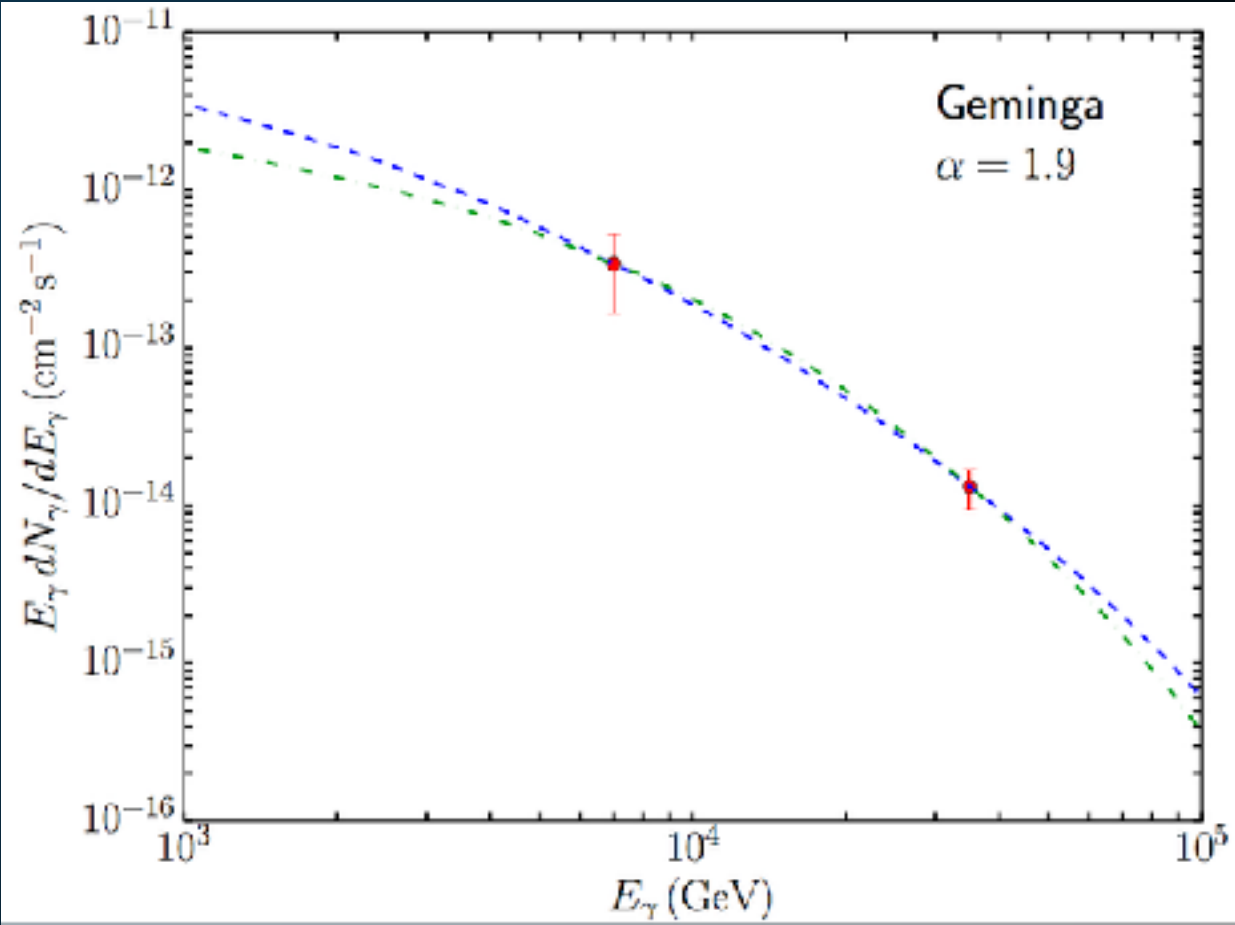
Geminga is Bright



Indicative of significant
electron cooling

Geminga has a hard-spectrum

| Name | Tested radius [°] | Index | $F_{\gamma} \times 10^{15}$ [TeV ⁻¹ cm ⁻² s ⁻¹] | TeVCat |
|----------------|----------------------|------------------|--|---------|
| 2HWC J0631+169 | - | -2.57 ± 0.15 | 6.7 ± 1.5 | Geminga |
| " | 2.0 | -2.23 ± 0.08 | 48.7 ± 6.9 | Geminga |
| 2HWC J0635+180 | - | -2.56 ± 0.16 | 6.5 ± 1.5 | Geminga |



Indicative of minimal
electron cooling

COSMIC-RAY DIFFUSION IN A TEV HALO

- ▶ Energy constraints demand that ~30 TeV electrons lose the majority of their energy before exiting TeV halo.

$$\tau = 3.1 \times 10^4 \text{ yr} \left(\frac{E_e}{10 \text{ TeV}} \right)^{-1}$$

- ▶ This strongly constrains the efficiency of particle propagation near the halo.

$$D = \frac{L^2}{6\tau} = \frac{(10 \text{ pc})^2}{6(3.1 \times 10^4 \text{ yr})} = \frac{(3.08 \times 10^{19} \text{ cm})^2}{5.86 \times 10^{12} \text{ s}}$$

$$D = 1.6 \times 10^{26} \frac{\text{cm}^2}{\text{s}}$$

- ▶ Provides strong evidence for new morphological feature.

TOTAL POWER OF TEV HALOS

- ▶ Measured Geminga flux translates to an intensity:

$$2.86 \times 10^{31} \text{ erg s}^{-1} \text{ at 7 TeV}$$

- ▶ For the best-fit spectrum, this requires an e^+e^- injection:

$$3.8 \times 10^{33} \text{ erg s}^{-1}$$

- ▶ Total Spindown Power of Geminga is:

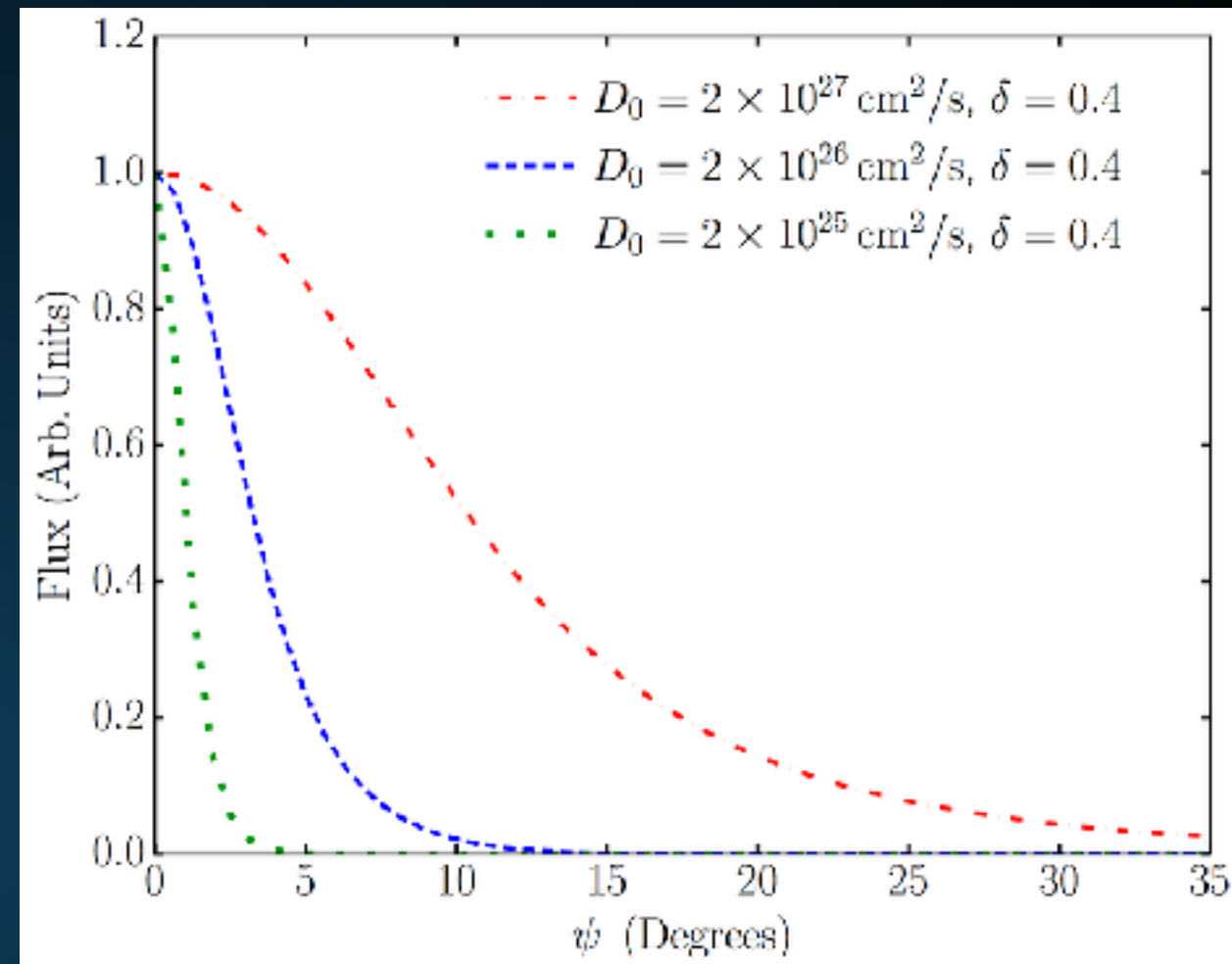
$$3.4 \times 10^{34} \text{ erg s}^{-1}$$

- ▶ Roughly 10% conversion efficiency to e^+e^- !

COSMIC-RAY DIFFUSION IN A TEV HALO

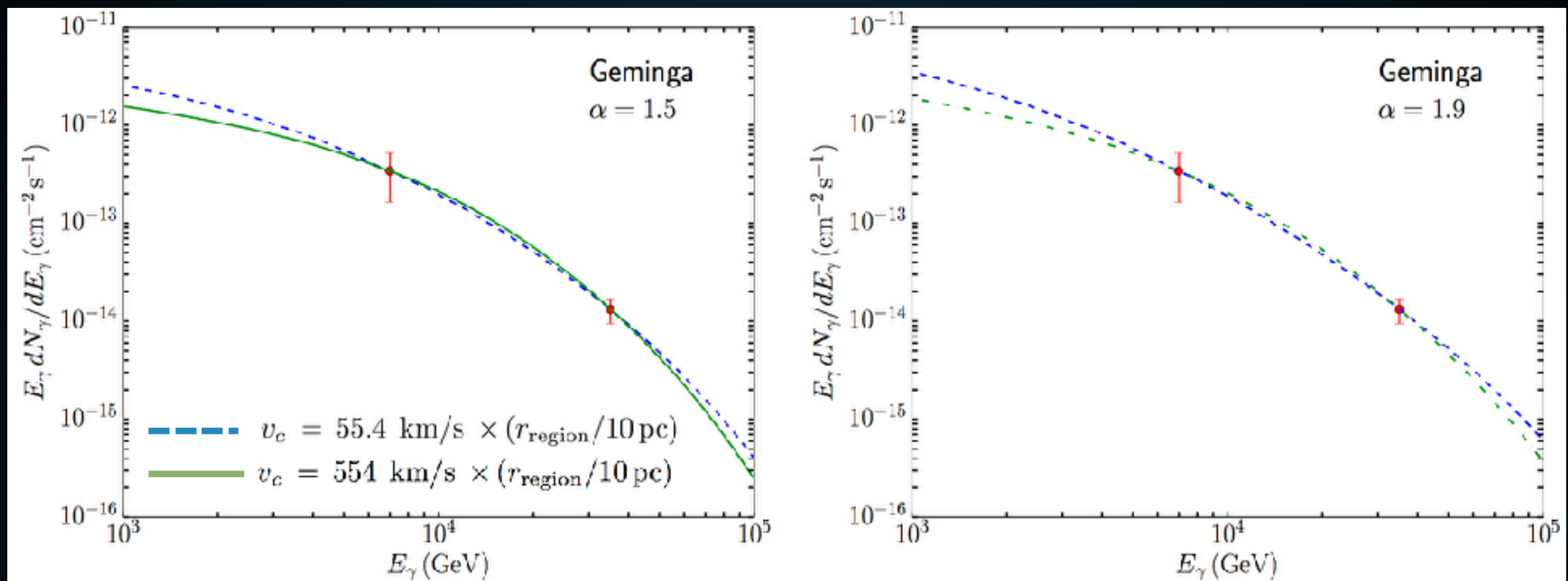
- ▶ **Actual source of particle propagation is unknown:**

- ▶ **Diffusion**
- ▶ **Advection**



- ▶ Particle propagation near pulsars must be orders of magnitude less efficient than typical for the ISM.
- ▶ Continues far outside the termination shock of a pulsar with no SNR.

GEMINGA SPECTRUM INDICATIVE OF CONVECTION



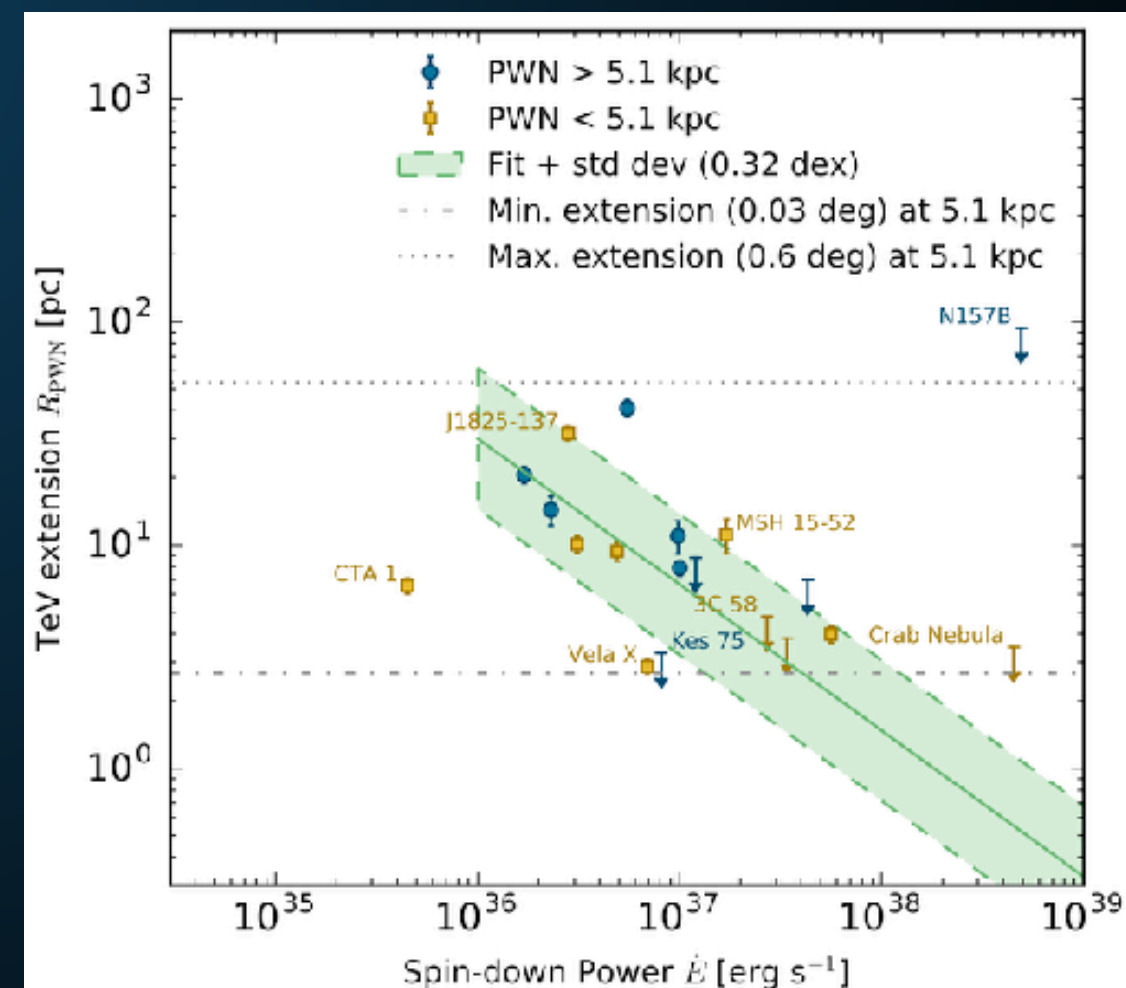
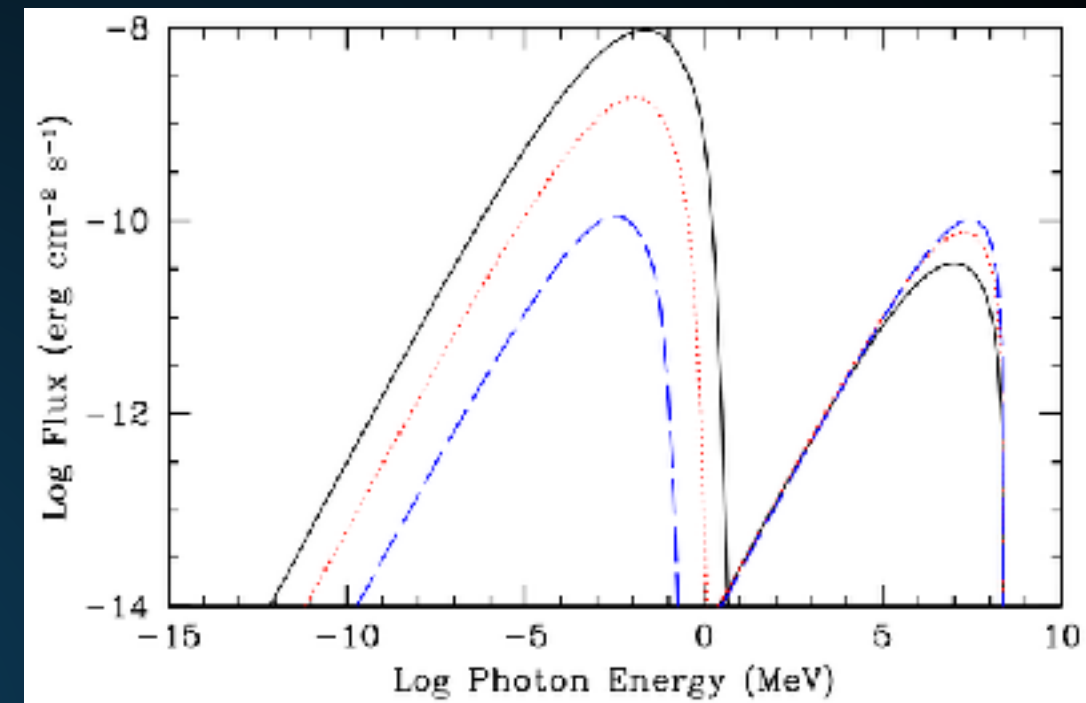
- ▶ However, Bohmian diffusion is incompatible with the gamma-ray spectrum.
- ▶ If low-energy electrons are cooled, the spectrum at 7 TeV should be significantly softer.

AN UPPER LIMIT ON THE TEV HALO SIZE

- ▶ These arguments only set a lower limit on the TeV halo size.
- ▶ What if TeV halos are much larger, but the TeV electrons die at ~ 10 pc?
- ▶ Will need to answer this question on the population level.

AN ALTERNATIVE EXPLANATION

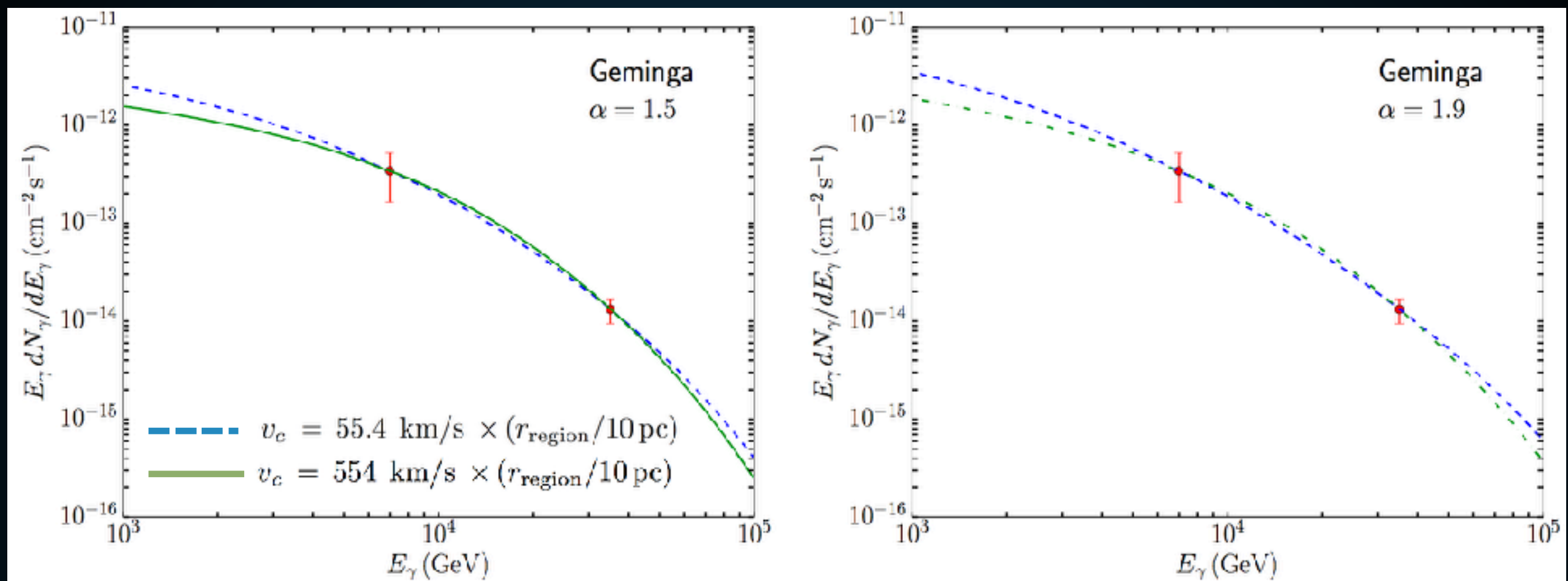
- ▶ Maybe TeV electrons propagate farther?
- ▶ Energy loss time-scale: E^{-1} .
- ▶ Propagation Distance in t: $E^{0.16}$.
- ▶ Size of Halo: $E^{-0.33}$.
- ▶ Moving from PeV to ~ 50 TeV electrons leads to 10x larger radius.



GEMINGA - A TEMPLATE FOR TEV HALOS

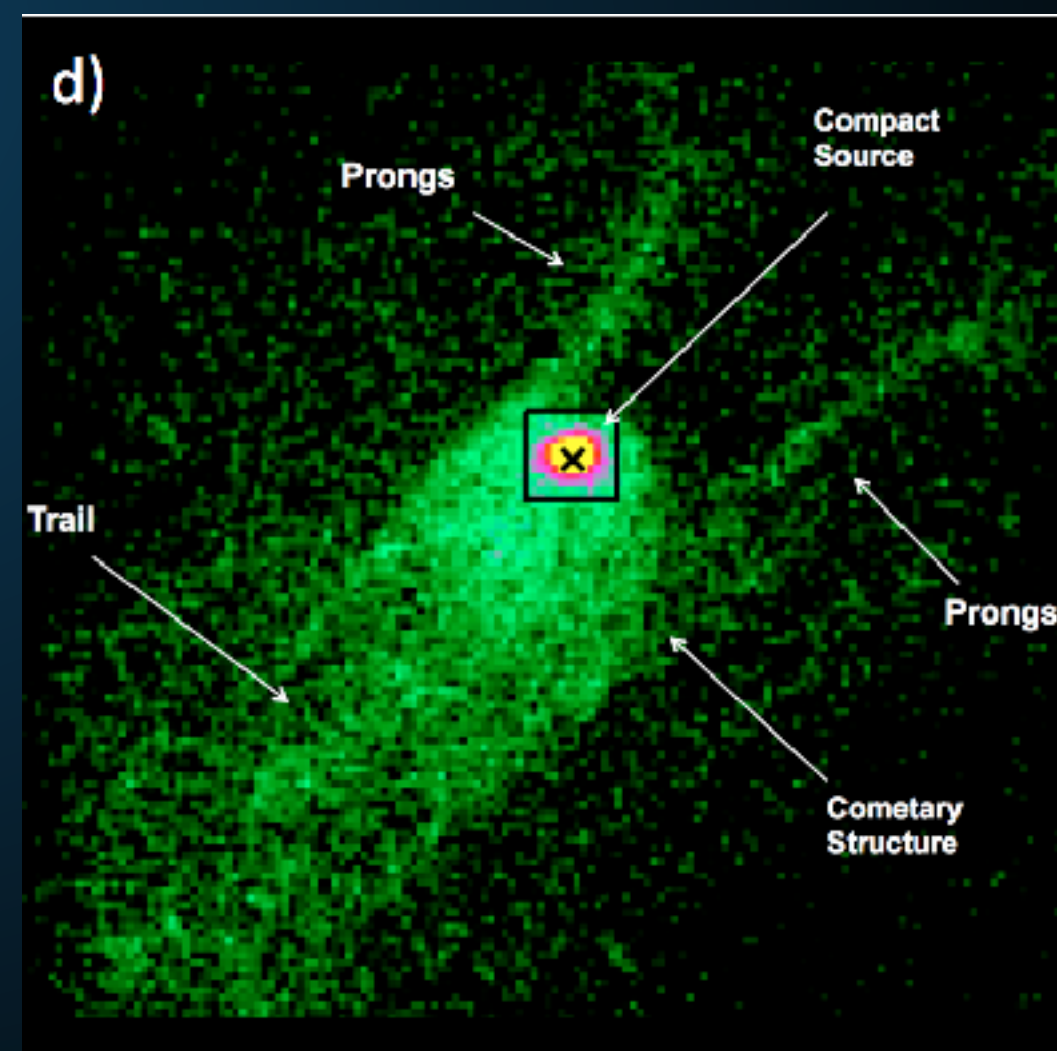
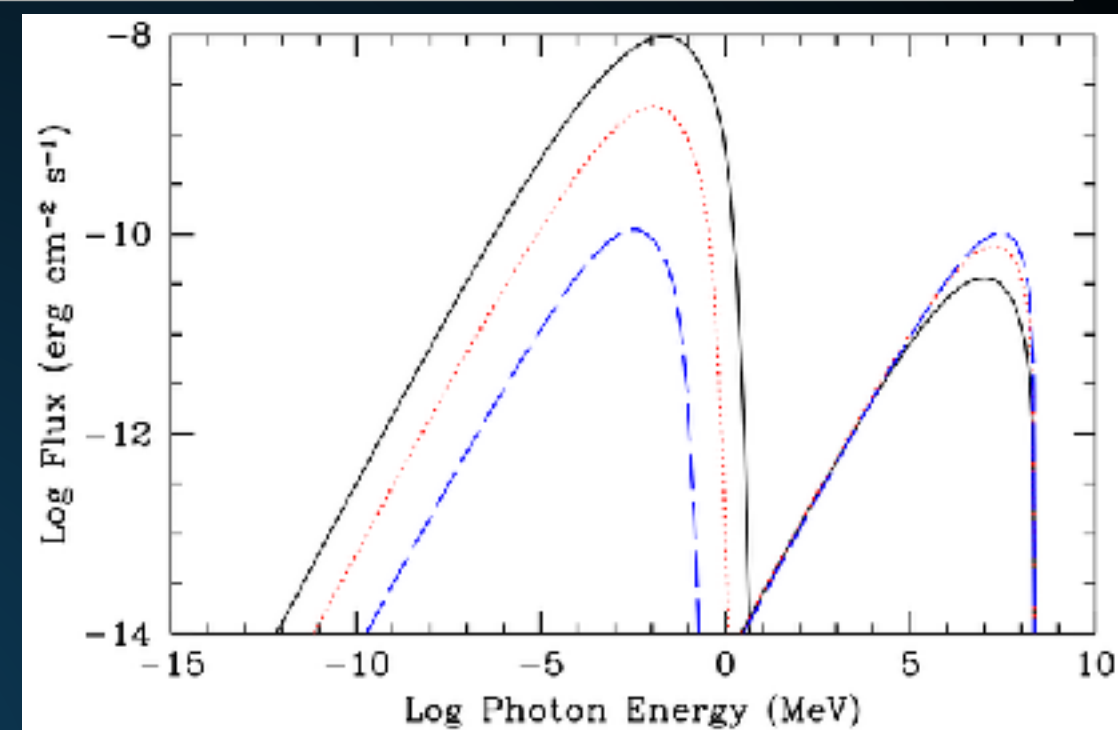
- ▶ **Will now use Geminga as a standard template for TeV halos.**
- ▶ **Bright (nearby)**
- ▶ **High latitude (low background)**
- ▶ **Middle-Aged (no associated SNR)**
- ▶ **Would get same (actually slightly better) results if we used Monogem.**

GEMINGA SPECTRUM INDICATIVE OF CONVECTION

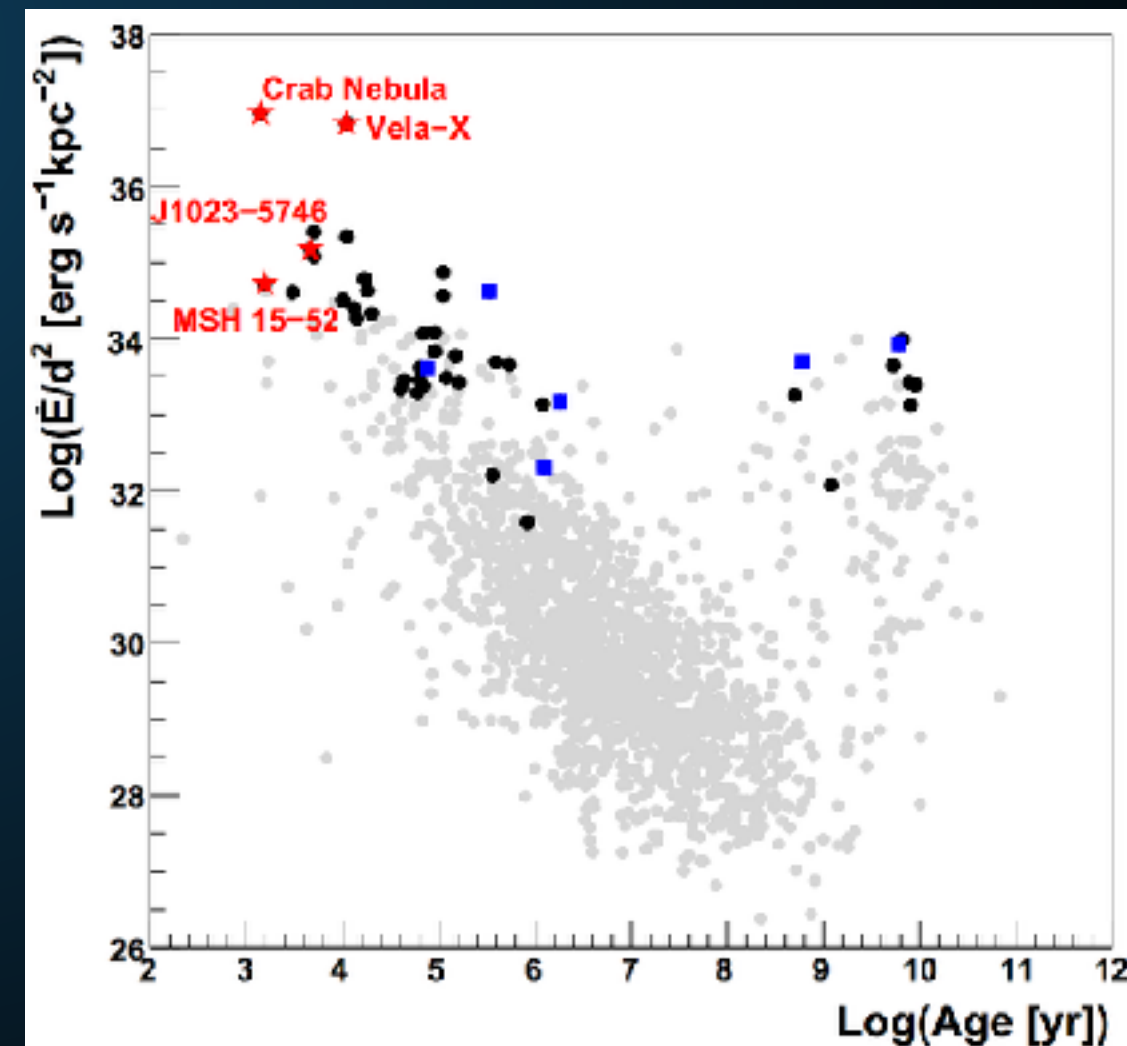
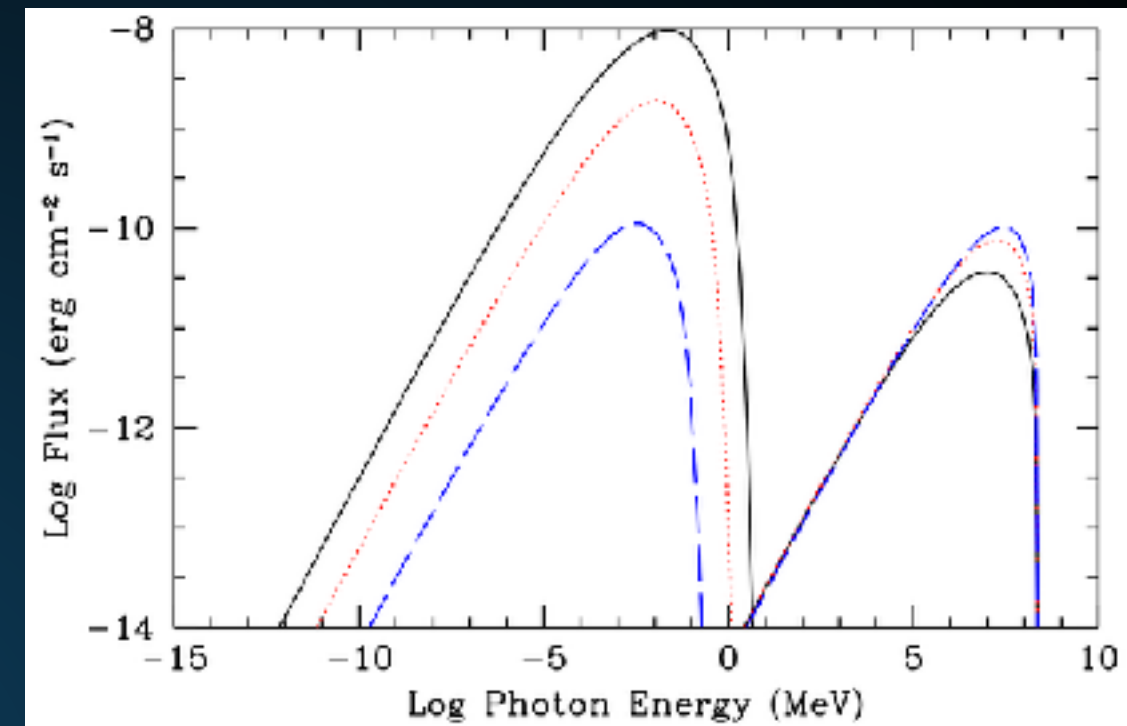


- ▶ Geminga spectrum is fit better with convective models.
- ▶ Energy-independent diffusion provides identical results
- ▶ Best-fit spectral-index (-2.23 ± 0.08) prefers high convection

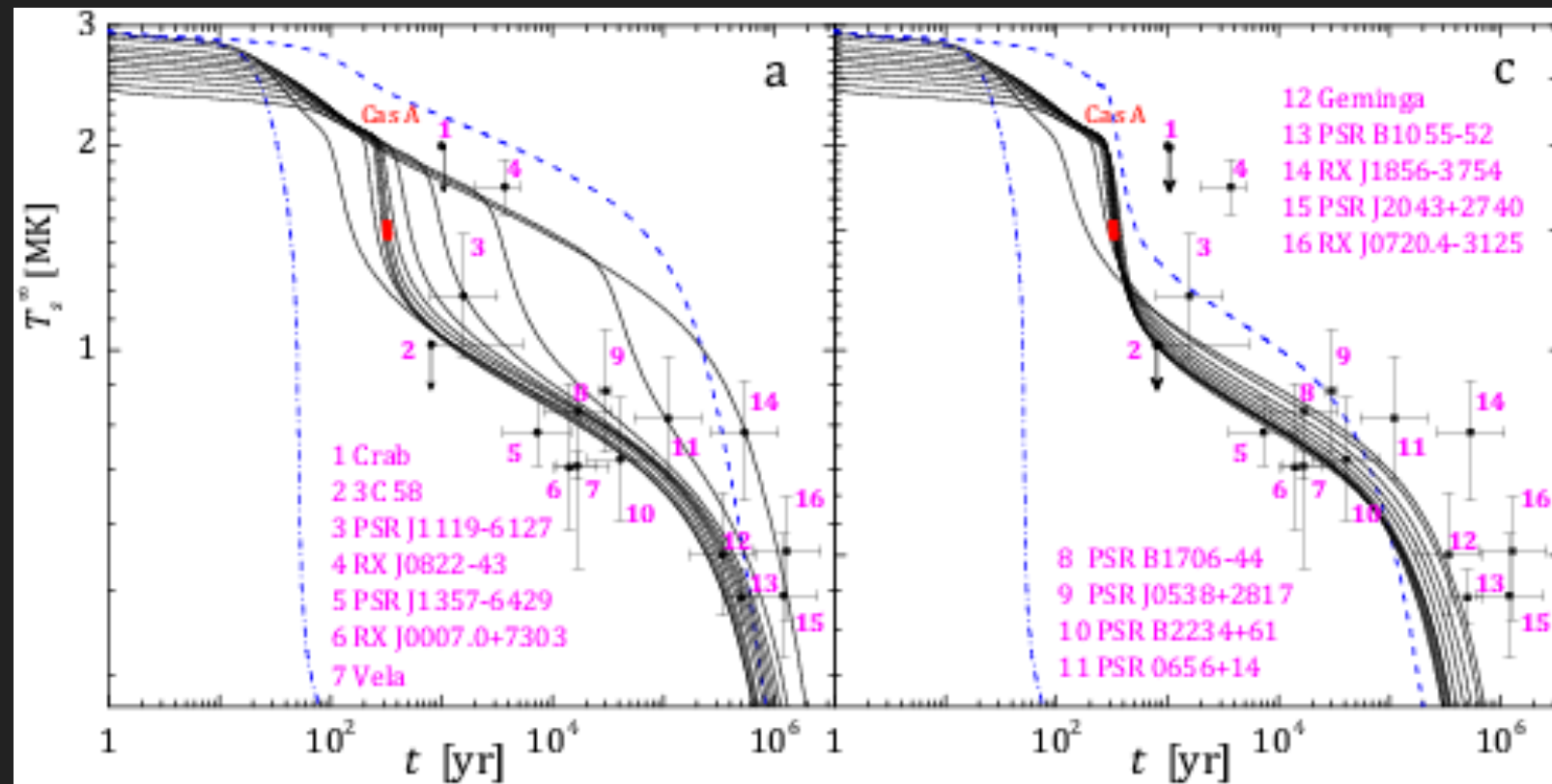
- ▶ Cooling dominated by 20 μG magnetic field.
- ▶ Energy loss time: ~ 40 years
- ▶ Distance Traveled: ~ 6 pc for standard diffusion constant. Real diffusion must be slower.
- ▶ The spectrum changes as a function of distance and time.



- ▶ Gamma-Ray produced through ICS should accompany synchrotron emission.
- ▶ Synchrotron observations imply very hard GeV gamma-ray spectrum.
- ▶ Conclusively prove leptonic nature of emission.

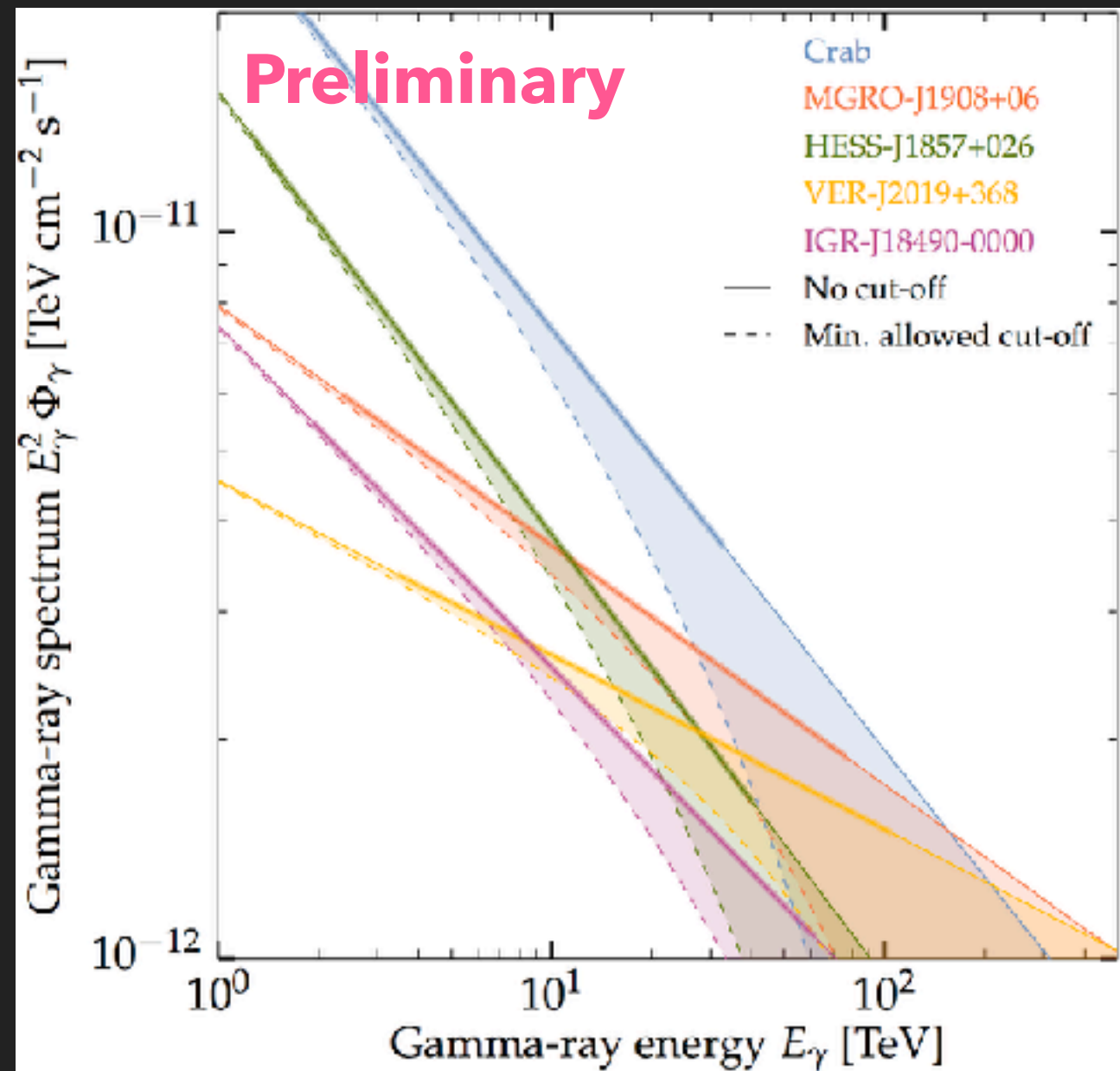


THERMAL PULSAR EMISSION

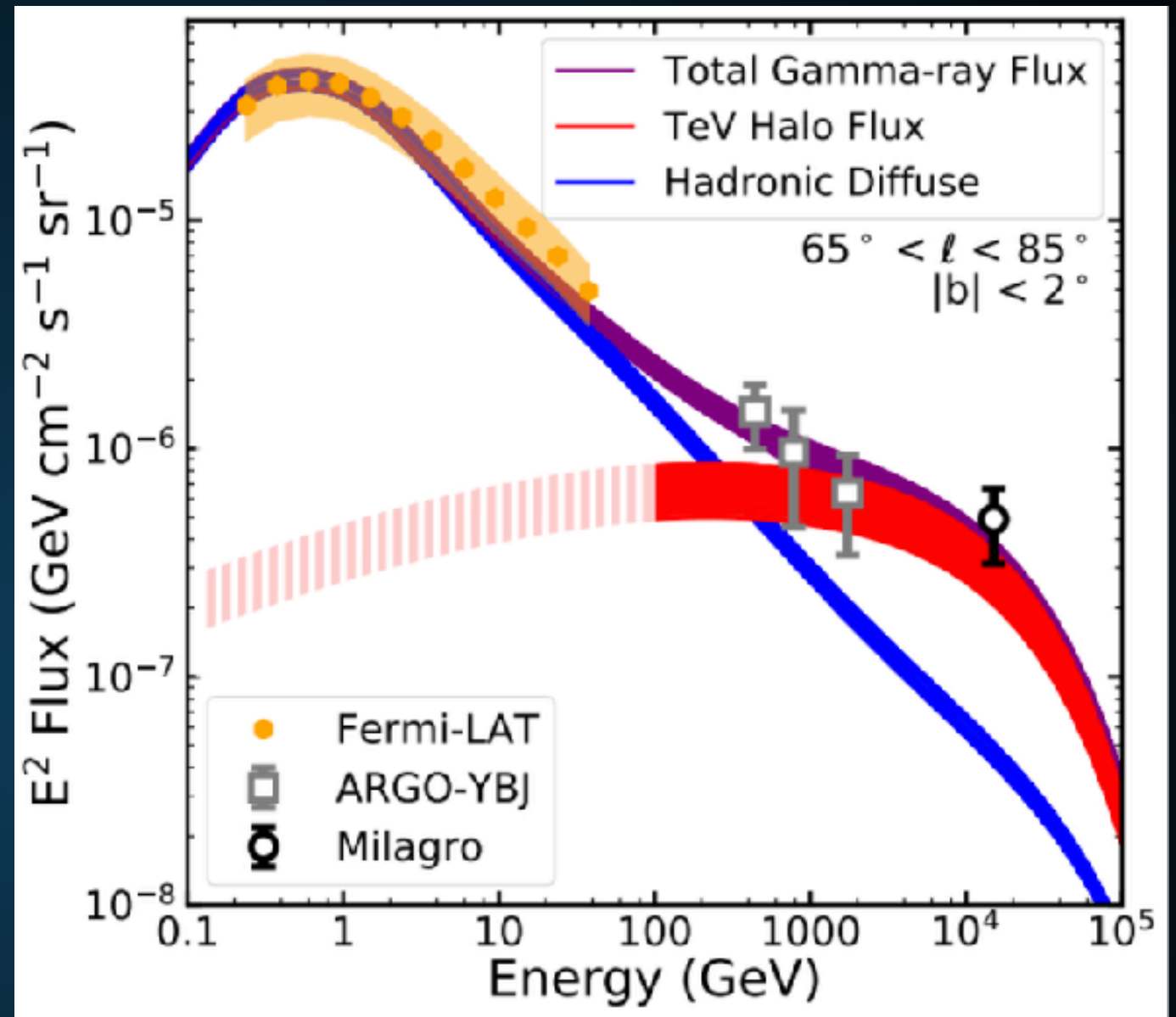


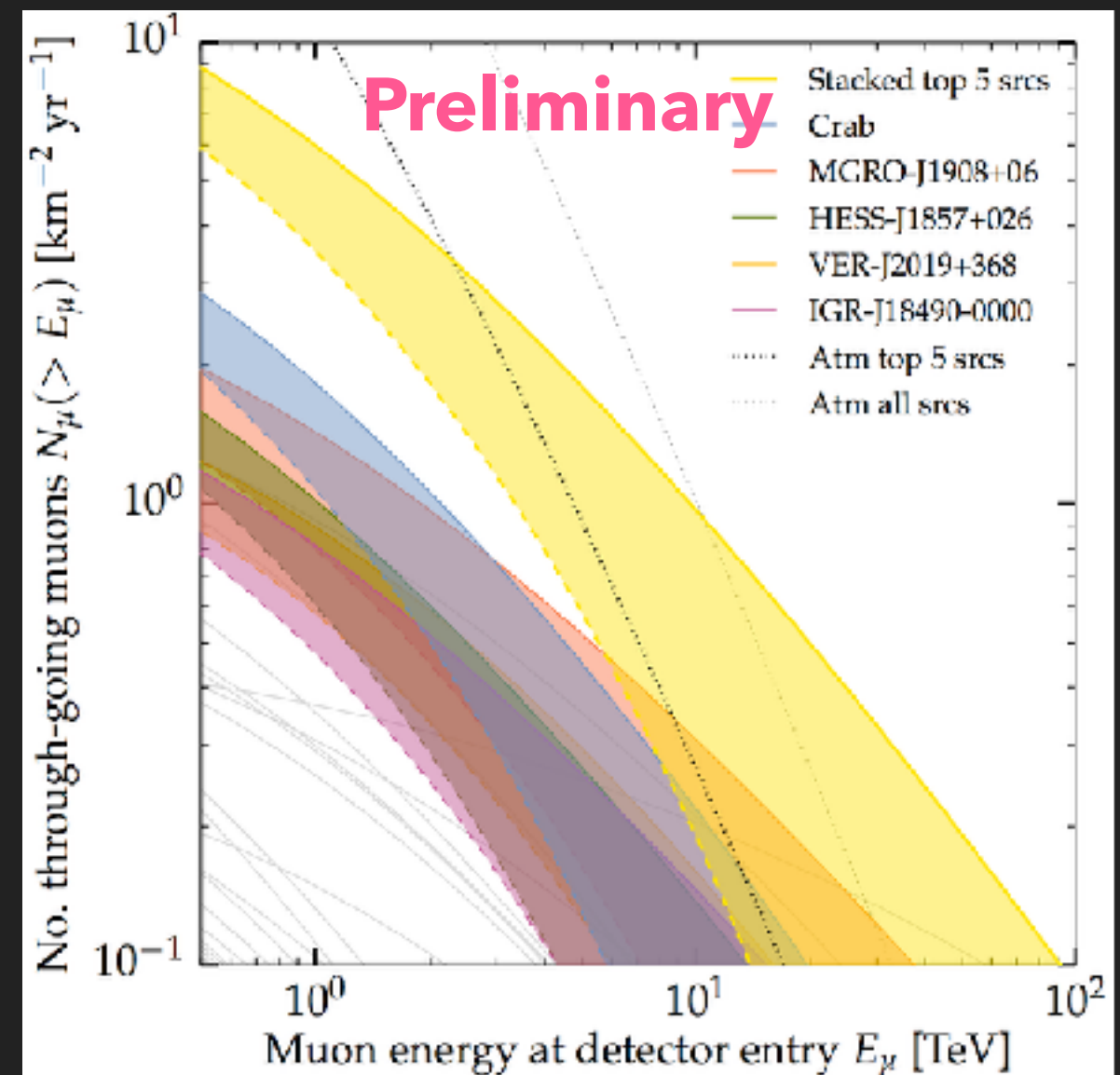
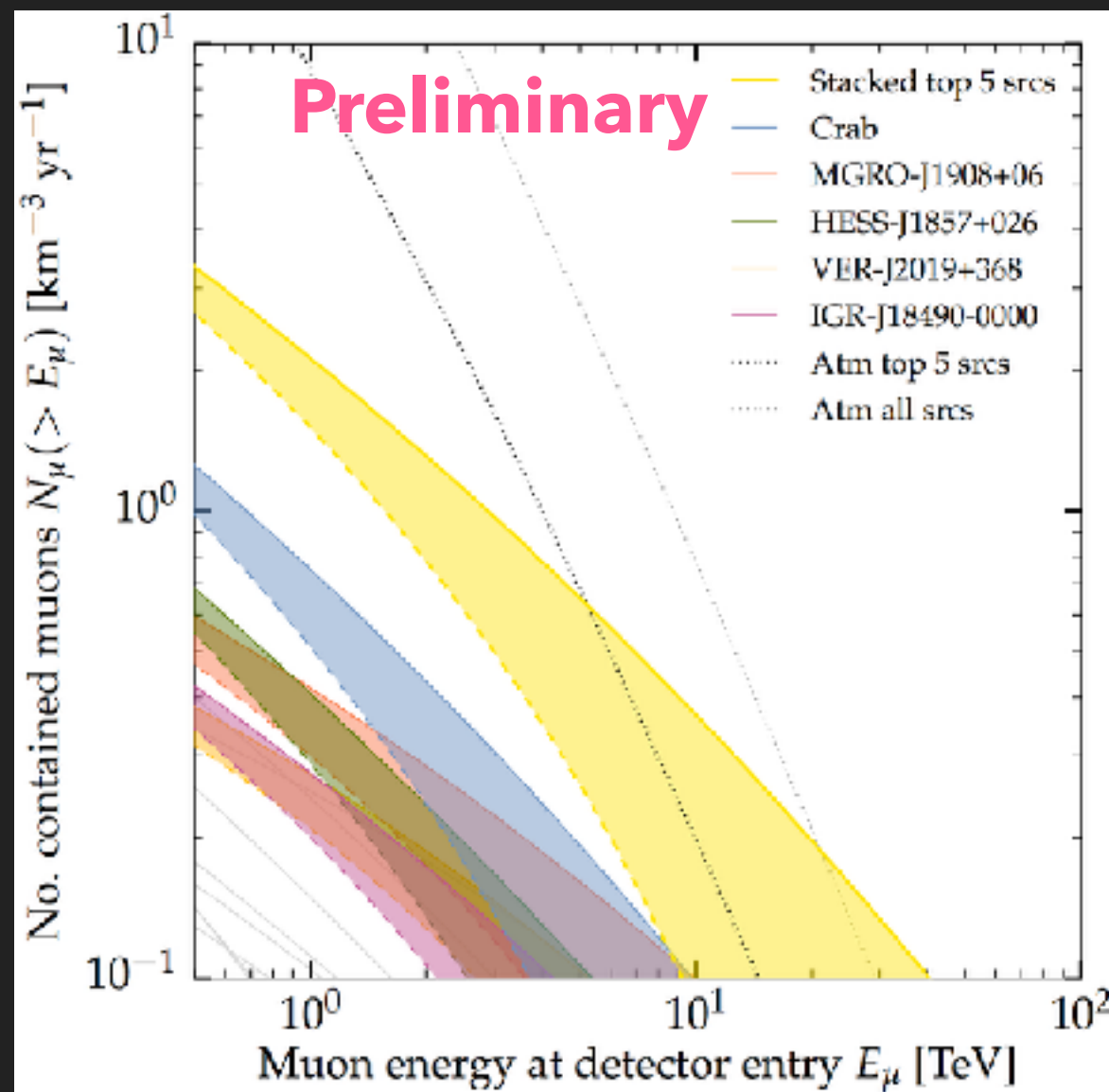
- ▶ Hot neutron stars can also be observed via their isotropic thermal emission.
- ▶ X-Ray observations can be sensitive to ~ 2 kpc for 10^6 K NS.
- ▶ Cooler NS extremely hard to see.
- ▶ Could potentially detect a system which has recently ceased producing TeV particles.

- ▶ **HAWC sources are potential IceCube neutrino sources.**
- ▶ **Spectral measurements of HAWC sources are imperative to calculating the expected neutrino flux.**
- ▶ Here we produce an analysis taking into account a 20% uncertainty in total flux, as well as spectral uncertainty due to an exponential cutoff.



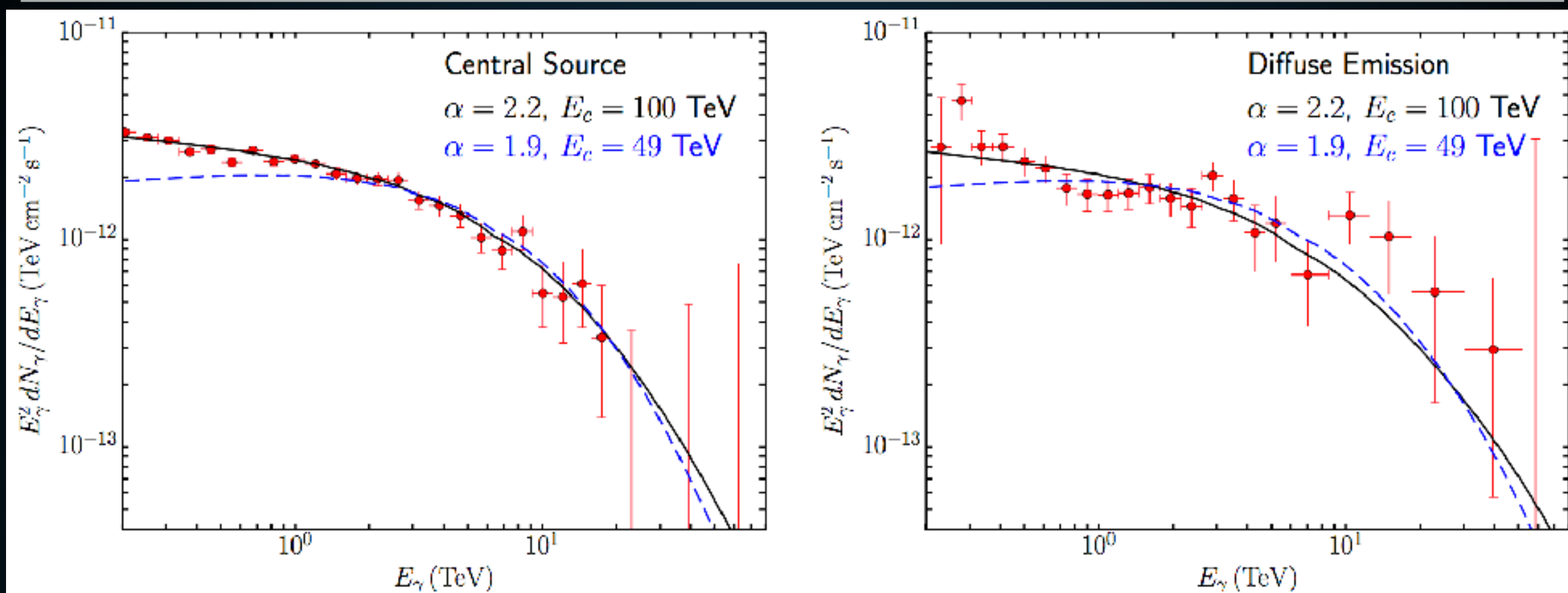
- ▶ Use Geminga as a template to calculate TeV halo intensity.
- ▶ Use Geminga spectrum with complete (diffuse) cooling.
- ▶ Hadronic background from Galprop models tuned to Fermi-LAT emission.
- ▶ TeV halos naturally explain the intensity and spectrum of the TeV excess.





- ▶ If these sources are hadronic, their stacked neutrino flux is detectable in current IceCube data.
- ▶ Alternatively, can place a strong constraint on the hadronic fraction of the brightest HAWC sources.

TeV HALOS PRODUCE THE PEVATRON SPECTRUM



- ▶ The TeV halo spectrum from Geminga naturally reproduces the HESS observations.
- ▶ Slightly softer spectra preferred.
 - ▶ Some evidence that Geminga spectrum is particularly hard.
 - ▶ Hadronic diffuse background contamination?

TWO DIFFERENT SOURCES OF INFORMATION

- ▶ This provides us two ways to learn about cosmic rays:
 - ▶ Investigating the cosmic-rays that directly hit satellites on Earth
 - ▶ Can directly detect cosmic-ray species
 - ▶ Only a local measurement
 - ▶ Solar Modulation
 - ▶ Investigating the gamma-ray signal from cosmic-ray interactions
 - ▶ Can understand propagation near sources
 - ▶ Don't directly know the cosmic-ray species, or even if the gamma-ray is galactic
 - ▶ Line of sight